

FC  
4565  
OFR  
79-1076

GL00052

UNITED STATES DEPARTMENT OF THE INTERIOR

GEOLOGICAL SURVEY

PRELIMINARY REPORT ON TERTIARY VOLCANISM  
AND URANIUM MINERALIZATION IN THE  
THOMAS RANGE AND NORTHERN DRUM MOUNTAINS,  
JUAB COUNTY, UTAH

by

David A. Lindsey

**UNIVERSITY OF UTAH  
RESEARCH INSTITUTE  
EARTH SCIENCE LAB.**

Open-File Report 79-1076

1979

This report is preliminary and has not been  
edited or reviewed for conformity with U.S.  
Geological Survey standards.

## Contents

	Page
Abstract -----	1
Introduction -----	3
Acknowledgments -----	5
Stratigraphy -----	5
Stratigraphic section -----	5
Age and correlation -----	6
Description of rock units -----	12
Drum Mountains Rhyodacite -----	12
Diorite -----	16
Mt. Laird Tuff -----	16
Joy Tuff -----	21
Crystal tuff member -----	21
Black glass tuff member -----	24
Landslide breccia -----	26
Breccia at Spor Mountain and breccia at Wildhorse Spring -----	26
Megabreccia of the northern Drum Mountains -----	28
Dell Tuff -----	29
Needles Range Formation -----	31
Spor Mountain Formation -----	33
Beryllium tuff member -----	33
Porphyritic rhyolite member -----	36
Topaz Mountain Rhyolite -----	38
Flows and domes of alkali rhyolite -----	38
Stratified tuff -----	40
Structural geology -----	43
Thomas caldera -----	44
Dugway Valley cauldron -----	47
Basin-and-range structure -----	48
Structural evolution -----	49
Some unsolved problems -----	52
Chemical composition of volcanic rocks -----	54
Rock types -----	54
Trace element associations -----	55
Relationship of volcanism to mineralization -----	60
Origin of volcanic rocks -----	62
Uranium occurrences -----	65
Uranium in fluorspar pipes -----	65
Uranium in the beryllium tuff member of the Spor Mountain Formation -----	66
Yellow Chief mine -----	71
Uraniferous opal -----	75

Uranium occurrences--cont.	
Uranium in stratified tuff of the Topaz Mountain Rhyolite	76
A model for uranium deposits and some suggestions for exploration -----	76
References cited -----	80

#### Illustrations

Figure 1.--Map showing location of the Thomas Range and Drum Mountains, other geographic features, and mineral occurrences -----	4
2.--Geologic map of Tertiary rocks in the Thomas Range and northern Drum Mountains, Juab County, Utah ---	8
3-12.--Photos and photomicrographs:	
3.--Drum Mountains Rhyodacite -----	13
4.--Mt. Laird Tuff -----	17
5.--Crystal tuff member of Joy Tuff -----	22
6.--Black glass tuff member of Joy Tuff -----	25
7.--Landslide breccia -----	27
8.--The Dell Tuff -----	30
9. Needles Range Formation -----	32
10.--Facies of the beryllium tuff member of the Spor Mountain Formation -----	35
11.--Porphyritic rhyolite member of the Spor Mountain Formation -----	37
12.--Topaz Mountain Rhyolite -----	39
13.--Features of the stratified tuff in the Topaz Mountain Rhyolite -----	42
14.--Aerial views of the the ring fracture zone of the Thomas caldera, showing the Joy graben and its northward extension in The Dell -----	45
15.--Geologic map showing the structure of The Dell ----	46
16.--Maps showing structural evolution of the Thomas Range and northern Drum Mountains -----	51
17.--Chemical composition including trace elements, of igneous rocks compared to age -----	56
18.--Total alkalis (Na <sub>2</sub> O plus K <sub>2</sub> O) versus silica content of igneous rocks -----	57
19.--AFM diagram of igneous rocks -----	59

Figures--cont.

	Page
20.--Histograms showing the abundance of uranium and thorium in the beryllium tuff member -----	67
21.--Distribution of uranium with respect to beryllium ore in beryllium tuff member at the Roadside beryllium deposit -----	69
22.--Histograms showing the abundance of beryllium oxide, uranium, and thorium, and a scattergram showing segregation of beryllium oxide and uranium in mineralized zones of the beryllium tuff member -----	70
23.--Location and analyses of geochemical samples in two ore lenses in the Yellow Chief Mine -----	73

Tables

Table 1.--Revised stratigraphy of the Tertiary rocks of the Thomas Range and northern Drum Mountains, Juab County, Utah -----	7
2.--Summary of age dates for volcanic formations of the Thomas Range and northern Drum Mountains, Juab County, Utah -----	9
3.--Analytical data for new fission track ages of igneous rocks in Juab and Millard Counties, Utah -----	10
4.--Comparison of mineral composition of volcanic rocks of the Thomas Range and northern Drum Mountain -----	14
5.--Section of Mt. Laird Tuff in drillhole east of Topaz Mountain -----	18
6.--Analytical data for uranium content of zircon in volcanic rocks of the Thomas Range -----	61
7.--Chemical analyses of samples from two ore lenses in the Yellow Chief mine -----	74
8.--(Appendix) Chemical analyses of igneous rocks of the Thomas Range and Drum Mountains -----	87

## ABSTRACT

The Thomas Range and northern Drum Mountains have a history of volcanism, faulting, and mineralization that began about 42 m.y. ago. Volcanic activity and mineralization in the area can be divided into three stages according to the time-related occurrence of rock types, trace element associations, and chemical nature of mineralization. Volcanic activity switched abruptly from rhyodacite-quartz latite (42-39 m.y. ago) to rhyolite (38-32 m.y. ago) to alkali rhyolite stages (21 and 6-7 m.y. ago); these stages correspond to periods of chalcophile and siderophile metal mineralization, no mineralization, and lithophile metal mineralization, respectively. Angular unconformities record episodes of cauldron collapse and block faulting between the stages of volcanic activity and mineralization. The youngest angular unconformity formed between 21 and 7 m.y. ago during basin-and-range faulting.

Early rhyodacite-quartz latite volcanism from composite volcanoes and fissures produced flows, breccias, and ash-flow tuff of the Drum Mountains Rhyodacite and Mt. Laird Tuff. Eruption of the Mt. Laird Tuff about 39 m.y. ago from an area north of Joy townsite was accompanied by collapse of the Thomas caldera. Part of the roof of the magma chamber did not collapse, or the magma was resurgent, as is indicated by porphyry dikes and plugs in the Drum Mountains. Chalcophile and siderophile metal mineralization, including copper, gold, and manganese, accompanied early volcanism.

The middle stage of volcanic activity was characterized by explosive eruption of rhyolitic ash-flow tuffs and collapse of the Dugway Valley cauldron. Eruption of the Joy Tuff 38 m.y. ago was accompanied by subsidence of this cauldron and followed by collapse and sliding of Paleozoic rocks from the west wall of the cauldron. Landslides in The Dell were covered by the Dell Tuff, erupted 32 m.y. ago from an unknown source to the east. An ash-flow of the Needles Range Formation was erupted 30-31 m.y. ago, probably from a distant source outside the volcanic field. The rhyolitic stage of volcanism was barren of mineralization.

The last stage of volcanism was contemporaneous with basin-and-range faulting and was characterized by explosive eruption of ash and pumice, forming stratified tuff, and by quiet eruption of alkali rhyolite as viscous flows and domes. The first episode of alkali rhyolite volcanism deposited the beryllium tuff and porphyritic rhyolite members of the Spor Mountain Formation 21 m.y. ago. After a period of block faulting, the stratified tuff and alkali rhyolite of the Topaz Mountain Rhyolite were erupted 6-7 m.y. ago along faults and fault intersections. Erosion of Spor Mountain may have provided abundant dolomite detritus to the beryllium tuff member. The alkali rhyolite of both formations is fluorine-rich, as is evident from abundant topaz, and contains anomalous amounts of lithophile metals. Alkali rhyolite volcanism was accompanied by lithophile metal mineralization which deposited fluorite, beryllium, and uranium.

The structure of the area is dominated by the Thomas caldera, and the younger Dugway Valley cauldron, which is nested within the Thomas caldera; the Thomas caldera is surrounded by a rim of Paleozoic rocks at Spor Mountain and Paleozoic to Precambrian rocks in the Drum Mountains. The Joy fault and Dell fault system mark the ring fracture zone of the Thomas caldera. These structural features began to form about 39 m.y. ago during eruption of the Mt. Laird Tuff and cauldron subsidence. The Dugway Valley cauldron sank along a series of step-like normal faults southeast of Topaz Mountain in response to collapse of the magma chamber of the Joy Tuff. The caldera structure was modified by block faulting between 21 and 7 m.y. ago, the time of widespread extensional faulting in the basin-and-range province. Vents erupted alkali rhyolite 6-7 m.y. ago along basin-and-range faults.

Uranium mineralization was associated with the stage of alkali rhyolite volcanism, extensional basin-and-range faulting, and lithophile metal mineralization; it occurred at least 11 m.y. after the end of the caldera cycle. Uranium, derived from alkali rhyolite magma, was concentrated in trace amounts by magmatic fluids and in potentially economic amounts by hydrothermal fluids and ground water. Hydrothermal fluids deposited uraniferous fluorite as pipes in carbonate rocks of Paleozoic age on Spor Mountain and uranium-bearing disseminated deposits of fluorite and beryllium in the beryllium tuff member of the Spor Mountain Formation. Uranium of hydrothermal origin is dispersed in fluorite and opal. Uranium in fluorite may be tetravalent(?) but that in opal is probably hexavalent; no primary minerals of tetravalent uranium are known to occur. Ground waters have concentrated significant ores of hexavalent uranium minerals in the beryllium tuff member of the Spor Mountain Formation at the Yellow Chief Mine, and are probably also responsible for widespread low concentrations (0.0X percent) of uranium that occur separately from beryllium ore in the beryllium tuff member. More deposits of the Yellow Chief type may occur in down-faulted sections of beryllium tuff beneath the Thomas Range. The ground water ores show no evidence of a reducing environment; instead, precipitation of hexavalent uranium minerals occurred by evaporation, decline in concentration of complexing ions such as carbonate, or some other mechanism. Reducing environments for hydrothermal deposits must be sought around rhyolite vents and in a hypothesized pluton of alkali rhyolite composition beneath Spor Mountain; for ground-water deposits, reducing environments may occur in basin fill such as that of the Dugway Valley cauldron.

## INTRODUCTION

The Thomas Range (fig. 1) contains important deposits of fluorspar, beryllium, and uranium. These mineral deposits are associated with a sequence of volcanic rocks that extends into the northern Drum Mountains and contains intermediate-composition flow rocks and tuffs, rhyolitic ash-flow tuffs, and large volumes of alkali rhyolite. The area is part of an east-west belt of mineral deposits, volcanic and intrusive rocks, and aeromagnetic high anomalies called the Deep Creek-Tintic mineral belt (Shawe and Stewart, 1976; Stewart, Moore, and Zietz, 1977), which also contains the beryllium belt of western Utah (Cohenour, 1963). A similar sequence of volcanic rocks, but with no known mineral deposits, crops out in the Keg Mountains, east of the Thomas Range.

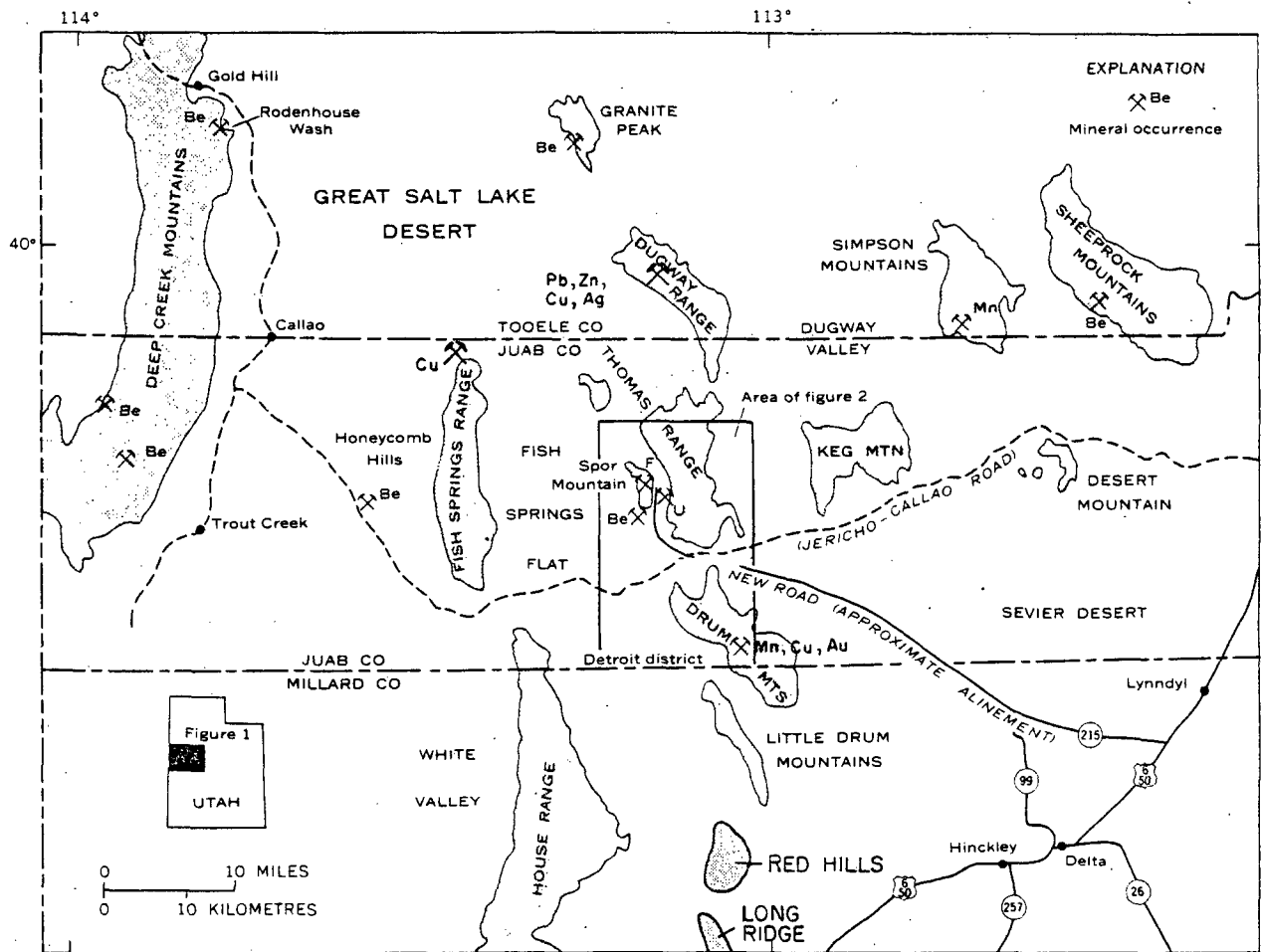
The volcanic rocks of the Thomas Range were first mapped and divided into two groups by Staatz and Carr (1964). Shawe (1972) reclassified the volcanic rocks of the Thomas Range into three assemblages of 1) flows and agglomerates, 2) ash-flow tuffs, and 3) rhyolite flows and tuff, all of which he was able to map throughout much of the Keg, Desert, and Drum Mountains. Geochronologic studies (Lindsey and others, 1975) confirmed much of Shawe's (1972) three-fold classification of the volcanic rocks of the region. Shawe also concluded that eruption of voluminous ash-flow tuffs of his middle assemblage was followed by caldera collapse in the Thomas, Keg, and Desert Mountain areas. The Joy fault was interpreted as part of the ring fracture of the Thomas caldera and such ring fractures were believed to have provided conduits that localized the deposits of ore-forming fluids. The northern Drum Mountains also were mapped by Newell (1971), who confirmed the general outline of the caldera model there. Recent mapping in the southwestern Keg Mountains by Staub (1975) did not confirm the Thomas caldera ring fracture that was projected there by Shawe (1972).

The mineral deposits of the Thomas Range were studied by Staatz and Osterwald (1959) and Staatz and Carr (1964), who described the fluorspar pipes and uranium occurrences there. Beryllium deposits in tuff were discovered at Spor Mountain in 1959, and studies of these deposits related them to fluorspar mineralization and rhyolite volcanism in the Thomas Range (Staatz and Griffitts, 1961; Shawe, 1968; Park, 1968; Lindsey, 1977). The manganese deposits of the Detroit district in the Drum Mountains have been studied by Crittenden, Straczek, and Roberts (1961) and the area's potential for gold, copper, and other mineral deposits has been examined by mapping and geochemical surveys (Newell, 1971) and geochemical studies of jasperoid found there (McCarthy and others, 1969).

The present study was conducted in response to the current (1978) high interest in uranium exploration in the Thomas Range and vicinity. Reconnaissance studies of the uranium potential of the area have been made (Leedom and Mitchell, 1978; Texas Instruments Incorporated, 1977),

Figure 1.--Map showing location of the Thomas Range and Drum Mountains, the other geographic features, and mineral occurrences. Location of mineral occurrences shown by a pick and hammer and the following symbols: U, uranium; Be, beryllium; F, fluorite; Mn, manganese; Cu, copper; Pb, lead; Zn, zinc; Au, gold; and Ag, silver.





but recent work (Lindsey, 1978) indicated that the history of volcanism and tectonism in the Thomas Range and Drum Mountains was still not sufficiently understood to relate it to uranium mineralization and to provide reliable guides for uranium exploration. A new stratigraphic framework, resembling that of Shawe (1972) in general outline but differing in many details, was developed from field mapping, geochronologic, petrographic, and trace element studies, and a new geologic map of the area was prepared (Lindsey, 1979). The results of the new mapping are summarized in figure 2 for reference here, but the reader should consult U.S. Geological Survey map I-1176 (Lindsey, 1979) for details. This report describes the geology of Tertiary rocks and uranium occurrences of the Thomas Range and northern Drum Mountains in detail, and proposes a model relating volcanism, tectonism, and mineralization for the area.

#### Acknowledgments

Many employees of the U.S. Geological Survey provided chemical analyses and assisted with other aspects of this study; they are acknowledged in the text and tables. D. R. Shawe, by many discussions of the area studied, J. C. Ratté, by discussion of cauldron-subsidence concepts, and R. K. Glanzman, by obtaining samples for uranium and thorium analyses, have contributed importantly to the present report. L. M. Osmonson and Ezekiel Rivera of the U.S. Geological Survey made mineral separations, and Louise Hedricks prepared photomicrographs. I thank many exploration geologists, including M. J. Bright, W. A. Buckovic, R. D. Dorman, D. E. Gorski, S. M. Hansen, S. H. Leedom, P. L. Nieson, J. M. Pratt, and W. A. Spears, for information about the geology of the area; and I also thank W. L. Chenoweth and D. A. Sterling of the U.S. Department of Energy and Charles Beverly, Michael Callaghan, and R. D. Cole of Bendix Field Engineering Corporation for geologic information and coordination with U.S. Department of Energy plans and programs in the area. I thank the employees of Brush Wellman for their cooperation and hospitality during fieldwork.

#### STRATIGRAPHY

##### Stratigraphic section

The Tertiary rocks of the Thomas Range and northern Drum Mountains are divided into nine formations (table 1). As revised here, the stratigraphy corresponds generally to the former subdivision of stratigraphic units into oldest (flows and agglomerates), middle (ash flow tuffs), and youngest (rhyolite flows and tuffs) assemblages or groups (Shawe, 1972; Lindsey and others, 1975). Each of these groups is characterized by a particular style of volcanism and separated by an angular unconformity. Minor unconformities occur between some formations, also.

All of the volcanic rocks with the probable exception of the Needles Range Formation have local sources. Flows of the Drum Mountains

Rhyodacite were probably extruded from local fissures and from central volcanos in the Black Rocks Hills and Little Drum Mountains (Leedom, 1974) about 42 m.y. ago. Quiet eruption of rhyodacite gave way to explosive eruption of ash-flow tuff from vents north of Joy townsite in the Drum Mountains and east of Topaz Mountain in the Thomas Range. The first explosive eruptions, from the Drum Mountains vent, deposited tuff of intermediate composition (Mt. Laird Tuff); whereas all later eruptions, from 38 m.y. to 32 m.y. ago, deposited rhyolitic tuff. One or more of these eruptions deposited the crystal tuff member of the Joy Tuff over an area that extends from Fish Springs Flat to Desert Mountain, a distance of 60 km. Collapse of cauldron walls 39-32 m.y. ago left landslide deposits of megabreccia and breccia interbedded with lava flows and ash-flow tuffs. Near the end of explosive rhyolite volcanism, about 30-31 m.y. ago, an ash-flow tuff of the Needles Range Formation was deposited in part of the area. All later volcanism consisted of explosive eruption of ash and quiet extrusion of alkali rhyolite lava as flows and domes at 21 m.y. ago (Spor Mountain Formation) and 6-7 m.y. ago (Topaz Mountain Rhyolite).

Four angular unconformities record periods of cauldron collapse, faulting, and erosion in the Tertiary section; these unconformities have regional extent throughout the volcanic field of the Thomas Range, Drum Mountains, and Keg Mountains. Unconformity A, at the base of the section, records some pre-volcanic period or periods of uplift and erosion of uncertain age. Unconformity B lies beneath the 38 m.y.-old crystal tuff member of the Joy Tuff, and records subsidence of the Thomas caldera that accompanied eruption of the Mt. Laird Tuff about 39 m.y. ago. Erosional detritus is lacking above the unconformity, indicating that it is mainly constructional. Cauldron collapse resulting from eruption of the Joy Tuff 38 m.y. ago was followed by deposition of the Dell Tuff 32 m.y. ago and the Needles Range Formation about 30-31 m.y. ago. Unconformity C represents a 9 m.y. period of quiescence after ash-flow eruption; it is partly constructional and partly erosional, as indicated by erosional detritus in the Spor Mountain Formation of 21 m.y. ago. Unconformity D, between the Spor Mountain Formation and the Topaz Mountain Rhyolite, formed during basin-and-range faulting between 21 and 6-7 m.y. ago.

#### Age and correlation

An attempt was made to date each rock unit in the Thomas Range and Drum Mountains, using both old and new data (table 2). The ages have been revised to reflect additional dating and recently adopted decay constants used in calculating ages by the potassium-argon and fission track methods. Methods used for fission track dates reported here are described by Naeser (1976).

The new fission-track ages extend the history of volcanism in western Utah to almost 42 m.y. ago (tables 2 and 3). A single age of  $41.8 \pm 2.3$  m.y. on zircon from the Drum Mountains Rhyodacite is somewhat older than two whole rock K-Ar ages of  $38.2 \pm 0.4$  m.y. (revised from

Table 1.—Revised stratigraphy of Tertiary rocks in the Thomas Range and northern Drum Mountains, Juab County, Utah. (Leaders (—) indicate information not available or not relevant.)

Age (m.y.) <sup>1/</sup>	Map symbol (on fig. 2)	Description of rocks <sup>2/</sup>
<1	Qal	ALLUVIUM AND COLLUVIUM (QUATERNARY)—Alluvial pediments and stream deposits of poorly sorted gravel, sand, and clay; colluvium covering slopes; playa sediments; beach sand and gravel deposits and lake-bottom clays deposited by Lake Bonneville at elevations below about 1580 m (5200 ft) elevation
		unconformity
6.3-6.8	Ttm <sub>1,2,3</sub>	TOPAZ MOUNTAIN RHYOLITE (UPPER MIOCENE)—Flows and extrusive domes of gray to red, topaz-bearing alkali rhyolite, black vitrophyre, and interbedded units of tan stratified tuff. Tuff units (Ttmc) seldom exceed 30 m in thickness, are local in extent, and have unconformable bases. Rhyolite contains sparse crystals of quartz, sanidine, biotite, and plagioclase except locally at Antelope Ridge and lower part of Fismire Wash, where phenocrysts are abundant. Maximum thickness of rhyolite is about 700 m
		angular unconformity D
21.3	Tsp	SPOR MOUNTAIN FORMATION, PORPHYRITIC RHYOLITE MEMBER (LOWER MIOCENE)—Flows and plugs of gray to red porphyritic alkali rhyolite; rhyolite contains abundant phenocrysts of dark quartz, sanidine, plagioclase, and biotite and abundant microscopic topaz in groundmass. Maximum thickness is about 300 m
(21.3)	Tsb	SPOR MOUNTAIN FORMATION, BERYLLIUM TUFF MEMBER (LOWER MIOCENE)—Stratified tan vitric tuff and tuffaceous breccia with abundant clasts of carbonate rocks. Tuff includes thin beds of ash-flow tuff, bentonite, and epiclastic tuffaceous sandstone and conglomerate in The Dell. Hydrothermal alteration of tuff to clay, fluorospar, and potassium feldspar is widespread. Maximum thickness is about 60 m
		angular unconformity C
30.4 <sup>3/</sup>	Tar	NEEDLES RANGE FORMATION (OLIGOCENE)—Simple cooling unit of pink to gray to red-brown ash-flow tuff with abundant small crystals of plagioclase, hornblende, and biotite. Partially welded. Tuff fills paleovalleys on northwest side of Drum Mountains. Maximum thickness is about 30 m
32.0	Td	DELL TUFF (OLIGOCENE)—Gray to pink rhyolitic ash-flow tuff that contains abundant crystals of euhedral quartz, sanidine, biotite, and plagioclase in a poorly welded to unwelded matrix of devitrified shards and pumice. The tuff resembles the older Joy Tuff, but may be distinguished from the Joy by the presence of abundant large quartz bipyramids and a loose, ashlike weathering aspect. Maximum thickness is about 180 m at the north end of The Dell
(<37)	Tld	LANDSLIDE BRECCIA, MEGABRECCIA OF THE NORTHERN DRUM MOUNTAINS (OLIGOCENE?)—Megabreccia of Cambrian limestone and dolomite overlying Joy Tuff in northern Drum Mountains. The megabreccia retains original stratigraphy of the Cambrian strata but contains intensely brecciated and rotated clasts of Cambrian rocks locally. Maximum thickness is about 60 m
(32-42)	Tls	LANDSLIDE BRECCIA, BRECCIA AT SPOR MOUNTAIN (OLIGOCENE?)—Breccia of Ordovician and Silurian dolomite, limestone, and quartzite. The breccia retains the original stratigraphy of Paleozoic rocks near the breakaway zone at the crest of Spor Mountain, but passes east into breccia with clasts of various strata mixed together and faintly stratified. Maximum thickness estimated very approximately at 80 m
(32-42)	Tlw	LANDSLIDE BRECCIA, BRECCIA AT WILDHORSE SPRING (OLIGOCENE?)—Breccia of mixed angular to subround clasts of Paleozoic rocks and Drum Mountains Rhyodacite in a matrix of rhyodacite fragments. The breccia underlies and passes laterally into the breccia at Spor Mountain, and is stratified at the top. Maximum thickness is estimated very approximately at about 20 m
		unconformity
~37	Tjb	JOY TUFF, BLACK GLASS TUFF MEMBER (LOWER OLIGOCENE)—Simple cooling unit of rhyolitic ash-flow tuff with sparse crystals of sanidine, quartz, plagioclase, and biotite and lithic fragments of limestone and volcanic rock. Most of the tuff is intensely welded, with abundant compacted black pumice in the lower part. The upper, unwelded part is tan and contains abundant light-colored pumice. Maximum thickness is about 30 m

Table 1.--cont.

Age (m.y.) <sup>1/</sup>	Map symbol (on fig. 2)	Description of rocks <sup>2/</sup>
38.0	Tjc	JOY TUFF, CRYSTAL TUFF MEMBER (UPPER EOCENE AND LOWER OLIGOCENE)-- Gray-pink to red-brown rhyolitic ash-flow with abundant euhedral and broken crystals of quartz, sanidine, plagioclase, and biotite in a moderately welded matrix of devitrified shards. Lower 10 m of tuff contains abundant compacted black pumice; light-colored pumice is present higher in section. Tuff contains abundant accessory sphene and rare cognate inclusions of lathlike plagioclase, biotite, and sphene that aid in distinguishing it from the Dell Tuff. Welding is strong near probable vents east of Topaz Mountain, where foliation is near vertical and breccia occurs. Maximum thickness is about 130 m at the type locality
		angular unconformity B
39 <sup>4/</sup>	Tml	MT. LAIRD TUFF (UPPER EOCENE)--pink quartz latitic ash-flow tuff with abundant euhedral crystals of white plagioclase (10 mm long), bronze biotite (5 mm across), and hornblende. Quartz phenocrysts with resorbed outlines occur in tuff northeast of Thomas Range. Pumiceous breccia and hydrothermally altered tuff occur near probable vent north of Joy townsite. Dikes and plugs of porphyry (Tml) very similar to Mt. Laird Tuff crop out 3 km south of Joy townsite; they are included in the unit. Maximum exposed thickness is about 80 m, but 500 m of tuff is interbedded with tuffaceous lacustrine sediments in the subsurface of Dugway Valley
(39-42)	Tdi	DIORITE (UPPER EOCENE)--Plugs of dark gray, massive, fine-grained diorite intrude Paleozoic strata 3 km southeast of Joy townsite. The diorite contains abundant calcic plagioclase and hornblende
42	Tdr	DRUM MOUNTAINS RHYODACITE (UPPER EOCENE)--Rusty-weathering black rhyodacite flows and breccias with phenocrysts of intermediate-composition to calcic plagioclase and pyroxene in an aphanitic to glassy matrix. Modally, this rock is a hypersthene andesite, but chemical analyses show the rock to be a rhyodacite in the classification of Rittmann (1952). Unit includes some interbedded tuffaceous sandstone and laharic debris flows in the Black Rock Hills and some aphanitic flow or dike rocks near Joy townsite. Maximum thickness is about 240 m in the Black Rock Hills
		angular unconformity A
-	Dp6	UNDIFFERENTIATED ROCKS (DEVONIAN TO PRECAMBRIAN)--Limestone, dolomite, quartzite, and shale. Formations are differentiated on maps of Staatz and Carr (1964) for the Thomas Range and Newell (1971) and Crittenden and others (1961) for the Drum Mountains. Maximum thickness exceeds 1200 m

<sup>1/</sup> Ages are averages of all valid K-Ar and fission track dates (table 3); ages in parentheses are inferred from stratigraphic relationships.

<sup>2/</sup> Many units have unconformable tops, so that the original thickness has been reduced by erosion.

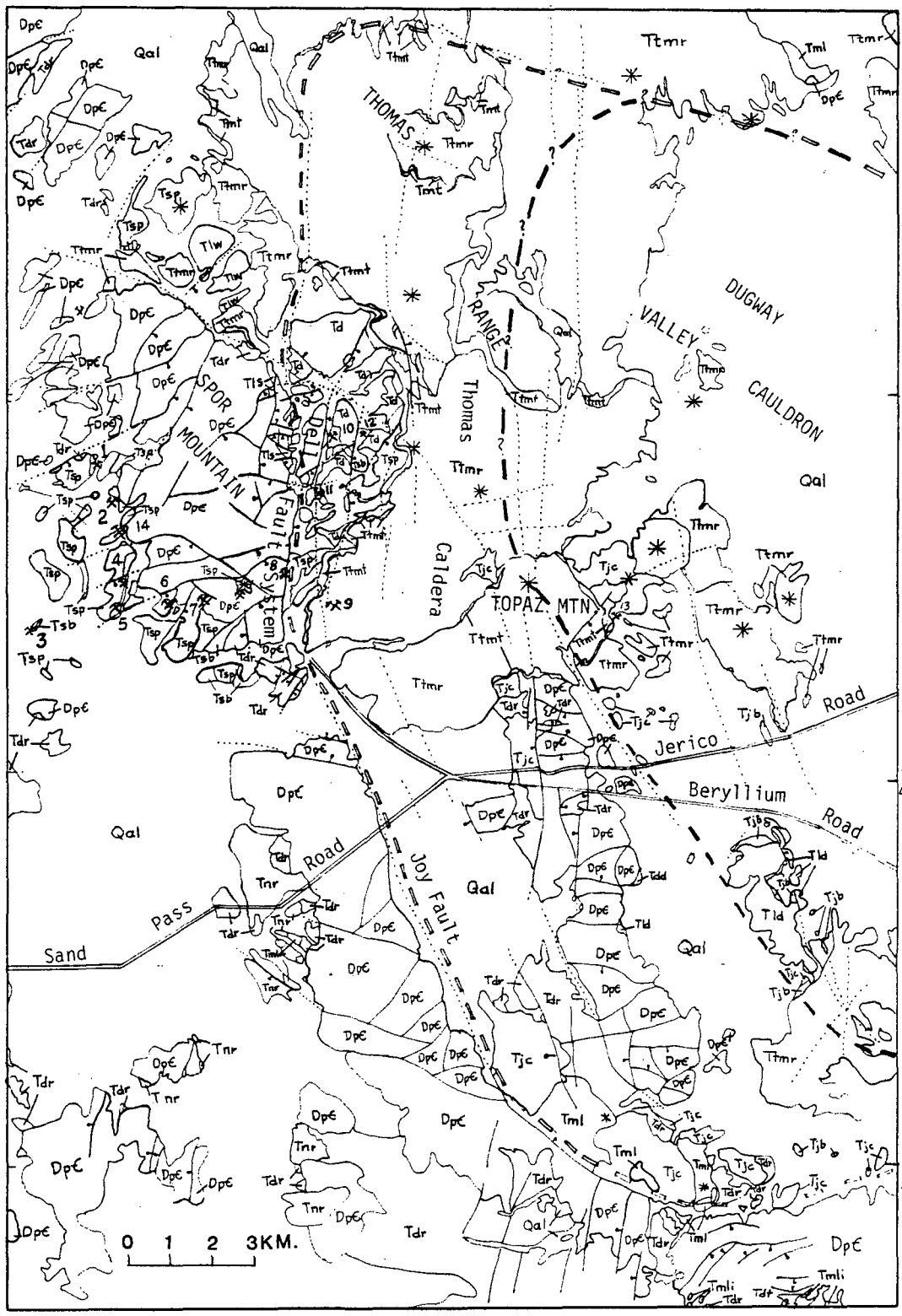
<sup>3/</sup> Average age of the Needles Range Formation (Armstrong, 1970); average of two ages from Little Drum Mountains is 31.4 m.y.

<sup>4/</sup> A single age of 36.4±1.7 m.y. on the Mt. Laird Tuff was determined (table 3), but the true age of the Mt. Laird Tuff is estimated at about 39 m.y. because it underlies the 38.0 m.y.-old crystal tuff member of the Joy Tuff.

Figure 2.—Geologic map of Tertiary rocks in the Thomas Range and northern Drum Mountains, Juab County, Utah (modified from Lindsey, (1979).

113° 15'

113° 00'



0 1 2 3KM.

EXPLANATION

Qal	Alluvium and colluvium (Quaternary)
Ttmr	Topaz Mountain Rhyolite (Upper Miocene) flows and domes of alkali rhyolite
Ttmt	Topaz Mountain Rhyolite (Upper Miocene) stratified tuff — angular unconformity D —
Tsp	Spor Mountain Formation (Lower Miocene) porphyritic rhyolite member
Tsb	Spor Mountain Formation (Lower Miocene) beryllium tuff member — angular unconformity C —
Tnr	Needles Range Formation (Oligocene)
Td	Dell Tuff (Oligocene)
Tld	Landslide breccia (Oligocene?) megabreccia in northern Drum Mountains
Tls	Landslide breccia (Oligocene?) breccia at Spor Mountain
Tlw	Landslide breccia (Oligocene?) breccia at Wildhorse Spring
Tjb	Joy Tuff (lower Oligocene) black glass tuff member
Tjc	Joy Tuff (Upper Eocene) crystal tuff member — angular unconformity B —
Tml	Mt. Laird Tuff (Upper Eocene) ash-flow tuff and breccia
Tmli	Mt. Laird Tuff equivalent (Upper Eocene) intrusive dike and plugs
Tdt	Diorite (Upper Eocene?) intrusive plugs
Tdr	Drum Mountains Rhyodacite (Upper Eocene) flows and breccias — angular unconformity A —
Dpε	Undifferentiated rocks (Devonian to Precambrian) limestone, dolomite, quartzite, and shale

— Contact, dashed where approximately located

— Fault, dotted where concealed  
ball and bar on downthrown side

\* Probable vent area

— Structural margin of Thomas caldera  
queries(?) where location uncertain

— Structural margin of Dugway Valley cauldron  
queries(?) where location uncertain

\* Mines and prospects in rocks of Tertiary age

1. North End (Be)
2. Taurus (Be)
3. Monitor (Be)
4. Roadside Mine (Be)
5. Fluro Mine (Be)
6. Rainbow (Be)
7. Blue Chalk Mine (Be)
8. Oversight (Be,U)
9. Buena no.1 (U)
10. Claybank (Be,U)
11. Hogsback (Be)
12. Yellow Chief Mine (U)
13. Autunite no. 8 (U)
14. Sigma Emma (Be)



Table 2.—Summary of age dates for volcanic formations of the Thomas Range and northern Drum Mountains, Juab County, Utah. [Ages determined from some formations in nearby areas are included. All fission track ages on zircon, sphene, and apatite have been recalculated using  $d_D = 1.551 \times 10^{-1} \text{ yr}^{-1}$  and  $d_F = 7.03 \times 10^{-17} \text{ yr}^{-1}$ . All K-Ar ages on sanidine have been recalculated using decay constants for  $K^{40}$  of  $\lambda_e = 0.581 \times 10^{-10} \text{ yr}^{-1}$  and  $d_3 = 4.962 \times 10^{-10} \text{ yr}^{-1}$  and  $^{40}\text{K}/\text{K} = 1.167 \times 10^{-4}$ .]

<u>Rock unit</u>	<u>Sample no.</u>	<u>Mineral dated</u>	<u>Age<math>\pm 2\sigma</math></u>	<u>Average age (<math>\pm</math> standard error of the mean)</u>
<b>Topaz Mountain Rhyolite</b>				
Younger flow, Topaz Mountain	177 <sup>1/</sup>	sanidine	6.1 $\pm$ 0.4	6.3 $\pm$ 0.1 m.y.
Younger flow, Topaz Mountain	T40-TR-A <sup>2/</sup>	sanidine	6.3 $\pm$ 0.4	
Younger flow, Topaz Mountain	T40-TR-A <sup>3/</sup>	zircon	6.3 $\pm$ 0.3	
Older flow, Topaz Mountain	T52-TR-A <sup>3/</sup>	zircon	6.2 $\pm$ 0.3	6.3 $\pm$ 0.1 m.y.
Older flow, Topaz Mountain	T52-TR-B <sup>3/</sup>	zircon	6.4 $\pm$ 0.3	
Older flow, Pismira Wash	T50-TR-A <sup>3/</sup>	zircon	6.8 $\pm$ 0.3	
<b>Spor Mountain Formation</b>				
Porphyritic rhyolite member	T53-TR-B <sup>4/</sup>	sanidine	21.2 $\pm$ 0.9	21.3 $\pm$ 0.2 m.y.
Do.	U26	zircon	21.5 $\pm$ 1.1	
<b>Needles Range Formation,</b>				
Little Drum Mountains	U229	zircon	30.6 $\pm$ 1.2	31.4 $\pm$ 0.8 m.y.
Do.	U229	apatite	32.2 $\pm$ 3.6	
Dell Tuff	T43-A <sup>3/</sup>	zircon	30.7 $\pm$ 6.3	32.0 $\pm$ 0.6 m.y.
Do.	T43-A <sup>3/</sup>	sphene	28.5 $\pm$ 1.2	
Do.	T43-A <sup>3/</sup>	apatite	32.8	
Do.	T42-A <sup>3/</sup>	zircon	33.0 $\pm$ 1.3	
Do.	T42-A <sup>3/</sup>	sphene	32.4 $\pm$ 1.4	
Do.	T42-A <sup>3/</sup>	apatite	33.3	
Do.	T54-A	zircon	29.4 $\pm$ 1.3	
Do., Keg Mountain Pass	K20-A <sup>3/</sup>	sphene	33.6 $\pm$ 1.8	
Do.	K48-A <sup>3/</sup>	sphene	32.5 $\pm$ 1.6	
Do.	K48-A <sup>3/</sup>	zircon	33.8 $\pm$ 1.3	
Joy Tuff, black glass tuff member	U141	sphene	37.0 $\pm$ 4.1	
Joy Tuff, crystal tuff member	T51-A <sup>3/</sup>	apatite	40.0	38.0 $\pm$ 0.7 m.y.
Do.	T51-A <sup>3/</sup>	sphene	38.5 $\pm$ 2.0	
Do.	U18B	sphene	39.7 $\pm$ 3.4	
Do.	U32	sphene	39.4 $\pm$ 2.8	
Do.	U34	sphene	38.4 $\pm$ 4.0	
Do.	U56	sphene	36.4 $\pm$ 2.3	
Do., Desert Mountain	U238	zircon	34.5 $\pm$ 1.3	
Do., Picture Rock Hills	U240	zircon	36.9 $\pm$ 1.7	
Mt. Laird Tuff	U57	zircon	36.4 $\pm$ 1.6	
Drum Mountains Rhyodacite	U10A	zircon	41.8 $\pm$ 2.3	

<sup>1/</sup> Armstrong (1970, table 3)

<sup>2/</sup> E. H. McKee, oral commun., 1975

<sup>3/</sup> Lindsey and others (1975)

<sup>4/</sup> H. H. Mehnert, oral commun., 1976, 1978

Table 3.--Analytical data for new fission track ages of igneous rocks in western Juab and Millard Counties, Utah  
 [All ages done by external detector method. Neutron dose determined by C. W. Haeser.]

Sample number	Rock unit	Geographic area	Sample location	Mineral	No. of grains	Fossil tracks		Induced tracks in detector		Neutron dosage (neutrons/cm <sup>2</sup> )	Age $\frac{1}{2}\sigma$
						Number counted	Density (tracks/cm <sup>2</sup> )	Number counted	2X Density (tracks/cm <sup>2</sup> )		
U26	Spor Mountain Formation porphyritic rhyolite member	north of Spor Mountain	NE1/4 sec. 9, T.12S., R.12W.	zircon	5	730	6.76x10 <sup>6</sup>	463	8.46x10 <sup>6</sup>	4.56x10 <sup>14</sup>	21.5±1.1
U7A	do.	The Dell	SW1/4 sec. 36, T.12S., R.12W.	zircon	1	156	4.33x10 <sup>6</sup>	119	6.61x10 <sup>6</sup>	4.60x10 <sup>15</sup>	18.1±4.6
U12B-1	Spor Mountain Formation beryllium tuff member (bentonite at Yellow Chief Mine)	The Dell	NW1/4 sec. 36, T.12S., R.12W.	zircon <sup>2/</sup>	4	321	2.74x10 <sup>6</sup>	338	5.78x10 <sup>6</sup>	9.97x10 <sup>14</sup>	28.3±1.8
				do. <sup>2/</sup>	2	346	5.77x10 <sup>6</sup>	257	8.57x10 <sup>6</sup>	9.97x10 <sup>14</sup>	40.0±7.0
U229	Needles Range Formation	south of Little Drum Mountains	NE1/4 sec. 23, T.16S., R.11W.	zircon	10	919	3.52x10 <sup>6</sup>	861	6.60x10 <sup>6</sup>	9.61x10 <sup>14</sup>	30.6±1.2
U229	do.	do.	do.	apatite	15	234	1.58x10 <sup>5</sup>	1002	1.35x10 <sup>6</sup>	4.62x10 <sup>15</sup>	32.2±3.6
T54-A	Dell Tuff	The Dell	SE1/4 sec. 26, T.12S., R.12W.	zircon	5	1031	6.29x10 <sup>6</sup>	1047	1.28x10 <sup>5</sup>	1.00x10 <sup>15</sup>	29.4±1.3
U141	Joy Tuff black glass tuff member	northeastern Drum Mountains	NE1/4 sec. 36, T.13S., R.11W.	sphene	12	262	6.07x10 <sup>5</sup>	1017	4.71x10 <sup>6</sup>	4.81x10 <sup>15</sup>	37.0±4.1
U18B	Joy Tuff crystal tuff member	east of Topaz Mountain	SW1/4 sec. 10, T.13S., R.11W.	sphene	12	488	1.13x10 <sup>6</sup>	350	1.62x10 <sup>6</sup>	9.55x10 <sup>14</sup>	39.7±3.4
U32	do.	south of Topaz Mtn.	NW1/4 sec. 22, T.13S., R.11W.	sphene	11	436	1.10x10 <sup>6</sup>	311	1.57x10 <sup>6</sup>	9.43x10 <sup>14</sup>	39.4±2.8
U34	do.	do.	NE1/4 sec. 20 T.13 S., R.11W.	sphene	10	366	1.02x10 <sup>6</sup>	1384	7.69x10 <sup>6</sup>	4.86x10 <sup>15</sup>	38.4±4.0
U56	do.	northwest of Joy townsite	NE1/4 sec. 21, T/14 S., R.11W.	sphene	10	369	1.03x10 <sup>6</sup>	1466	8.14x10 <sup>6</sup>	4.84x10 <sup>15</sup>	36.4±2.8
U238	do.	east of Desert Mtn.	NW1/4 sec. 29, T.12S., R.6 W.	zircon	10	789	3.02x10 <sup>6</sup>	656	5.03x10 <sup>6</sup>	9.61x10 <sup>14</sup>	34.5±1.3
U240	do.	Picture Rock Hills	NW1/4 sec. 23, T.13S., R.10W.	zircon	8	1005	5.28x10 <sup>6</sup>	782	8.23x10 <sup>6</sup>	9.61x10 <sup>14</sup>	36.9±1.7
U57	Mt. Laird tuff	northwest of Joy Townsite	NE1/4 sec. 21, T.14S., R.11 W.	zircon	8	966	3.98x10 <sup>6</sup>	886	3.65x10 <sup>6</sup>	1.12x10 <sup>15</sup>	36.4±1.6
U29B	Keg granodiorite of Staub (1975)	western Keg Mountains	SE1/4 sec. 24, T.12S., R.10W.	zircon	6	727	3.89x10 <sup>6</sup>	598	6.40x10 <sup>6</sup>	1.01x10 <sup>15</sup>	36.6±1.6
U10A	Drum Mountains Rhyodacite	The Dell	SW1/4 sec. 35, T.12S., R.12W.	zircon	8	518	1.80x10 <sup>6</sup>	345	2.40x10 <sup>6</sup>	9.33x10 <sup>14</sup>	41.8±2.3

1/ Computed using  $\lambda_D = 1.551 \times 10^{-10}/\text{yr}$  and  $\lambda_F = 7.03 \times 10^{-17}/\text{yr}$ .  $\lambda_D$  = Total decay constant for <sup>238</sup>U;  $\lambda_F$  = decay constant for spontaneous fission of <sup>238</sup>U

2/ Zircon believed to be detrital; abundant (90%) zircon with high U content could not be dated.

37.3±0.4 m.y. reported by Leedom, 1974, to account for the change in constants) for flow rocks that overlie the rhyodacite in the Little Drum Mountains. The zircon age is considered reliable because it is not subject to the effects of weak alteration that pervades much of the rhyodacite; also, uranium and the resultant fission tracks are distributed uniformly in the zircon dated so that counting errors that may attend dating of zoned grains are not a problem.

The age of the crystal tuff member of the Joy Tuff is estimated at 38.0±0.7 m.y. by eight fission track dates on sphene, zircon, and apatite. The date of the Joy Tuff marks the onset of extensive eruptions of rhyolitic ash-flow tuff. A single zircon age of 36.4±1.6 m.y. on the Mt. Laird Tuff, which unconformably underlies the Joy Tuff, is probably not significantly different from the age of the Joy Tuff. Accordingly, the true age of the Mt. Laird Tuff is believed to be about 39 m.y. The age of the black glass tuff member of the Joy Tuff, which overlies the crystal tuff member, was checked by a single determination of 37.0±4.1 m.y. on sphene. The age is supported by the close chemical and spatial association of the two members of the Joy Tuff, and sets them apart from the younger Dell Tuff, which has an average age of 32.0±0.6 m.y. as determined by ten fission track dates on zircon, sphene, and apatite.

The age of the ash-flow tuff correlated with the Needles Range Formation (Pierce, 1974) was determined to check that correlation. Tuff of the Needles Range Formation was described from outcrops south of the Little Drum Mountains (Leedom, 1974; Pierce, 1974), and mapped by me (Lindsey, 1979) along the northwest side of the Drum Mountains. Fission track ages of 30.6±1.2 m.y. on zircon and 32.2±3.6 m.y. on apatite confirm assignment of the tuff to the Needles Range Formation, which was estimated by Armstrong (1970) to be 30.4 m.y. old (age adjusted to account for different decay constants).

The 21 m.y. age of the Spor Mountain Formation is confirmed by a new zircon date of 21.5±1.1 m.y. on the plug of porphyritic rhyolite near Wildhorse Spring. H. H. Mehnert dated the porphyritic rhyolite flow at the Roadside pit at 21.2±0.9 m.y. by the K-Ar method on sanidine (Lindsey, 1977). An age of 18.1±4.6 m.y. was obtained for porphyritic rhyolite at the east side of The Dell, but was not used in estimating the average age (table 2) because only a single grain of zircon could be dated.

An attempt to date zircon from bentonite in the Yellow Chief pit, a facies of the beryllium tuff member of the Spor Mountain Formation, was not successful. Detrital zircon from the bentonite comprises about ten percent of the total zircon and is dated as 28.3±1.8 and 40.0±7.0 m.y. old; it reflects the ages of the older volcanic rocks. The remaining 90 percent of the zircon has high track densities and could not be dated; it contains 2200-4500 ppm uranium, which is well above that of zircon from the older volcanic rocks and within the range of high uranium content typical of zircon in the overlying porphyritic rhyolite

member. Field relationships presented in following sections indicate that the age of the bentonite and the rest of the beryllium tuff member is close to that of the overlying porphyritic rhyolite.

The history of igneous activity is approximately the same in the Thomas Range, Drum Mountains, Keg Mountains, and Desert Mountain (Shawe, 1972; Lindsey and others, 1975). Each range has local intrusive and volcanic rocks, however, and only the ash-flow tuffs provide stratigraphic markers that extend into all of the ranges. The Keg Spring andesite and latite of Erickson (1963) is  $39.4 \pm 0.7$  m.y. old and is confined to the northwest part of the Keg Mountains. The Keg Spring is overlain by the Mt. Laird Tuff north of Keg Pass; thus it occupies the same stratigraphic position in the Keg Mountains as the Drum Mountains Rhyodacite does in the Thomas Range. A newly recognized stock of granodiorite (Staub, 1975; H. T. Morris, 1976, oral commun.), dated here at  $36.6 \pm 1.6$  m.y. by the fission track method on zircon, intrudes the Keg Spring andesite and latite west of Keg Pass. Both of these rocks are unconformably overlain by the crystal tuff member of the Joy Tuff in the Picture Rock Hills, which suggests that the zircon age of the granodiorite stock may be about 1-2 m.y. too young. The Dell Tuff unconformably overlies the Keg Spring andesite and latite and the Mt. Laird Tuff north of Keg Pass, where three fission track ages yield an average of  $33.1 \pm 0.4$  m.y. (Lindsey and others, 1975). The crystal tuff member of the Joy Tuff is well exposed on the east side of Desert Mountain, where it has been dated at  $34.5 \pm 1.3$  m.y. by the fission track method. This age may be too young because the tuff has been intruded by the stock of Desert Mountain (Shawe, 1972); the granitic facies of the stock was emplaced about 28-31 m.y. ago (Lindsey and others, 1975; Armstrong, 1970), and that event may have reset slightly the zircon age of the tuff. Stratified tuff and rhyolite considered to be equivalent in part to the Topaz Mountain Rhyolite were erupted from the Keg Mountains about 8-10 m.y. ago. Alkali rhyolite and basalt at the north end of the Fumarole Butte were erupted about 6-7 m.y. ago (Mehnert and others, 1978; Peterson and others, 1978). The last volcanic activity in the region was the eruption of basaltic lava at Fumarole Butte 0.88 m.y. ago (Peterson and others, 1978).

## DESCRIPTION OF ROCK UNITS

### Drum Mountains Rhyodacite

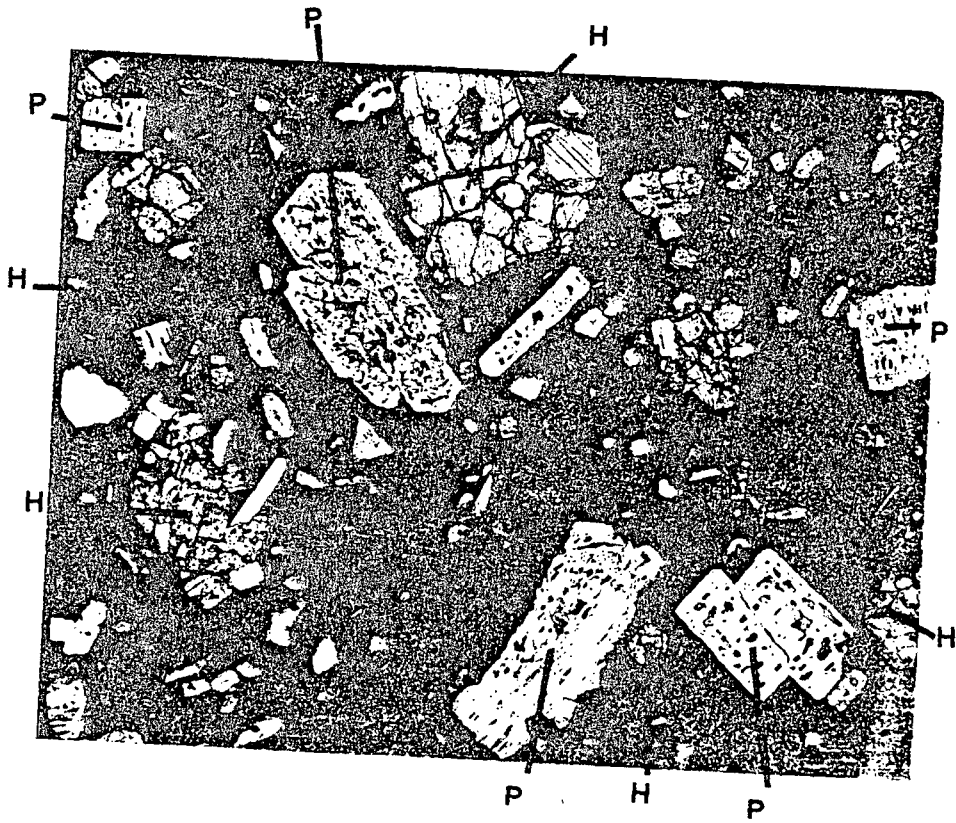
The oldest formation of volcanic rocks in the mapped area consists of dark, rusty-brown weathering flows and flow breccias having the chemical composition of rhyodacite and, to a lesser extent, quartz latite<sup>1</sup>.

---

<sup>1</sup> Nomenclature of Rittmann (1952) is used throughout this report, unless otherwise stated.

---

Figure 3.--Photomicrograph of Drum Mountains Rhyodacite showing partially resorbed plagioclase (P) and clusters of hypersthene (H) and plagioclase in a groundmass of microlites. Crossed polars. Sample from sec. 20, T. 13 S., R. 11 W.



1 mm.

Table 4.--Comparison of the mean and range (in parentheses) of mineral composition and the occurrence of accessory minerals in volcanic rocks in the Thomas Range and northern Drum Mountains. [Mineral composition estimated from point counts on three to six thin sections and cobaltinitrite-stained slabs of each rock type by C. A. Brannon. Accessory minerals identified by binocular microscope and X-ray methods by the writer using mineral concentrates prepared by heavy liquid and electromagnetic separation. tr, trace; x, present; leaders (--) indicate not present.]

Mineral composition in percent									
	1	2	3	4	5	6	7	8	9
quartz	0.1(0-0.4)	0.3(0-1)	29(22-36)	5(3-7)	20(14-25)	3(0-5)	18(13-27)	6(4-10)	16(12-19)
k-feldspar	-	-	24(15-35)	3(2-6)	21(16-26)	-	19(12-29)	7(3-10)	13(11-14)
plagioclase	25(20-27)	17(9-29)	8(3-14)	5(1-7)	8(5-11)	31(26-37)	2(0-3)	<1(0-1)	3(1-3)
biotite	-	3(1-5)	7(0-8)	<1(0-1)	3(1-5)	7(2-11)	1(0-3)	-	-
hornblende	-	6(0-11)	tr	-	-	9(6-13)	-	-	-
hypersthene and augite	10(1.5-13)	4(1-5)	-	-	-	7(0-1)	-	-	-
rock fragments	-	tr	1(0-13)	8(6-11)	<1(0-1)	<1(0-1)	-	-	-
opaque minerals	2(1-6)	1.5(0-3)	tr	<1(0-1)	tr	2.6(1-4)	tr	<1(0-1)	<1(0-1)
other accessory minerals	-	0.8(0-2.4)	1.0(0-2)	<1(0-1)	tr	tr	tr	tr	tr
matrix	63(52-74)	68(61-72)	34(26-49)	79(77-89)	48(40-54)	46(42-52)	60(46-72)	87(74-96)	68(63-73)
composition of matrix	glass and crystals	devitrified shards and pumice	devitrified shards and pumice	glassy to devitrified shards and pumice	devitrified shards and pumice	glassy to devitrified shards and pumice	devitrified glass	devitrified glass	devitrified glass
Occurrence of accessory minerals									
magnetite	x	x	x	x	x	x	x	-	-
specular hematite	-	-	-	-	-	-	-	x	x
allanite	-	-	x	x	x	-	-	-	-
sphene	-	-	x	x	x	-	-	-	-
zircon	tr	x	x	x	x	x	tr	tr	tr
apatite	tr	x	x	x	x	x	-	-	-
topaz	-	-	-	-	-	-	x	x	x

1. Drum Mountains Rhyodacite
2. Mt. Laird Tuff
3. Crystal tuff member of Joy Tuff
4. Black glass tuff member of Joy Tuff
5. Dell Tuff
6. Needle Range Formation
7. Porphyritic rhyolite member of Spar Mountain Formation
8. Flows and domes of alkali rhyolite, Topaz Mountain Rhyolite
9. Local flows and domes of porphyritic alkali rhyolite, Topaz Mountain Rhyolite

Named the Drum Mountains Rhyodacite for exposures in the Drum Mountains (Lindsey, 1979), the rhyodacite crops out discontinuously around Spor Mountain and is well exposed in the Black Hills, where it is believed to have been erupted from a small central volcano. It is about 240 m thick in the Black Rock Hills and about 150 m thick in the southern part of The Dell. Volcaniclastic sandstone and laharic breccias are interbedded with the lower part of the rhyodacite in the Black Rock Hills. Some dark aphanitic flow rocks were mapped with the more porphyritic rhyodacite near Joy townsite; these are seen under the microscope to have similar petrographic features. Much rhyodacite in the northern Drum Mountains and around Spor Mountain is broken into many blocks about 100-300 m across of diverse orientation; this may reflect shattering of the formation as it subsided into the Thomas caldera. The rhyodacite everywhere unconformably overlies rocks of Paleozoic age, and is overlain by the Mt. Laird Tuff locally, by the Joy Tuff at many localities, and by landslide breccia, Dell Tuff, and the Spor Mountain Formation around Spor Mountain.

The rhyodacite contains an average of 35 percent euhedral phenocrysts of plagioclase and pyroxene as large as 3-4 mm in a groundmass of plagioclase microlites and glass (table 4) (fig. 3). Plagioclase is mainly andesine and labradorite, but sodic rims are common; pyroxene is mainly hypersthene, but lesser amounts of augite are present and pigeonite has been reported (Staatz and Carr, 1964). Euhedral magnetite is abundant, traces of quartz occur at a few localities, and very small amounts of accessory apatite and zircon also occur locally. Along the east side of Spor Mountain, the mafic minerals in the rhyodacite are commonly altered to chlorite and brown hydromica(?).

The texture of the rhyodacite indicates that the phenocrysts were not in equilibrium with the magma at the time of eruption and cooling of the groundmass. Intratelluric crystallization of the phenocrysts evidently proceeded in an andesitic magma; somehow, either by addition of another magma, contamination with wall rocks, or differentiation, the melt became more silicic and alkali-rich than the original magma, so that plagioclase phenocrysts were partially resorbed and overgrown with sodic rims. The interiors of some plagioclase have a sieve texture of holes filled with glass; these may indicate change in composition of the melt or, alternatively, of temperature and pressure. When erupted, the remaining lava cooled quickly to form microlites and glass. Chemical analyses confirm that the groundmass of the rhyodacite is much more silicic (59-63 percent  $\text{SiO}_2$ ) than the phenocrysts would indicate. The modal phenocryst content suggests the rock is a hypersthene andesite, but most chemical analyses show it to be rhyodacite and quartz latite in the classification of Rittmann (1952).



## Diorite

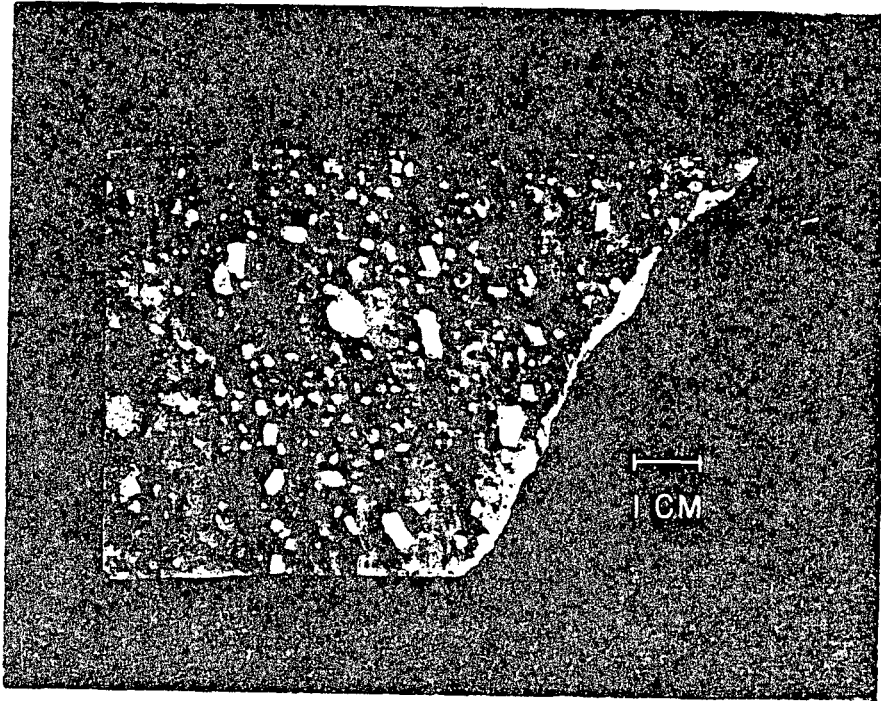
Plugs of diorite crop out in the Drum Mountains 3 km southeast of Joy townsite; they were first mapped by Crittenden, Straczek, and Roberts (1961) as quartz diorite and were examined only briefly by me. Fresh specimens of the rock are dark brown in color, like the Drum Mountains Rhyodacite, but the rock is phaneritic, unlike the aphanitic-porphyrific texture of the rhyodacite. In thin section, the rock is seen to contain about 56 percent elongate, subparallel grains of calcic plagioclase and about 22 percent hornblende that is highly altered. Other minerals include about 7 percent anhedral brown biotite, about 9 percent anhedral potassium feldspar, 5 percent magnetite, and accessory apatite. Although Crittenden, Straczek, and Roberts (1961) called the rock quartz diorite, no quartz could be identified with certainty. The diorite is assigned an Eocene age on the basis of overall compositional similarity to other rocks of that age and on the basis of cross-cutting by dikes considered equivalent to the Mt. Laird Tuff. Crittenden, Straczek, and Roberts and others (1961, pl. 20) mapped dikes of quartz monzonite porphyry cutting the diorite. Reexamination of their quartz monzonite dikes 2-3 km south and southwest of Joy townsite showed them to be nearly identical to the Mt. Laird Tuff. Similar, but hydrothermally altered, dikes cut one diorite plug indicating that the diorite is older than the Mt. Laird Tuff.

## Mt. Laird Tuff

The Mt. Laird Tuff, called plagioclase crystal tuff by Staatz and Carr (1964, p. 78-79), is about 80 m thick in the type area near Mt. Laird in the north-central Drum Mountains. It overlies the Drum Mountains Rhyodacite and is unconformably overlain by the Joy Tuff. The Mt. Laird Tuff has a wide but scattered distribution: it crops out northeast of the Thomas Range, where it overlies rocks of Paleozoic age (Staatz and Carr, 1964), and in the northern part of the Keg Mountains, where it overlies the Keg Spring andesite and latite of Erickson (1963). The formation is more than 500 m thick in the subsurface 2-3 km east and northeast of Topaz Mountain, where drilling has revealed a section consisting of 1) 95 m of ash flow tuff, 2) 62 m of tuffaceous sediments, 3) 75 m of ash-flow tuff, 4) 85 m of tuffaceous sediments, and 5) 199 m of ash-flow tuff to the bottom of the hole (table 5). The drilled section contains three major intervals of ash-flow tuff, and variation in size and type of lithic inclusions within these suggests that each may consist of more than one ash flow. Much of the tuff is partly welded, devitrified and further altered to clay and calcite.

Outcrops of the Mt. Laird Tuff vary from gray to pink to lavender and the tuff can be recognized easily in the field by conspicuous white plagioclase phenocrysts as much as 10 mm long and bronze-colored biotite phenocrysts as much as 5 mm across (fig. 4A). Locally, the Mt. Laird Tuff displays distinct lamination reflected by compacted dark pumice.

Figure 4.--Mt. Laird Tuff. A) Photo showing large euhedral crystals of white plagioclase and dark biotite in a foliated matrix. Sample collected from upper part of Mt. Laird Tuff in SW 1/4 sec. 16, T. 14 S., R. 11 W. B) Photomicrograph of same rock showing crystals of plagioclase (P), oxidized hornblende (H), and biotite (B) in an altered matrix; no vitroclastic texture is evident. Crossed polars. Sample locality same as A. C) Photomicrograph of ash-flow tuff showing broken crystals and vitroclastic texture, from drill core 216 m below surface at SW1/4 NW1/4 sec. 3, T. 13 S., R. 11 W. D) Photo showing core of tuffaceous sandstone and siltstone from 391 m below surface in drill hole at SW1/4 NW1/4 sec. 3, T. 13 S., R. 11 W.; note flame structure, graded bedding (top), and carbonaceous laminae. E) Photo of core showing carbonaceous siltstone and mudstone with mud chips and matrix-supported conglomerate of mudflow origin (right core). Left core is from 401 m below surface; right core is from 334 m; both from same drill hole as D). F) Probable vent breccia in the Mt. Laird Tuff northwest of Joy Townsite, NE1/4 sec. 21, T. 14 S., R. 11 W.



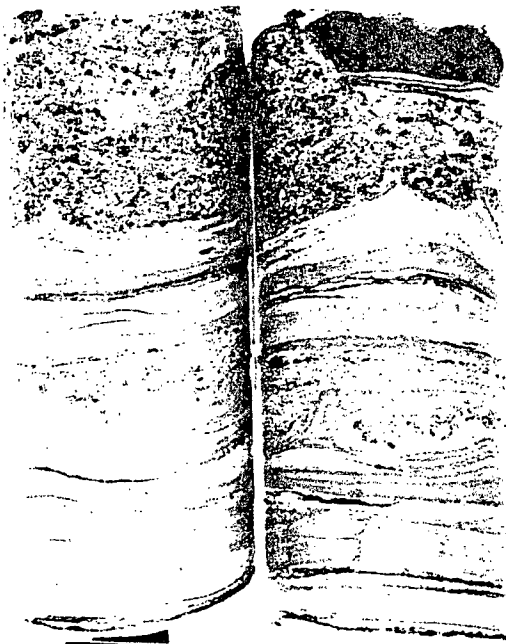
A.



B.



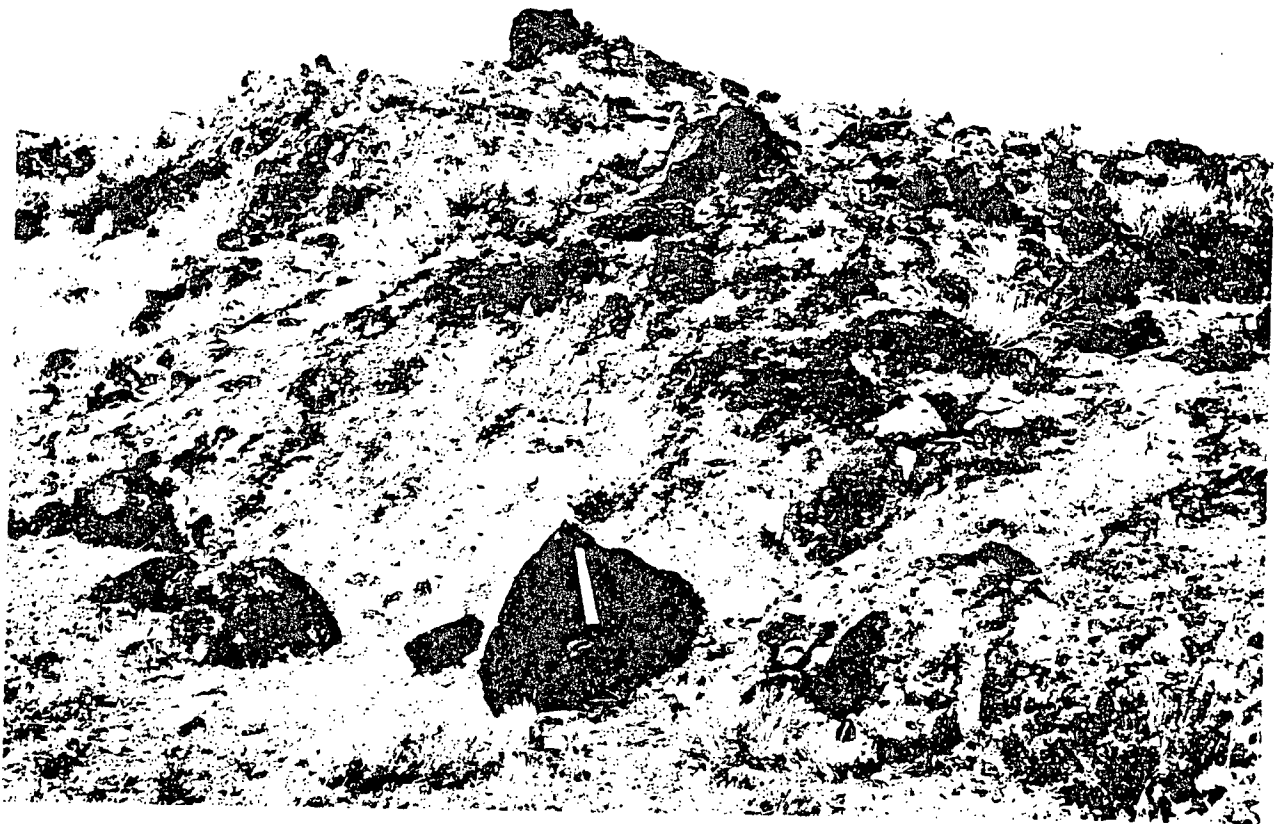
C.



D



E



F

Table 5.--Section of Mt. Laird Tuff in drill hole east of Topaz Mountain. Taken from log by Charles Beverly of hole 7 drilled for Bendix Field Engineering, revised after study of core and thin sections. Location of drillhole is SW 1/4 NW 1/4 sec. 3, T. 13 S., R. 11 W. Ground elevation, 1,669 m (5,475 ft); total depth, 608 m (1,995 ft)

Top of unit, meters below surface	Formation name	Description of core and thin sections
0	Topaz Mountain Rhyolite	Crystal-poor alkali rhyolite flow.
70	Joy Tuff; crystal tuff member	Crystal-rich (quartz, sanidine, biotite, and plagioclase) rhyolitic welded ash-flow tuff.
90	Mt. Laird Tuff (top approximate)	Crystal-rich (plagioclase, biotite, hornblende) quartz latitic welded ash-flow tuff. Thin sections at 98 m show glassy, perlitic matrix; at 152 m, matrix is devitrified and crystals are euhedral and mostly unbroken. At 158 m, matrix is devitrified but contains relict pumice, and broken crystals are common.
185		Fault (?) breccia.
187		Tuffaceous sediments of probable lacustrine origin include carbonaceous laminated mudstone, siltstone, sandstone, and minor conglomerate. Ash-flow tuff interbedded with sediments below 239 m. Thin sections at 202 m are of tuffaceous sandstone containing altered pumice, plagioclase, biotite, quartz, and lithic fragments of rhyodacite, tuffaceous siltstone, quartzite, and carbonate rock; all fragments are angular. At 210 m, same as at 202 m but with birefringent clay or sericite. At 240 m, unwelded ash-flow tuff containing broken plagioclase, biotite, quartz, hornblende altered to calcite, and altered pumice. Lithic fragments of flow rock.

Mt. Laird Tuff--cont.

- 249 Crystal-rich (plagioclase, biotite, quartz, and hornblende), latitic ash-flow tuff with abundant lithic fragments of carbonate rock and volcanic rocks to 292 m and below 305 m. Minor to no welding. Thin sections at 277 m and 306 m contain many broken crystals, relict pumice, and an altered matrix.
- 324 Tuffaceous sediments of probable lacustrine origin include black laminated carbonaceous mudstone with pyrite, siltstone, sandstone, minor conglomerate and some interbedded ash-flow tuff. Sediments contain abundant graded bedding, flame structure, mud chips, and cross-lamination. Thin sections at 335 and 392 m contain abundant angular quartz, plagioclase, biotite, carbonate rock, and altered volcanic rock fragments.
- 409 Crystal-rich (plagioclase, biotite, altered hornblende) quartz latitic welded ash-flow tuff. Large lithic clasts to 433 m. Thin sections at 514 m show crystals to be euhedral and unbroken but accompanied by relict pumice in a devitrified matrix. At 575 m, many crystals are broken and large resorbed quartz crystals are common.
- 608 Bottom of hole.

As seen under the microscope, the tuff contains 9-29 percent plagioclase, 1-5 percent red-brown biotite, and as much as 11 percent hornblende and 5 percent pyroxene (table 4) (fig. 4B). Crystals in the upper part of the Mt. Laird are remarkably euhedral and unbroken for an ash-flow tuff, and it is possible that this rock, with no preserved vitroclastic texture, may be flow rock instead of tuff. Broken crystals and relict pumice and shards are common in the rest of the tuff (fig. 4C). Northeast of the Thomas Range, the tuff differs from the type area in that it contains conspicuous quartz. Plagioclase (labradorite) in the Mt. Laird Tuff is typically zoned; some is euhedral but other crystals have sieve texture and rounded, resorbed boundaries with zones and overgrowths that follow these boundaries. Hornblende is partly to completely altered to iron oxide minerals and, locally, plagioclase is altered to chlorite and sericite. Accessory magnetite and traces of apatite and colorless zircon are present. The groundmass of the tuff near Joy townsite contains abundant plagioclase microlites and small hornblende crystals that are altered to iron oxide minerals; all are set in a matrix that was probably glassy, but evidence of vitroclastic texture has been destroyed by alteration.

Study of core and thin sections from drill holes (table 5) that penetrated the Mt. Laird Tuff east of Topaz Mountain confirms the abundance of ash-flow tuff in the formation. Only the upper 70 m contains large, euhedral crystals with little or no vitroclastic texture preserved. The matrix is perlitic glass at 8 m, but completely devitrified at 62 m below the top of the Mt. Laird Tuff. The latter resembles the upper part of the Mt. Laird 3-4 km northwest of the type locality. Perhaps the uppermost part of the Mt. Laird is a flow, but more likely it formed by eruption of a very hot, viscous ash flow. Below the top 70 m of Mt. Laird Tuff the drilled section contains much ash-flow tuff distinguished by broken crystals and relict pumice and shards (fig. 4C). At 485 m below the top of the tuff, near the bottom of the drill hole, large crystals of resorbed quartz are common, as is also the case in tuff northeast of the Thomas Range.

Two intervals of tuffaceous sediments are interbedded with the Mt. Laird Tuff in the subsurface east of Topaz Mountain (table 5). The sediments contain laminated carbonaceous mudstone, siltstone, sandstone, and conglomerate (figs. 4D, E) derived mainly from the Mt. Laird ash flows and Drum Mountains Rhyodacite. The sediments contain abundant graded bedding, flame structures, mud chips, and cross lamination; conglomerates are matrix supported, indicating a mud-flow origin. Such features, taken together, indicate rapid sedimentation. Mudstones contain small amounts of organic carbon and pyrite indicating that they may have been deposited in stagnant water. The Mt. Laird sediments were probably deposited in a lake that formed during eruption of the Mt. Laird Tuff and attendant cauldron subsidence.

Some features of the Mt. Laird Tuff indicate that it was erupted from the vicinity of Mt. Laird in the Drum Mountains. At the type locality and also 3-4 km northwest of Mt. Laird, the lower part of the

tuff contains a distinctive breccia of abundant large (30 cm) pumiceous tuff clasts in a similar matrix (fig. 4F). Such monolithologic breccias may represent fallback into the vent during eruption. Alternatively, the breccia could result from collapse of earlier-formed ash-flow sheets during eruption. Kaolinitic and pyritic altered areas, now oxidized, occur at the surface in tuff on the north side of Mt. Laird; these may represent post-eruption alteration by fluids from the magma of the Mt. Laird Tuff.

An area of porphyry intrusion and mineralization in the Detroit mining district of the Drum Mountains may be part of the Mt. Laird magma chamber that did not collapse, or may represent resurgence and shallow intrusion of the Mt. Laird magma after eruption of the tuff. Small dikes and plugs of porphyritic rock, mapped as quartz monzonite porphyry by Crittenden, Straczek, and Roberts (1961), are very similar to the Mt. Laird Tuff. Most intrude rocks of Cambrian and Precambrian age, but one dike intrudes a diorite plug of probable Eocene age. The westernmost group of dikes retain most of their original plagioclase phenocrysts, but mafic minerals and matrix have been hydrothermally altered. The eastern group contains only relict textures of feldspar and biotite phenocrysts. Study of X-ray diffraction patterns and thin sections show that the eastern intrusions are altered to quartz, kaolinite, well-crystallized sericite and minor pyrophyllite; such alteration is typical of the phyllic zone of the Lowell and Gilbert porphyry copper model (Hollister, 1978). The easternmost plug contains a stockwork filled with jarosite and is partly surrounded by quartzite pebble breccias derived from the country rock of Prospect Mountain Quartzite. The intrusions of porphyritic rock are believed to be apophyses from a buried pluton (Stalker, cited in Newell, 1971) that is the uncollapsed or resurgent portion of the magma chamber of the Mt. Laird Tuff. The area of porphyry intrusion and mineralization is only 4-6 km south of the probable vent breccias of the Mt. Laird Tuff, and the original mineralogy of the porphyry so closely matches that of the tuff that the two are considered to have been derived from the same magma.

#### Joy Tuff

The Joy Tuff was named for excellent exposures in hills 3-5 km northwest of Joy townsite in the Drum Mountains (Lindsey, 1979). The tuff consists of two members: a lower crystal tuff member about 180 m thick and an upper black glass tuff member about 30 m thick. In the type area, the lower crystal tuff member overlies the Mt. Laird Tuff and the Drum Mountains Rhyodacite along angular unconformity B. The black glass tuff member is present only in the northeastern part of the Drum Mountains and southeast of Topaz Mountain; it overlies the crystal tuff member.

Crystal tuff member--The crystal tuff member of the Joy Tuff extends from Fish Springs Flat to the east side of Desert Mountain, a distance of 60 km (fig. 1). It is well exposed in the Joy graben (fig. 5A), where it is 180 m thick in hills northwest of Joy Townsite and 70 m



Figure 5.--Crystal tuff member of Joy Tuff. A) Photo showing section of crystal tuff in the type locality (sec. 22, T. 14 S., R. 11 W.), B) photo showing compacted black pumice in lower 10 m of tuff (sec. 29, T. 13 S., R. 11 W.), C) photo of probable vent breccia of crystal tuff fragments in welded matrix of the same, D) photomicrograph showing broken crystals of quartz and sanidine with lesser plagioclase (P) and biotite (B), and E) photomicrograph of cognate inclusion (left half of photo) with abundant sphene (S). Crossed polars. Photomicrographs of sample from Searle Canyon (sec. 5, T. 13 S., R. 11 W.).

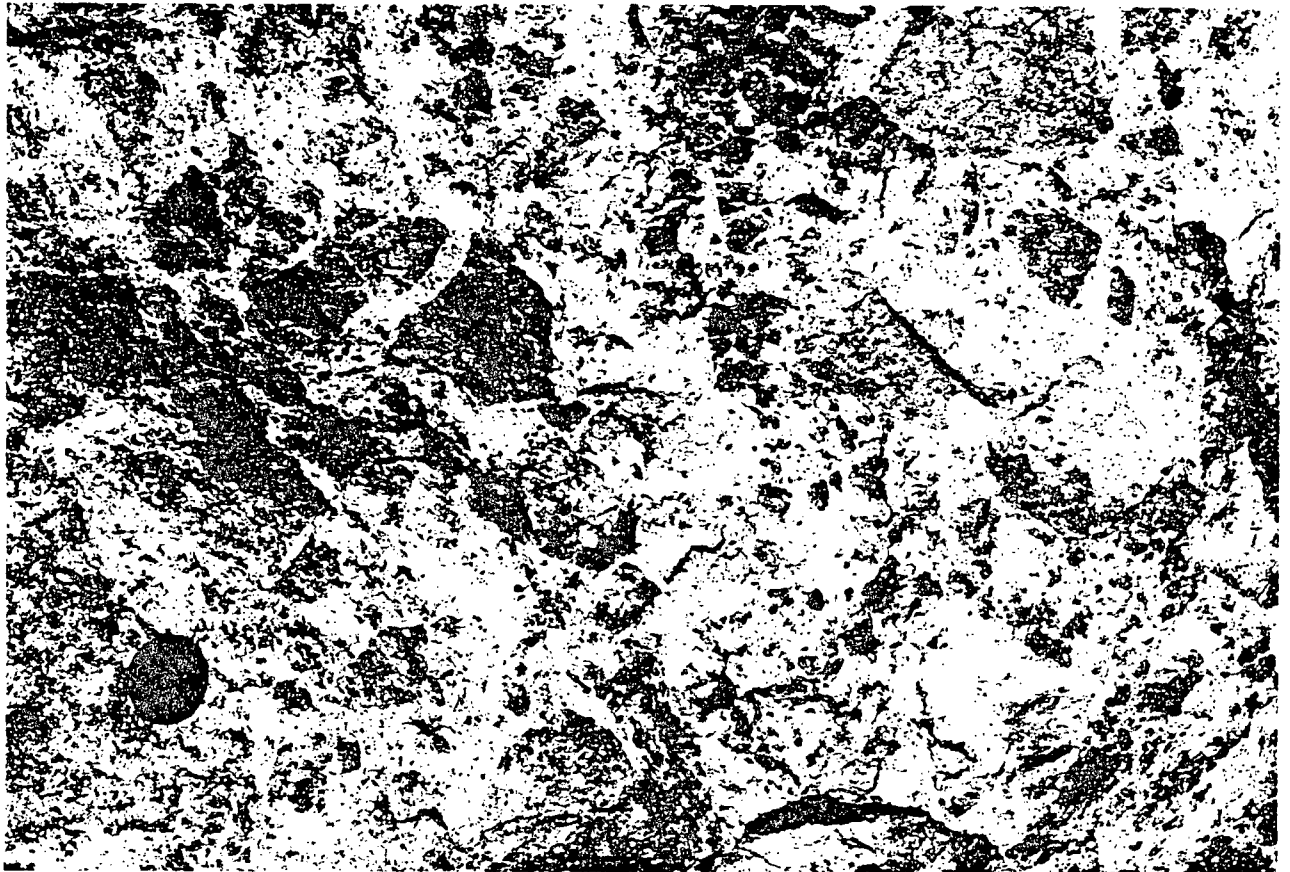


A



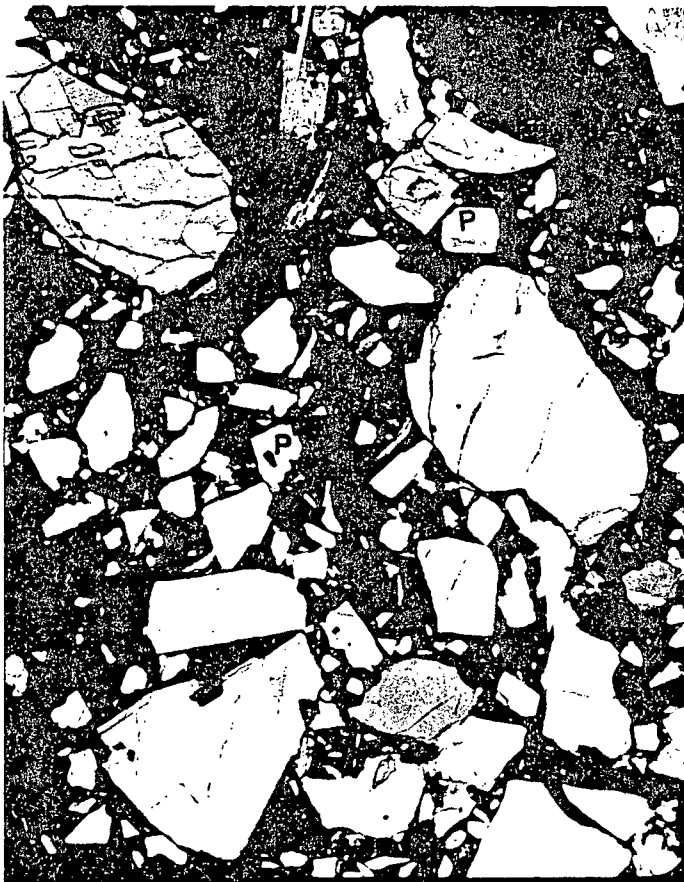
B

22a



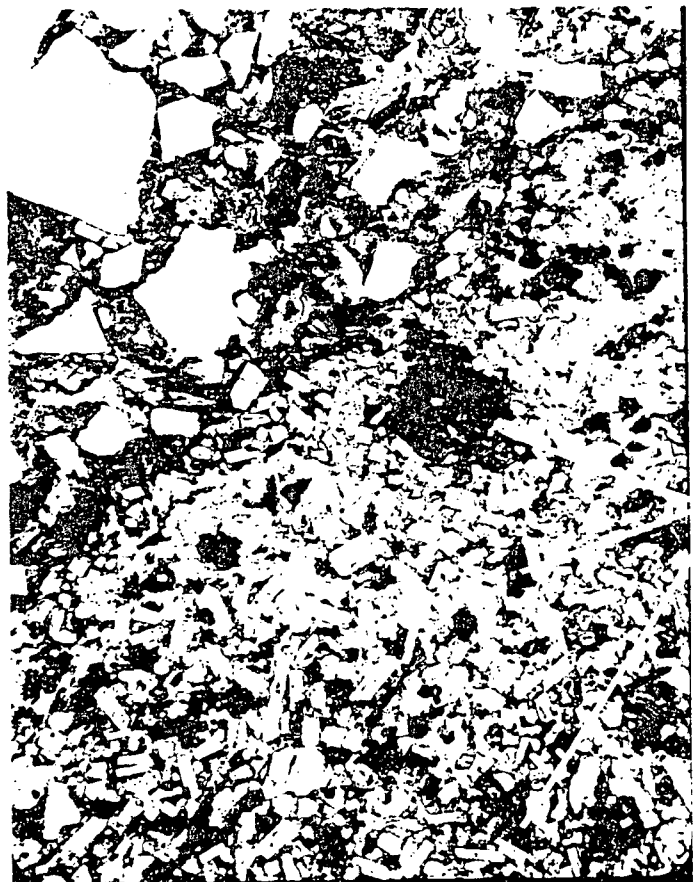
C.

B



D.

0 1 mm.



E.

0 1 mm.

thick on the south side of Topaz Mountain, in the Picture Rock Hills of the southwestern Keg Mountains, where it is about 150-200 m thick, and on the east side of Desert Mountain (fig. 1). Locally, the lowermost 10 m contains abundant compacted black pumice fragments (fig. 5B); the degree of welding and amount of black pumice decrease upward. Sections of the tuff in cliffs northwest of Joy townsite have a distinct parting that may be a partial cooling break within a compound cooling unit (fig. 5A). No compositional zoning of the crystal tuff is evident.

The source of the Joy Tuff is believed to be the Dugway Valley cauldron, which is located generally east of Topaz Mountain and perhaps in the subsurface northeast of Topaz Mountain. The tuff east of Topaz Mountain is strongly welded and contains steeply dipping (60-90°) foliation of somewhat variable northeasterly strike, in contrast to the more friable and less-welded tuff with gentle dips in the Joy graben. Monolithologic tuff breccia with unrotated and slightly rotated clasts in a welded matrix occurs east of Topaz Mountain (fig. 5C), and similar breccia was encountered in drill holes that penetrated the tuff 3 and 5 km north of Topaz Mountain. One small outcrop of crystal tuff in the northeast Drum Mountains has near-vertical foliation. Such welded tuff breccia and tuff with steep foliation may indicate vents; possibly, the north-south distribution of such occurrences along faults may indicate a system of eruption fissures. Alternatively, it is possible that the tuff breccias formed by collapse of the ash-flow into the cauldron during eruption. Such might be the explanation for large areas of steeply dipping foliation in the tuff; these could be large blocks that fell into the cauldron.

The crystal tuff member ranges from gray to reddish brown in outcrop; it contains abundant broken crystals of sanidine, quartz, and lesser quantities of plagioclase (oligoclase-andesine) brown biotite and euhedral magnetite (table 4) (fig. 5D). The crystals reach as much as 4 mm across and comprise an average of about 65 percent of the tuff. Sphene, apatite, allanite, and colorless zircon occur as accessory minerals, but large euhedral crystals of sphene are so abundant and conspicuous that they can be seen in some hand specimens. Abundant sphene and the darker, more compact appearance of outcrops are the most reliable characteristics that can be used to distinguish the Joy Tuff from the Dell Tuff, which it resembles closely. The matrix of the Joy Tuff consists of welded shards that have been devitrified and altered to potassium feldspar and cristobalite. Accidental inclusions of the Drum Mountains Rhyodacite occur in the crystal tuff member east of Topaz Mountain, and distinctive cognate inclusions consisting of normally zoned plagioclase, brown biotite, sphene and interstitial glass occur in the tuff at the head of Searle Canyon (fig. 5E). The cognate inclusions contain smaller, unbroken phenocrysts, in contrast to the tuff, and evidently represent an early stage of crystallization of the Joy Tuff within the magma chamber. Chemical analyses show that the crystal tuff member has a rhyolitic composition.

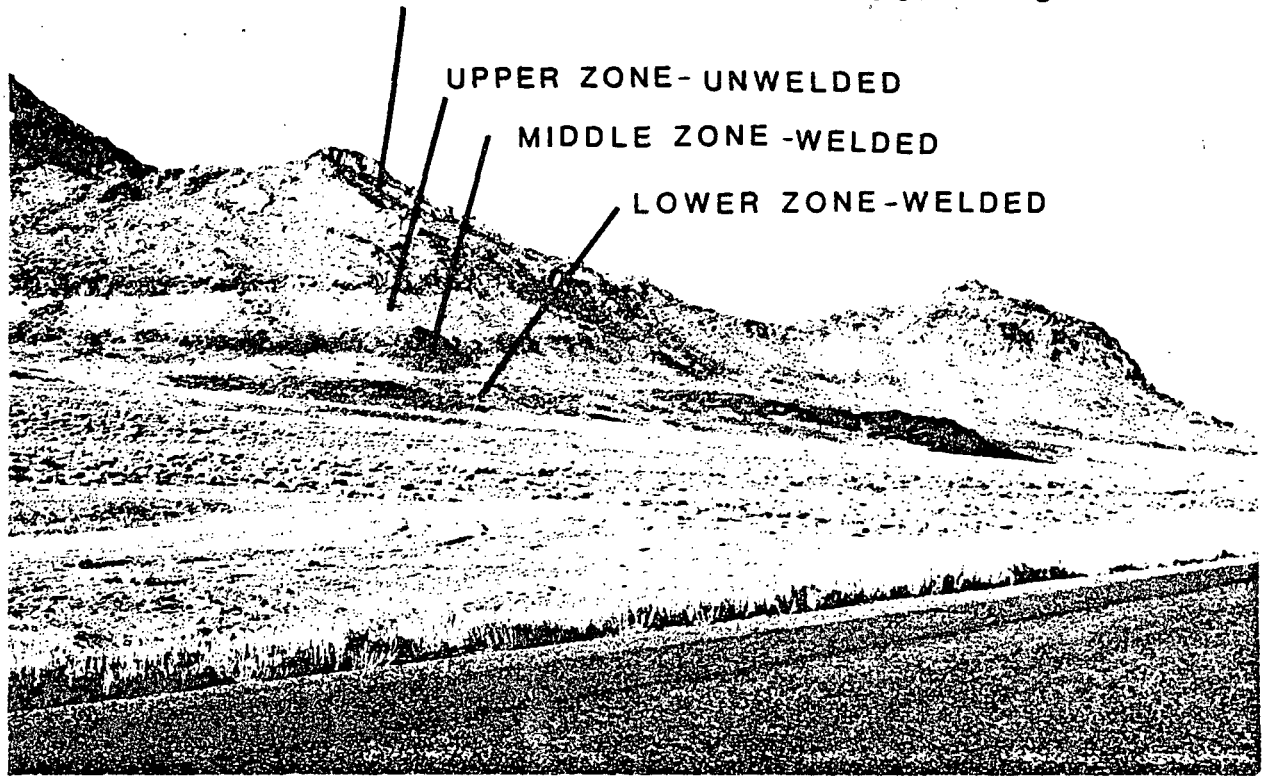
Black glass tuff member--The upper member of the Joy Tuff is a simple cooling unit of ash-flow tuff. It consists of three zones that reflect differing degrees of welding (fig. 6A): a densely welded lower zone consisting almost entirely of black glassy pumice, a partly welded middle zone of gray glassy tuff with locally abundant compacted black pumice (fig. 6B), and an upper zone of unwelded tan glassy tuff. At some localities the welded zones are more readily divisible into a lower black glassy zone and an upper gray-brown devitrified zone; both are overlain by unwelded tan tuff. The tuff crops out east of Topaz Mountain (Staatz and Carr, 1964, p. 84) and in the northeastern Drum Mountains. A section about 30 m thick is well exposed in sec. 36, T. 13 S., R. 11 W., where all three of the welding zones occur in approximately equal thickness, and where the tuff is overlain by a landslide of Tertiary age. The limited local extent of the black glass tuff, together with its small thickness and densely welded lower zone, indicate that it was a local, hot ash flow erupted from the Dugway Valley cauldron.

The black glass tuff contains an average of only 13 percent small inconspicuous crystals of quartz, sanidine, zoned plagioclase, brown biotite, and magnetite (table 4) (fig. 6C). Sphene is a conspicuous accessory mineral, as it is in the underlying crystal tuff member. Accidental inclusions of the crystal tuff, Mt. Laird Tuff, Drum Mountains Rhyodacite, and Paleozoic rocks are common in all zones. Glass shards and pumice comprise the rest of the tuff; these are highly compacted and deformed in the welded zones (figs. 6B and 6C), but uncompact, porous and partly altered to clinoptilolite in the upper, unwelded zone.

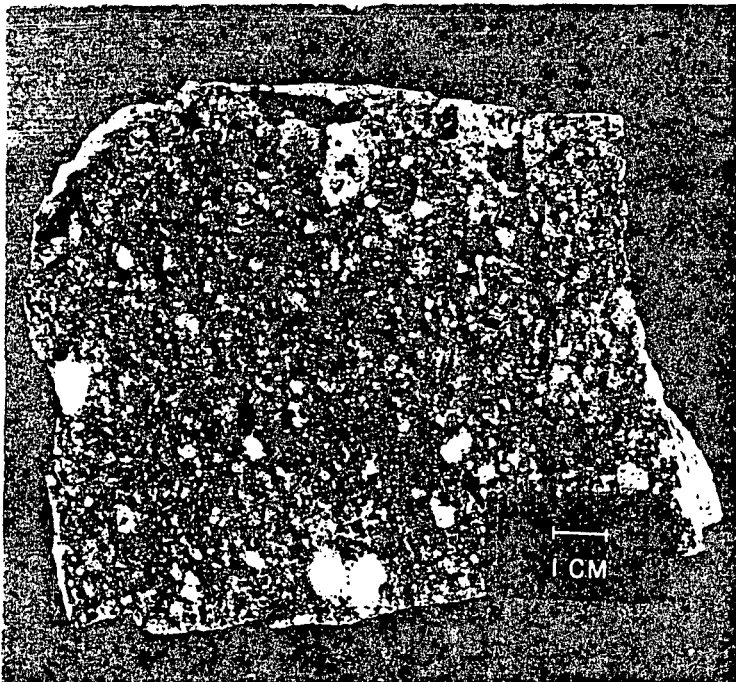
The correct stratigraphic assignment of the upper, unwelded zone of the black glass tuff is critical to the age of the overlying landslide megabreccias and their role in the volcanic and tectonic history of the area. The unwelded zone resembles tuff that is interbedded with younger rhyolite flows, and was mapped as water-laid tuff of the youngest volcanic group by Shawe (1964) and Newell (1971). The unwelded zone is not clearly stratified, however, and its contact with the underlying welded zone is conformable and sharply gradational. Chemical analyses show the composition of the unwelded zone to be consistent with leached tuff that had the same composition as the underlying welded zones. Stratified tuffs interbedded with young alkali rhyolite have a distinct trace element signature comprised of anomalous Be, Li, Nb, U, Th, and Y that is not present in any of the black glass tuff, including the upper, unwelded tuff. The unwelded zone has been partly altered to clinoptilolite and leached of alkali and alkaline earth elements, and perhaps some trace elements, but such leaching does not remove the distinctive trace element signature of the younger tuffs (Lindsey, 1975).

Figure 6.--Black glass tuff member of Joy Tuff. A) Photo showing zones of welding in the type locality of the black glass tuff, ranging from the densely welded, black lower zone, the partly welded middle zone, to the unwelded upper zone. Also shown is the landslide megabreccia of the northern Drum Mountains, which overlies the unwelded zone of the black glass tuff. B) Photo of specimen of partly welded middle zone, showing compacted black pumice, and C) photomicrograph showing glassy shards and pumice (P) and accidental inclusions (I) of rhyodacite in middle zone. Crossed polars. Samples B and C from outcrop in secs. 25 and 26, T. 13 S., R. 11 W.

MEGABRECCIA OF DRUM MOUNTAINS



A.



B.



C.

## Landslide breccias

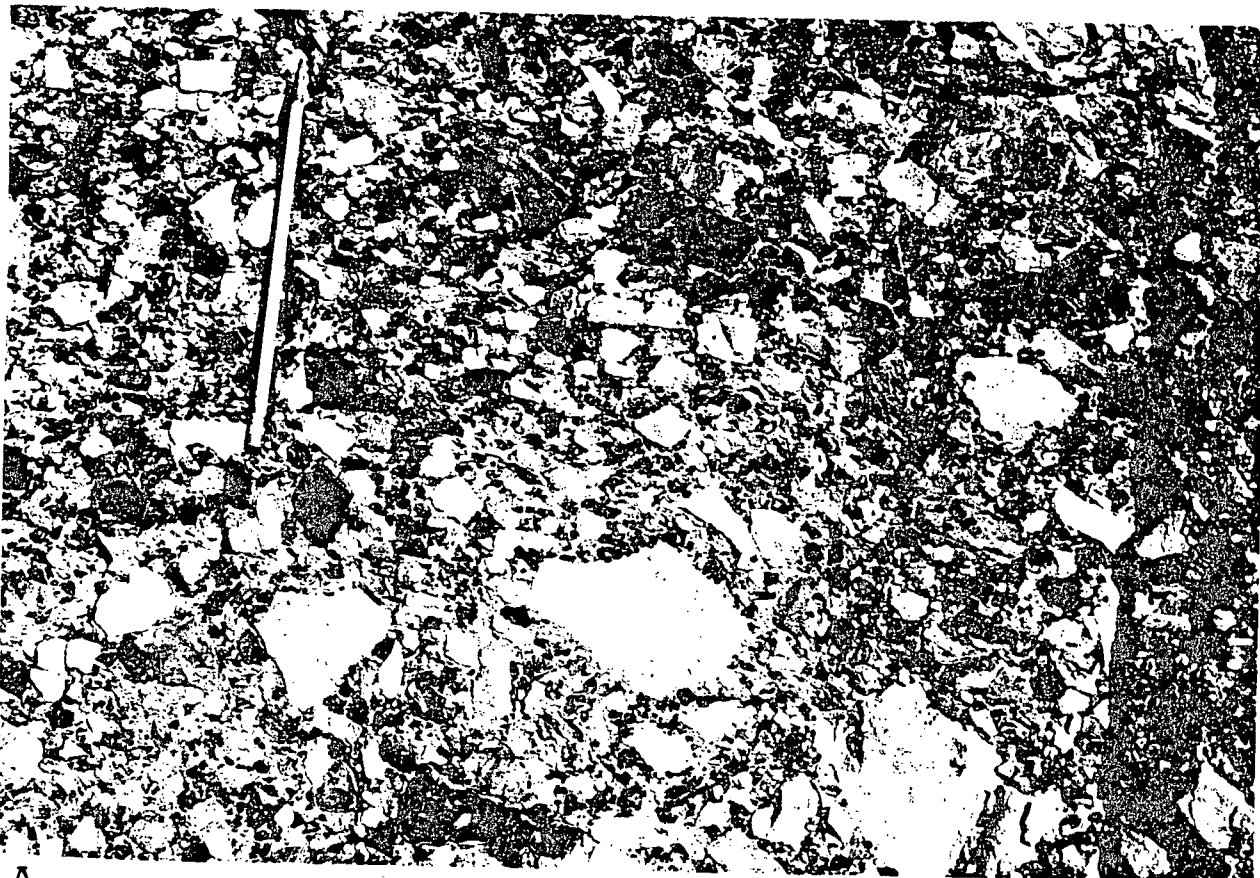
Large masses of breccia interpreted by me as landslide deposits and related debris flows occur at Spor Mountain and in the northeastern part of the Drum Mountains; they are associated with the time of ash flow eruption and probably record collapse of caldera walls. The breccias were mapped as three lithologically and geographically distinct informal units: breccia at Spor Mountain, breccia at Wildhorse Spring, and megabreccia of the northern Drum Mountains.

Breccia at Spor Mountain and breccia at Wildhorse Spring--These are discussed together because they are spatially and genetically associated. The breccia at Spor Mountain consists of angular clasts of Paleozoic rocks as large as 1 m across in a matrix of the same material (fig. 7A). Breccia at Wildhorse Spring contains subrounded clasts (<0.5 m) of Paleozoic rocks and rhyodacite in a matrix of pulverized rhyodacite (fig. 7B). The two units are associated locally but can be distinguished readily in the field. The breccia at Spor Mountain overlies the Drum Mountains Rhyodacite along the east side of Spor Mountain and overlies the breccia at Wildhorse Spring 1 km southwest of that locality (fig. 7C). The breccia at Spor Mountain is overlain by the Dell Tuff in the northern part of The Dell and probably west of the Yellow Chief mine, although relations at the latter locality may be complicated by faulting. Thus stratigraphic relationships indicate that the age of the breccias is between 42 and 32 m.y., the ages of the rhyodacite and Dell Tuff, respectively (table 2).

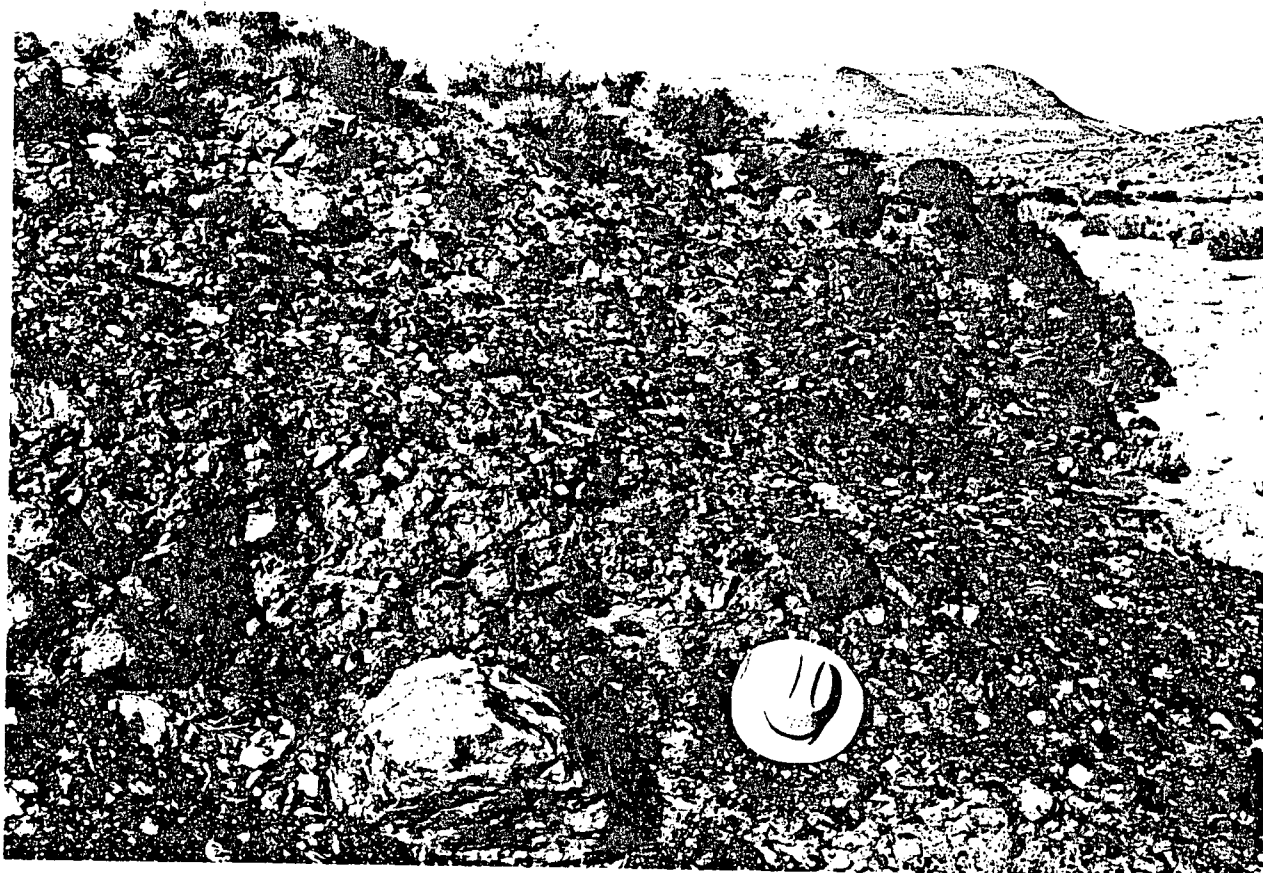
The breccias have long been considered to be of intrusive origin (Staatz and Carr, 1964, p. 85), but new evidence presented here indicates that they formed from landslides and related debris flows along a steep escarpment that followed the present north and east sides of Spor Mountain. Three types of evidence support my view that the breccias are landslide deposits: (1) The breccia at Spor Mountain contains rotated and mixed clasts of dolomite, limestone, and Swan Peak Quartzite in a nonigneous matrix (fig. 7A); it can be traced continuously westward from the east side of Spor Mountain to monolithologic dolomite breccia having healed fractures between unrotated and slightly rotated fragments (fig. 7D). Both of these facies were mapped as breccia at Spor Mountain (Lindsey, 1979). The monolithologic dolomite breccia retains the original stratigraphy of the Paleozoic rocks and resembles the "crackle breccia" of Tertiary landslides in Arizona described by Krieger (1977). All stages of brecciation from bedded but fractured dolomite to breccia of mixed Paleozoic lithologies are present in a small area about 2 km north-south and less than 0.3 km east-west that extends along the east side of the crest of Spor Mountain; I interpret this area as the breakaway zone for a landslide. (2) Both the breccias at Spor Mountain and at Wildhorse Spring are for the most part massive and unsorted, but they are faintly bedded locally, and the contact between the breccias southwest of Wildhorse Spring is distinctly bedded (fig. 7C). Massive structure and clasts of mixed lithology, set in abundant fine material, indicate



Figure 7.--Landslide breccia. A) Photo of breccia at Spor Mountain, showing clasts of mixed lithologies derived from rocks of early Paleozoic age on Spor Mountain (sec. 27, T. 12 S., R. 12 W.). B) Photo of breccia at Wildhorse Spring showing large clasts of rhyodacite and Paleozoic rocks in a matrix of pulverized rhyodacite (sec. 15, T. 12 S., R. 12 W.). C) Photo of the contact between breccia at Wildhorse Spring and overlying breccia at Spor Mountain, which contains clasts 1 m in diameter. Note layering defined by concentration of clasts along the contact between breccias, above map case and pick (sec. 16, T. 12 S., R. 12 W.). D) Photo of breccia at Spor Mountain showing monolithologic crackle breccia of dark dolomite in the breakaway zone (sec. 27, T. 12 S., R. 12 W.).



A.



B.



C.



D.

turbulent mass transport, but bedding in the breccias indicates a transport mechanism capable of incomplete sorting of fragments. Massive breccias may represent landslides which moved when on steep slopes or when saturated by moisture, and faintly bedded breccias may represent water-saturated debris flows deposited during heavy rainfall. (3) Only Paleozoic rocks are present as clasts and matrix of the breccia at Spor Mountain; Paleozoic rocks and rhyodacite are both present as clasts and matrix of the breccia at Wildhorse Spring; nowhere is an igneous matrix other than fragments of rhyodacite present. A few areas of breccia occur in small plugs of intrusive alkali rhyolite on Spor Mountain, such as above the Lost Sheep mine, but these are related to later faulting and to intrusion of the rhyolite.

The breccias at Spor Mountain were formed by sliding and flowage off a northerly trending break-away zone on Spor Mountain, west of Eagle Rock Ridge; the slides travelled east and northeast over a valley floor covered by rhyodacite. Somewhat similar breccias form by collapse of caldera walls (Lipman, 1976), by landsliding along upthrown fault blocks (Krieger, 1977), and by sliding along scarps of erosional origin (Shreve, 1968); the geologic environment of ash-flow eruption and cauldron collapse in the Thomas Range favors an origin by collapse of caldera walls. The breccia at Spor Mountain probably began moving as coherent masses (fractured and brecciated dolomite) which disintegrated into landslides (breccia with rotated clasts of mixed lower Paleozoic lithologies) and debris flows during heavy rainfall. Where slides and debris flows travelled over rhyodacite, they incorporated rhyodacite detritus into them, forming the breccia at Wildhorse Spring. Evidently, the two most important agents responsible for formation of the breccias were steep scarps and abundant moisture. There is no reason to believe that the slides travelled on a cushion of air, as was concluded in the case of the Blackhawk slide described by Shreve (1968), in part because the total distance travelled was probably not more than 5 km. Localization of sliding and flowage along north- and northwest-trending scarps that follow the Dell fault system suggests that these faults originated during times of ash flow eruption and cauldron collapse 42 to 32 m.y. ago, even though the faults now displace rocks as young as 21 m.y. old.

Megabreccia of the northern Drum Mountains--This megabreccia overlies the upper, unwelded zone of the black glass tuff member of the Joy Tuff over an area of about 5 km<sup>2</sup> (fig. 6A). It occurs as more or less coherently bedded slabs, some hundreds of meters across in size, of Cambrian limestone and dolomite; locally, the slabs exhibit large-scale contortion (fig. 6A) and intense brecciation. Breccia zones have been thoroughly recemented with fine particles of Cambrian rocks. The underlying tuff has not been appreciably disturbed. A breakaway zone may be preserved along the east side of the north-central Drum Mountains, where small amounts of breccia crop out in an upthrown fault block of Cambrian rocks that contain the same formations as the breccia.

The megabreccia of the Drum Mountains was first identified as a late Tertiary gravity slide (Shawe, 1964) and later as a Quaternary landslide (Newell, 1971). According to both interpretations, the megabreccia overlay water-laid tuff of the youngest volcanic group. The tuff is considered by me to be the upper unwelded zone of the black glass tuff member of the Joy Tuff, thus permitting the megabreccia to be as old as 37 m.y. and within the age range of the breccia at Spor Mountain and Wildhorse Spring. The top of the tuff is nearly flat and has not been eroded; thus sliding must have taken place soon after deposition of the tuff so that it was protected from erosion.

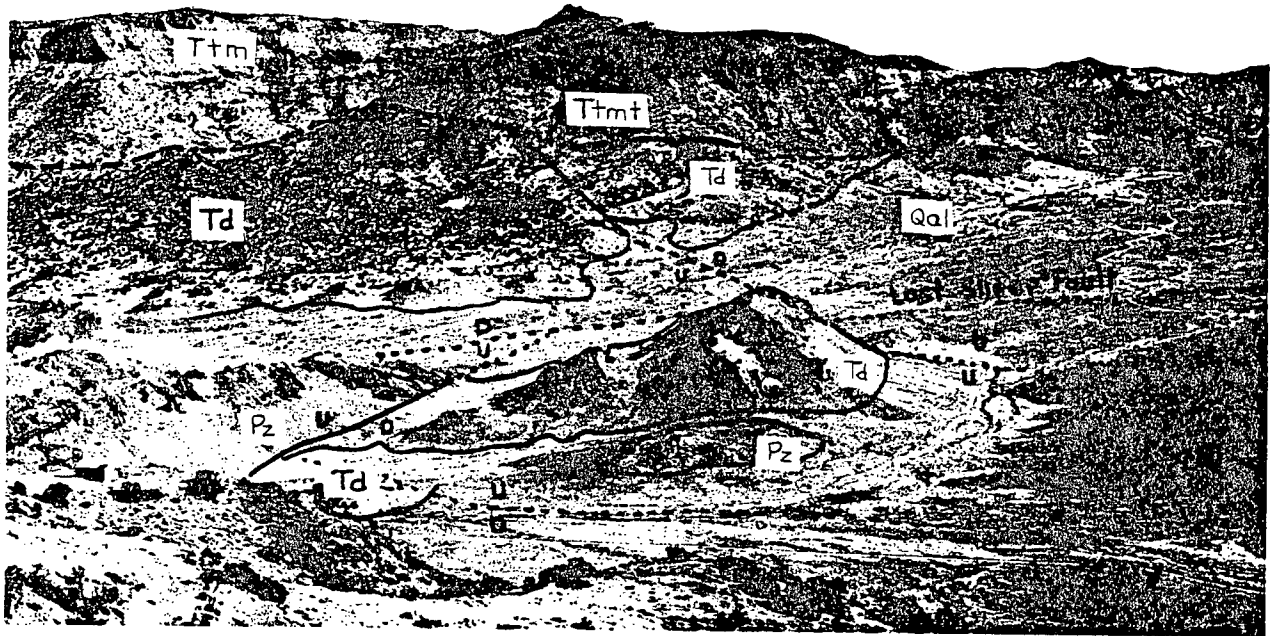
#### Dell Tuff

The name Dell Tuff was given (Lindsey, 1979) to slightly welded gray to pink rhyolitic ash-flow tuff that crops out extensively in The Dell; the tuff appears to be a simple cooling unit. A section about 180 m thick is exposed at the north end of The Dell (fig. 8A). The Dell Tuff unconformably overlies the Drum Mountains Rhyodacite and landslide breccia at Spor Mountain and is unconformably overlain by tuffaceous sandstone of the beryllium tuff member at the Yellow Chief mine, by the beryllium tuff and porphyritic rhyolite members of the Spor Mountain Formation elsewhere in The Dell, and by the Topaz Mountain Rhyolite at the north end of The Dell. As much as 200 m of Dell Tuff crops out northeast of Keg Pass in the Keg Mountains. There, it unconformably overlies the Keg Spring Andesite and latite of Erickson (1963) and the Mt. Laird Tuff, and is unconformably overlain by stratified tuff and alkali rhyolite of the Topaz Mountain Rhyolite.

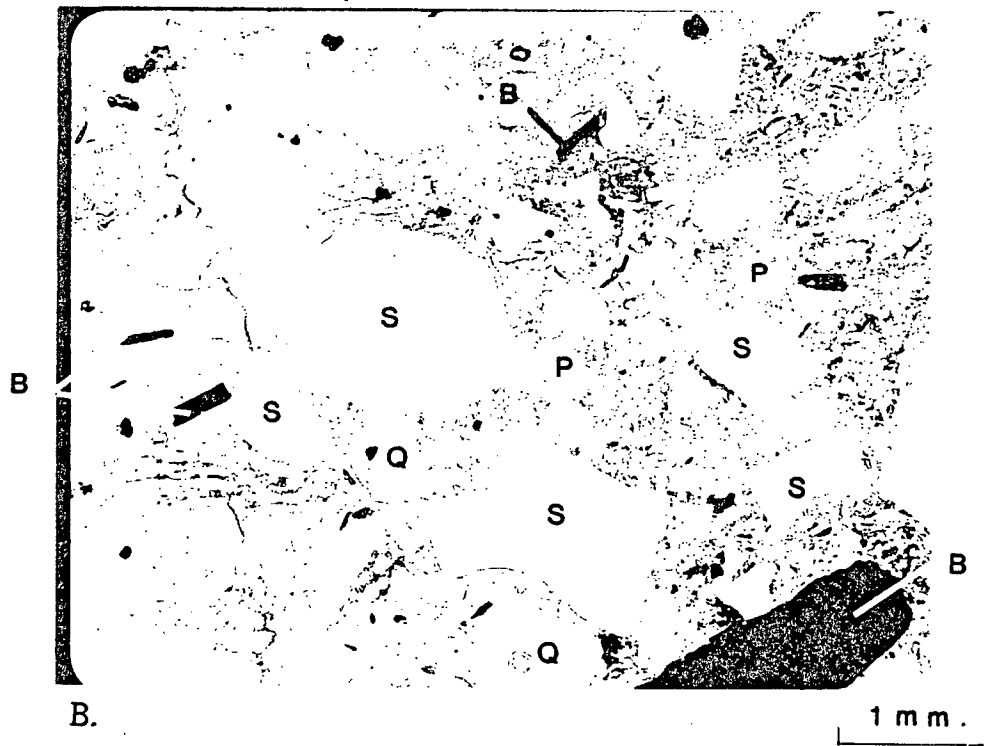
The source of the Dell Tuff has not been located. The tuff is limited to the Thomas Range and Keg Mountains, indicating that the source should be within or near these ranges. Intrusive rocks of about the same age and composition as the Dell Tuff occur as dikes in the Keg Mountains and in the granite facies of the stock of Desert Mountain.

The Dell Tuff was called quartz-sanidine crystal tuff by Staatz and Carr (1964, p. 80-81) because it contains large (>5 mm) euhedral crystals of quartz and sanidine and lesser amounts of plagioclase and brown biotite (fig. 8B). The tuff contains an average of 52 percent crystals (table 4). Minor euhedral magnetite and accessory allanite, sphene, apatite, and colorless zircon are present, also. The matrix consists of white pumice and shards that are only slightly welded. Tuff along the east side of The Dell and at Keg Pass is so poorly indurated that exposures weather to loose crystals in soft, ashy soil. Pumice and shards show both vapor phase crystallization and devitrification textures, but hydrothermal fluids have partially altered some of the tuff to smectite and sericite and introduced minor amounts of fluorite. Chemical analyses show that the tuff has a rhyolitic composition.

Figure 8.--A) Photo of the type locality of the Dell Tuff, north end of The Dell (secs. 23 and 24, T. 12 S., R. 12 W.), showing Topaz Mountain Rhyolite unconformably overlying faulted Dell Tuff. Ttm, Topaz Mountain Rhyolite; Ttmt, stratified tuff in Topaz Mountain Rhyolite; Td, Dell Tuff; Tls, breccia at Spor Mountain; Pz = Paleozoic rocks. B) Photomicrograph of the Dell Tuff, showing vitroclastic texture of devitrified shards and abundant crystals of quartz (Q), sanidine (S), plagioclase (P), and biotite (B). Plain light. Sample from SE1/4 sec. 2, T. 13 S., R. 12 W.



A.



B.

## Needles Range Formation

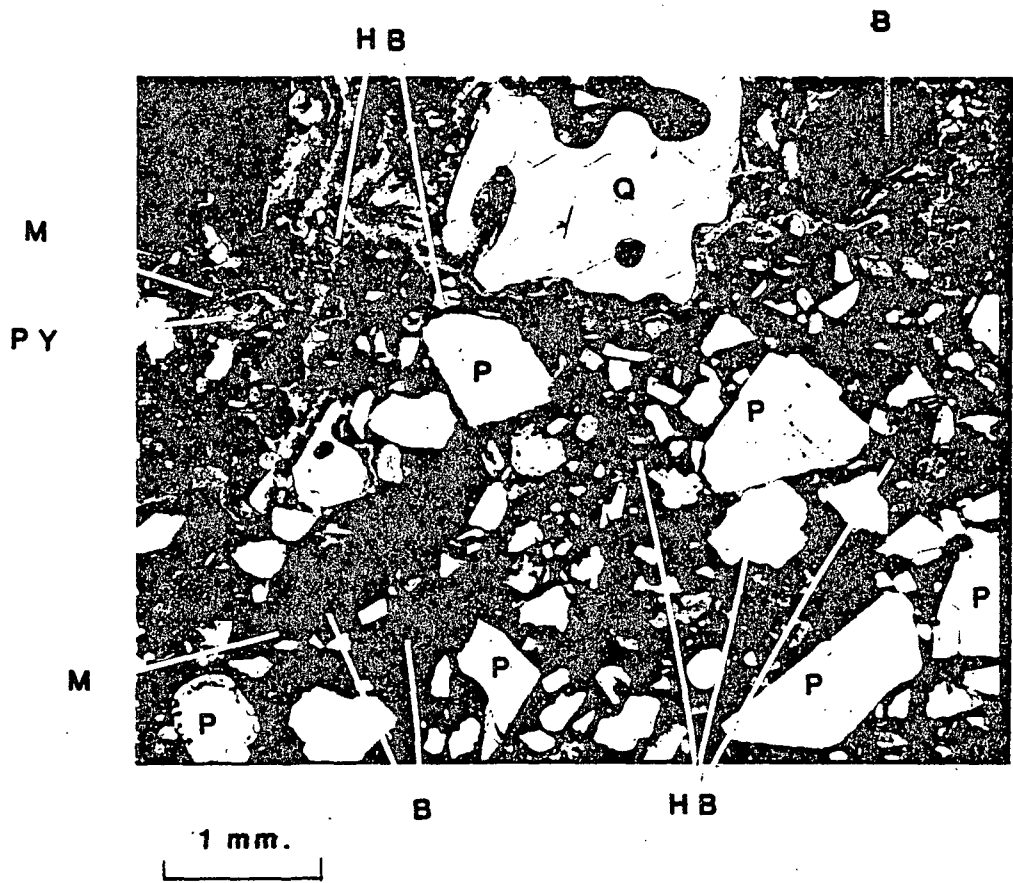
A simple cooling unit of ash-flow tuff that probably belongs to the Wah Wah Springs Tuff Member of the Needles Range Formation crops out discontinuously along the west side of the Drum Mountains from the Sand Pass road southward to the Little Drum Mountains. It is also well-exposed over a distance of 25 km south from the Little Drum Mountains through the Red Hills and Long Ridge, where it forms long escarpments about 30 m high. The tuff was first identified in outcrops on the south flank of the Little Drum Mountains by Leedom (1974) and Pierce (1974), whose petrographic studies demonstrated its similarity to the Needles Range Formation. Ages reported here (table 3) confirm this correlation. Its thickness is difficult to judge, but is probably near that of the 30 m estimated south of the Little Drum Mountains. The Needles Range Formation is about 70 m thick in the subsurface south of The Dell, at the center of sec. 23, T. 13 S., R. 12 W., where it overlies about 25 m of Dell Tuff(?) and Drum Mountain Rhyodacite. The Needles Range unconformably overlies lower Paleozoic rocks, Drum Mountains Rhyodacite, and Mt. Laird Tuff along the west side of the Drum Mountains, but it has not been observed in contact with the Joy and Dell Tuffs at the surface. The tuff fills valleys in dolomite and Drum Mountains Rhyodacite in secs. 23 and 26, T. 14 S., R. 12 W.

Tuff mapped as Needles Range Formation is typically red-brown and crystal-rich, the crystals being small (1-2 mm) plagioclase (26-37 percent) of intermediate composition, conspicuous biotite (2-11 percent), small green-brown hornblende (6-13 percent), and minor resorbed quartz, magnetite, and hypersthene (fig. 9). Accessory minerals include apatite and colorless zircon; no sphene was observed. The matrix is glassy to devitrified pumice and shards that have been moderately welded. Collapsed black pumice and lithic inclusions of Mt. Laird Tuff are abundant in the lower part of the tuff south of the Little Drum Mountains to Long Ridge; the lithic inclusions are abundant also in the drilled section of tuff south of The Dell. A few meters of tan, crudely stratified, loosely indurated tuff with stones of Mt. Laird Tuff and Drum Mountains Rhyodacite crop out in the basal part of the Needles Range Formation about 0.5 km south of the Jerico road.

The source of the tuff mapped as Needles Range is uncertain. The greatest thickness and development of the Needles Range is in southwestern Utah, about 150 km south of the Drum Mountains (Best and others, 1973; Cook, 1965). The close resemblance, in petrography and age, between the type Needles Range and tuff mapped as Needles Range in the Drum Mountains and southward to Long Ridge indicates a distant source in southwest Utah. Abundant lithic inclusions of Mt. Laird Tuff, particularly in the thickest section found to date by drilling just within the Thomas caldera, indicate a possible source within that structure. If the tuff is indigenous to the Thomas caldera, then the unlikely possibility of nearly simultaneous eruption of Needles Range tuff from multiple sources over a large area of Utah and Nevada must be considered.



Figure 9.--Photomicrograph of the Needles Range Formation, showing crystal-rich tuff containing quartz (Q), plagioclase (P), biotite (B), hornblende (Hb), pyroxene (Py) and Magnetite (M) in a matrix of devitrified shards. Crossed polars.



## Spor Mountain Formation

The Spor Mountain Formation consists of two informal members, the beryllium tuff and an overlying porphyritic rhyolite, both of which in most places occur together and are restricted to the vicinity of Spor Mountain. The beryllium tuff member contains all of the important deposits of beryllium and uranium discovered as of 1978, and the 21 m.y.-old porphyritic rhyolite is an important reference point for establishing the onset of alkali rhyolite volcanism, the maximum age of beryllium and uranium mineralization, and the age of block-faulting in this part of the basin and range province. The close spatial association of the two members of the Spor Mountain Formation indicates that eruption of the porphyritic rhyolite followed soon after deposition of the beryllium tuff.

Angular unconformities separate the Spor Mountain Formation from older rocks (unconformity C) and the younger Topaz Mountain Rhyolite (unconformity D). The two members of the Spor Mountain Formation are conformable to one another. The beryllium tuff member unconformably overlies Paleozoic rocks, Drum Mountains Rhyodacite and Joy Tuff (in the subsurface only) west of Spor Mountain, and Drum Mountains Rhyodacite and Dell Tuff in The Dell. Unconformity C is partly of erosional origin as is evident from abundant detritus of older volcanic rocks in the beryllium tuff member. Unconformity D is erosional as indicated by angular relationships in The Dell. There, the Spor Mountain Formation dips as much as 20° west along the east side of The Dell, where it is unconformably overlain by flat-lying Topaz Mountain Rhyolite.

Beryllium tuff member--About 60 m of the beryllium tuff member occurs beneath porphyritic rhyolite in drilled sections and beryllium mines south and west of Spor Mountain. In The Dell, about 60 m of the tuff, including bentonite and tuffaceous sandstone, is exposed in the Yellow Chief mine, and a partial section of 22 m occurs at the Claybank prospect. Drilling in the southern part of The Dell shows that the beryllium tuff thins from about 60 m near Spor Mountain to thin, discontinuous lenses on the east side of The Dell.

The beryllium tuff member contains five facies: 1) tuffaceous breccia with abundant clasts of altered and unaltered dolomite (figs. 10A, B), 2) thinly stratified tuff with a few small lithic fragments (fig. 10C), 3) bedded, massive ash-flow tuff with sparse to moderate lithic fragments, 4) bentonite composed mostly of altered pumice (fig. 10D), and 5) tuffaceous sandstone and conglomerate (fig. 10D). The dominance of a particular facies varies from one section to another. Tuffaceous breccia with distinctive dolomite clasts that have been hydrothermally altered to fluorite, clay, and silica minerals (Lindsey and others, 1973) grades laterally and vertically into ash-flow tuff and thinly stratified tuff with sparse dolomite clasts in the vicinity of the beryllium mines. These facies persist eastward into The Dell, where tuffaceous breccia with carbonate clasts comprises only a minor part of a section dominated by ash-flow tuff, bentonite, and tuffaceous

sandstone and conglomerate. In The Dell, tuffaceous breccia with altered dolomite clasts occurs in thin zones at the top of the tuff, as at the Hogsback prospect and the west side of the Yellow Chief pit; thin ash-flow tuffs are interbedded with bentonite at the Claybank prospect. The Yellow Chief section (modified from Bowyer, 1963) illustrates the composition of the beryllium tuff member in The Dell:

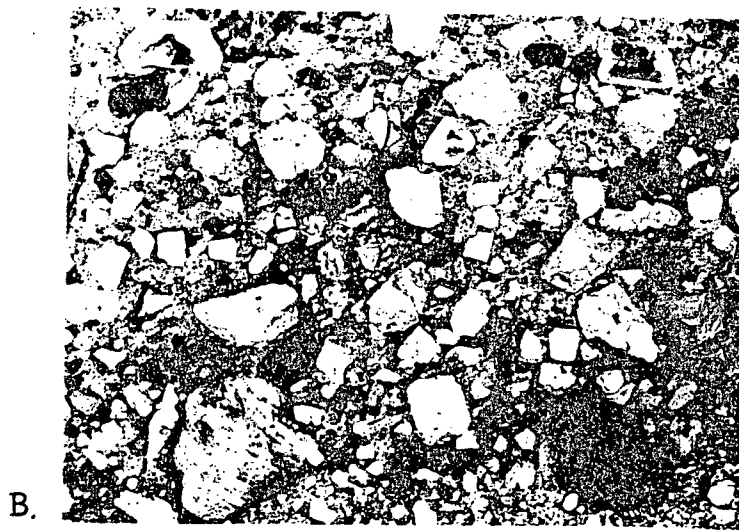
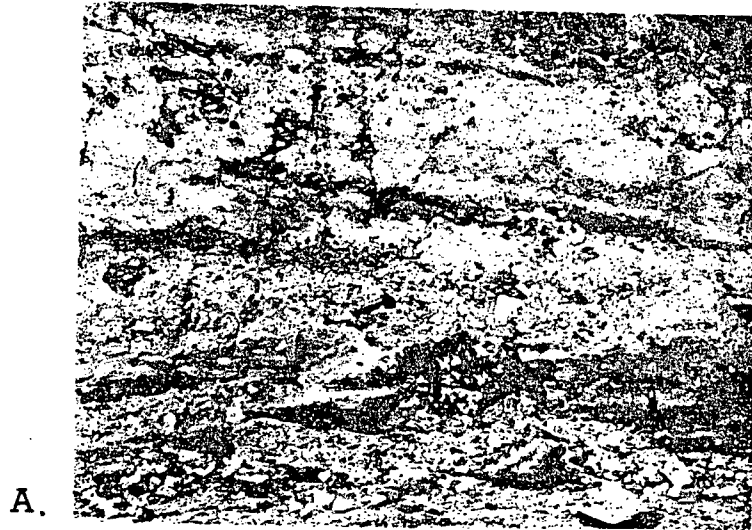
top of section	Beryllium tuff member:
3 m	tuffaceous breccia with altered dolomite clasts
15 m	bentonite
2 m	limestone pebble and cobble conglomerate with tuffaceous sandstone matrix
18 m	tuffaceous sandstone with abundant quartz and sanidine derived from the Dell Tuff
18 m	tuffaceous conglomerate and sandstone; cobbles and boulders are mostly rhyodacite
8 m	stratified tuff with volcanic rock fragments (only exposed south of pit in 1977, 8 m reported by Bowyer, 1963, when pit was freshly dug)
bottom of section	Dell Tuff

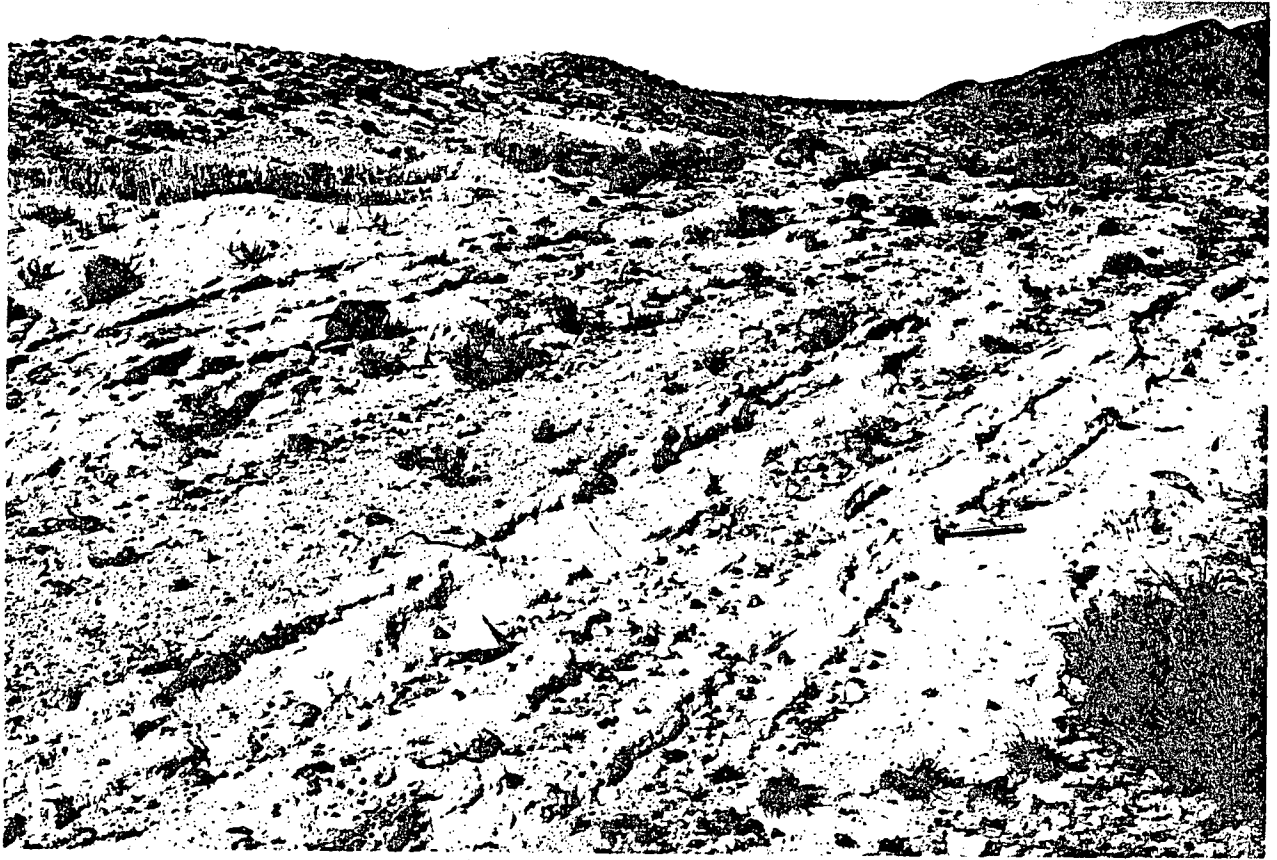
A partial section at the Claybank prospect illustrates the marked local variation in thickness of tuffaceous sandstone and conglomerate in the lower part of the beryllium tuff member:

top of section	fault with remnants of mineralized tuffaceous breccia containing altered dolomite clasts
	Beryllium tuff member:
4 m	bentonite
0.5 m	massive ash-flow tuff with volcanic rock fragments
3 m	bentonite
2 m	massive ash-flow tuff with volcanic rock fragments and compacted pumice
7 m	bentonite
1.5 m	massive ash-flow tuff with volcanic rock fragments, minor quartzite, and compacted pumice
5 m	tuffaceous sandstone with abundant quartz and sanidine derived from the Dell Tuff
bottom of section	Drum Mountains Rhyodacite

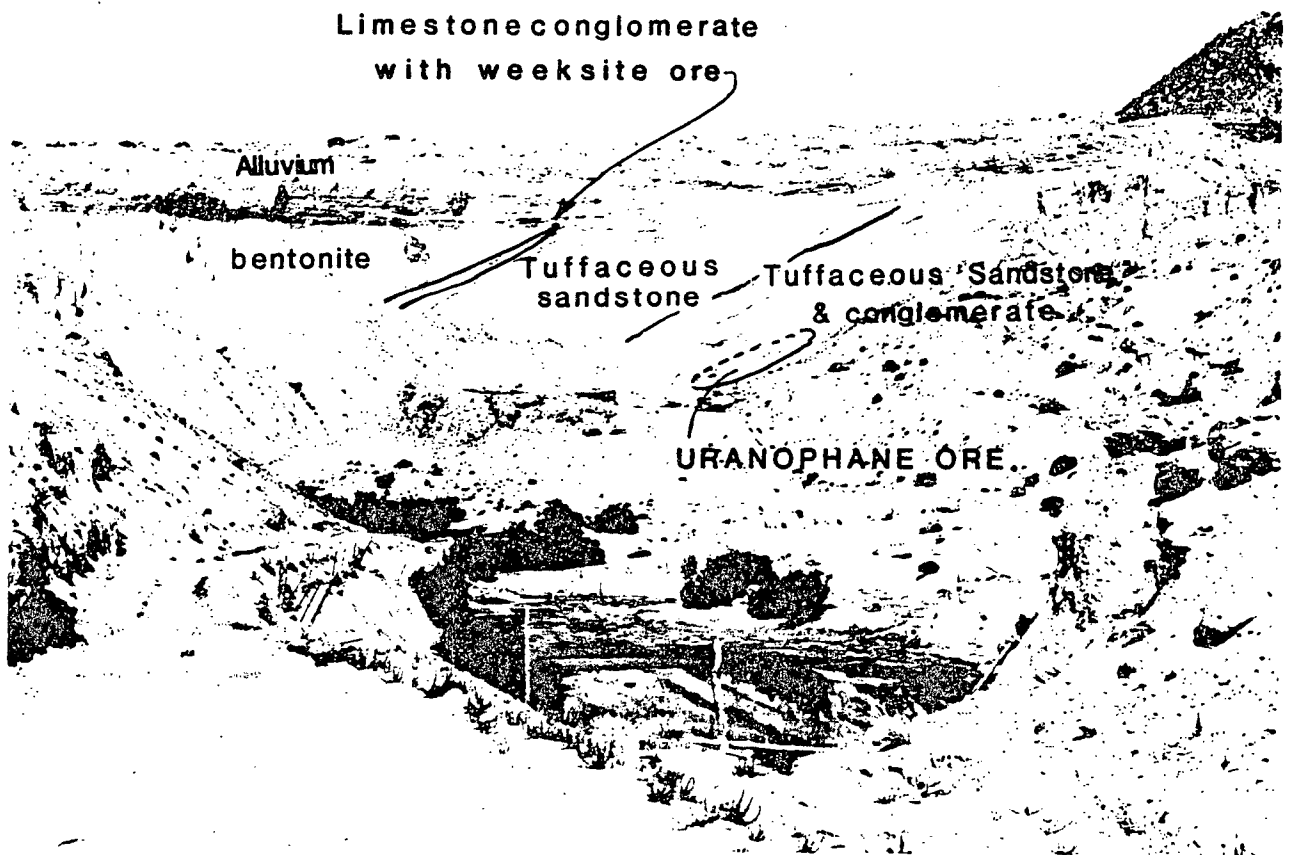
Studies of the beryllium tuff member by thin section and X-ray diffraction methods (Lindsey and others, 1973) show that most of the clasts in the tuff are dolomite from Spor Mountain, nodules derived from the alteration of dolomite to calcite, silica minerals, clay and fluorite, and fragments of volcanic rocks and Swan Peak Quartzite. Dolomite fragments dominate in the breccia facies and volcanic rock fragments dominate in thinly stratified tuff and ash-flow tuff. The matrix of all three facies contains abundant pumice and shards that range from glassy to completely altered; diagenetic alteration formed clinoptilolite and possibly potassium feldspar, and hydrothermal alteration produced smectite, sericite, potassium feldspar, and

Figure 10.--Facies of the beryllium tuff member of the Spor Mountain Formation. A) Tuffaceous breccia with abundant clasts of carbonate rock south of Blue Chalk pit (sec. 9, T. 13 S., R. 12 W.). Pick for scale. B) Closeup view of tuffaceous breccia with clasts of carbonate rock. C) Thinly stratified tuff with sparse clasts of volcanic and sedimentary rock south of Blue Chalk pit (sec. 9, T. 13 S., R. 12 W.). D) Section of bentonite and epiclastic tuffaceous sandstone and conglomerate at the Yellow Chief mine (secs. 25 and 36, T. 12 S., R. 12 W.).





C.



D.

crystalite. About 10-20 percent broken crystals of quartz, sanidine, plagioclase, and biotite are scattered through the matrix.

Porphyritic rhyolite member--Porphyritic rhyolite crops out as flows in The Dell and south and west of Spor Mountain and as plugs and extrusive domes that may have been the source for some of the flows and the pyroclastic debris in the beryllium tuff member. The largest (6 km<sup>2</sup>) dome is both intrusive and extrusive; it intrudes the Drum Mountains Rhyodacite west of Wildhorse Spring, and reached the surface, as judged from local lenses of beryllium tuff encountered by drilling beneath the rhyolite nearby. The intrusive contact is well exposed at NE 1/4 sec. 17, T. 12 S., R. 12 W. A small plug, in sec. 10, T. 13 S., R. 12 W., is only 0.25 km<sup>2</sup> in area; it has a chilled margin of dark vesiculated glass that has been incompletely altered to clay and uraniferous fluor spar. A third vent might be under the Thomas Range east of The Dell, where more than 80 m of porphyritic rhyolite extends east beneath stratified tuff of the Topaz Mountain Rhyolite.

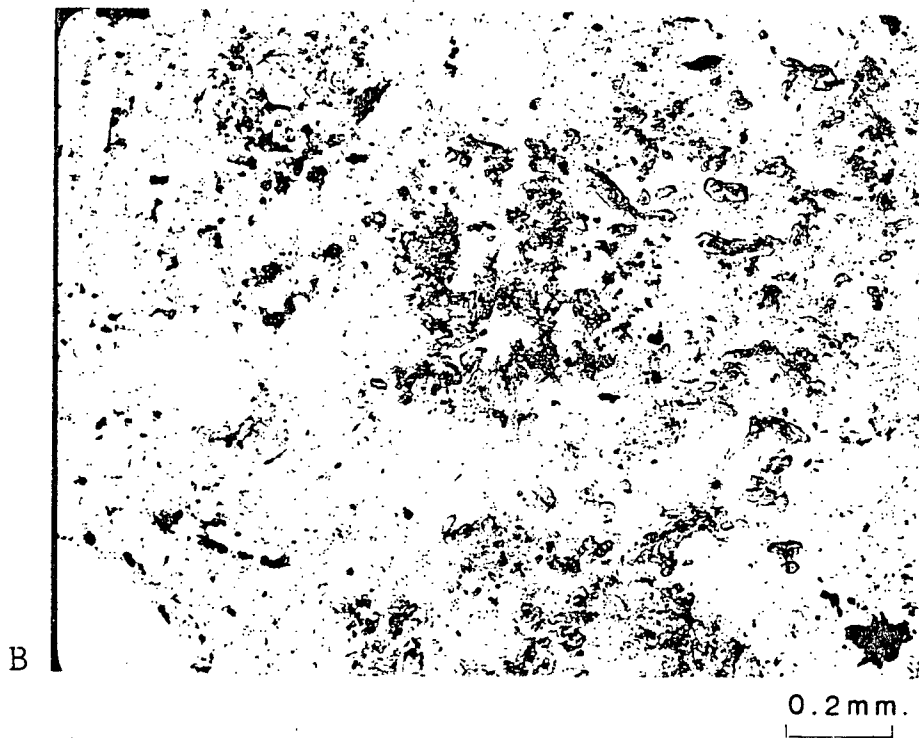
The porphyritic rhyolite contains abundant (average of 40 percent) phenocrysts of euhedral sanidine, quartz, plagioclase (andesine) and biotite; the phenocrysts are conspicuous (3 mm across) and serve to distinguish the rhyolite from most of the Topaz Mountain Rhyolite (table 4). The dome west of Wildhorse Spring contains as much as 60 percent phenocrysts locally, with quartz and sanidine as much as 5 mm across (fig. 11A). Sanidine phenocrysts are commonly chatoyant. Biotite occurs in the rhyolite as euhedral black phenocrysts with abundant magnetite inclusions, in contrast to the ragged, red appearance of biotite in the Topaz Mountain Rhyolite. Small, pink zircon occurs in trace amounts; the zircon is distinctive from that of older volcanic rocks in that it contains an average of about 10 times as much uranium. Southwest of Spor Mountain, the rhyolite contains numerous dark lithic inclusions that resemble the Drum Mountains Rhyodacite; the inclusions contain conspicuous (10-20 mm) large zoned plagioclase crystals with vermicular intergrowths of plagioclase, potassium feldspar, and glass.

The groundmass of the porphyritic rhyolite, as seen under the microscope, is commonly a coarse-grained (0.1-0.2 mm) mosaic of crystals, although fine-grained and spherulitic textures are common, also. The groundmass consists mostly of potassium feldspar and crystalite with lesser disseminated magnetite, fresh gray-brown biotite, and cavity fillings of quartz and topaz (fig. 11B). The groundmass biotite is unique because it is completely fresh and free of magnetite; it occurs also as overgrowths on the earlier-formed biotite phenocrysts which are brown and filled with magnetite inclusions.

Chemical analyses show that the porphyritic rhyolite is borderline between rhyolite and alkali rhyolite in the classification of Rittmann (1952). The rhyolite is clearly allied to the younger Topaz Mountain Rhyolite; both have high alkali and fluorine contents and anomalous traces of Be, Li, Nb, Sn, Th, U, and Y.



Figure 11. Photomicrographs of porphyritic rhyolite member of the Spor Mountain Formation. A) Porphyritic rhyolite at Wildhorse Spring with abundant phenocrysts of quartz (Q) and perthitic sanidine (S). Crossed polars. Sample from sec. 9, T. 12 S., R. 12 W. B) Groundmass of porphyritic rhyolite with abundant acicular and prismatic topaz (high relief). Plain light. Sample from Hogsback prospect, sec. 35, T. 12 S., R. 12 W.



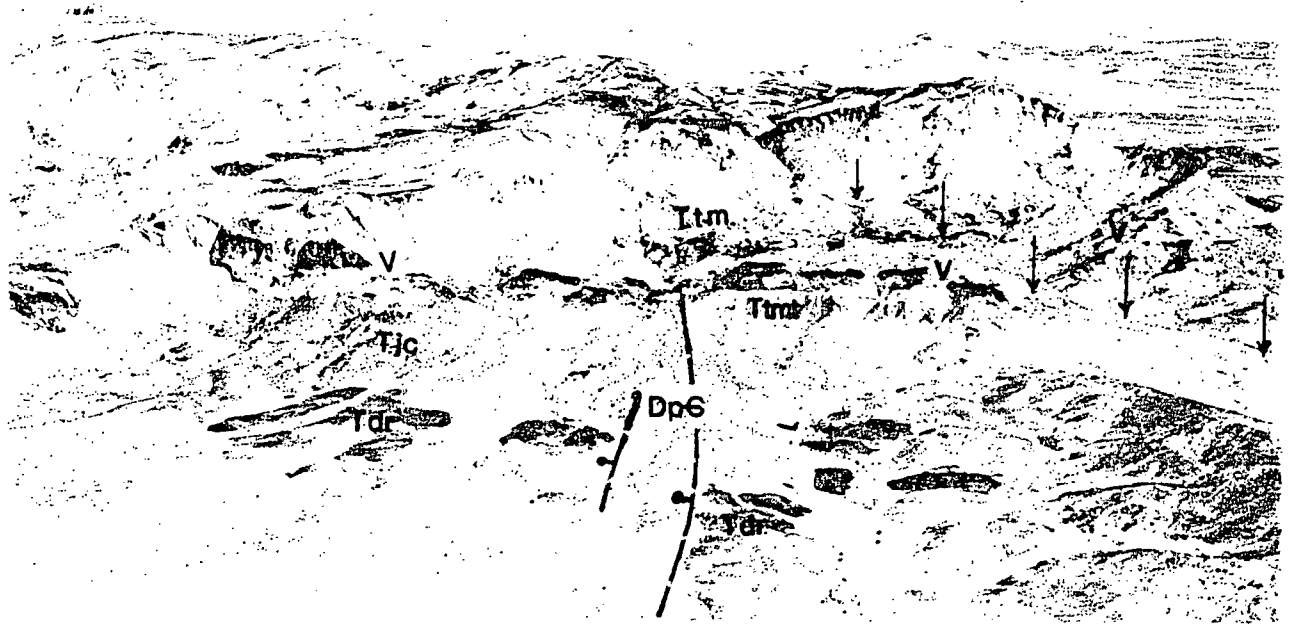
## Topaz Mountain Rhyolite

The Topaz Mountain Rhyolite is a large complex of alkali rhyolite flows, domes, and interbedded local units of stratified tuff. The entire complex unconformably overlies older volcanic rocks that have been faulted and tilted. Unconformities are also present beneath stratified tuff that separates older from younger flows of the Topaz Mountain Rhyolite. These unconformities do not show visible angular discordance and may be constructional in part, but paleotopography is clearly visible beneath stratified tuff at Topaz Mountain and in the upper reaches of Pismire Wash. Age dates indicate short quiescent intervals, of perhaps 100,000 years on Topaz Mountain to perhaps 500,000 years in Pismire Wash, between eruption of major flows and domes.

The Topaz Mountain Rhyolite contains distinctive sequences of lithologies (fig. 12A) that are repeated several times in vertical sections; the sequence is stratified tuff, breccia, vitrophyre, and flow layered rhyolite (Staatz and Carr, 1964, p. 86-90). Flows that extend several kilometers or more are commonly underlain by stratified tuff, whereas some domes and short flows have only breccia or vitrophyre at their base. Staatz and Carr (1964) divided the Topaz Mountain Rhyolite into five subgroups having implied lateral continuity, but my mapping shows that each subgroup is actually a complex of flows and domes derived from numerous vents. Flows and domes have been mapped separately by me (Lindsey, 1979) as far as was practical, but the location of the contact between adjacent flows remains obscure in many places.

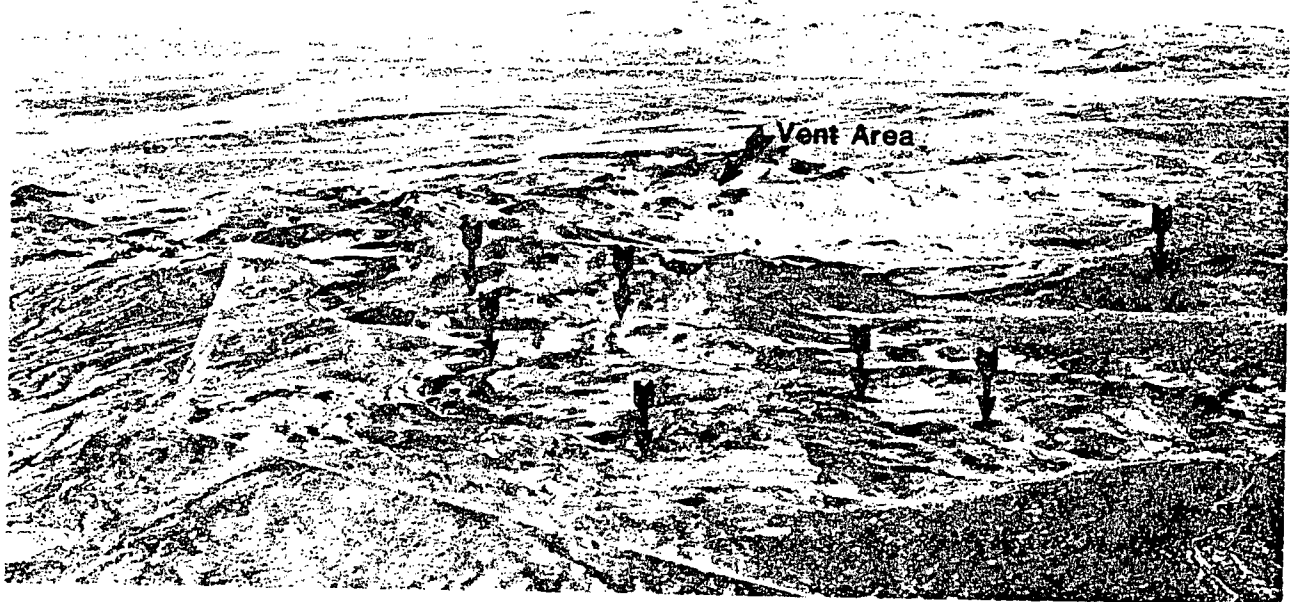
Flows and domes of alkali rhyolite--Flows and extrusive domes of alkali rhyolite have been mapped and their vent areas identified on the basis of lines of viscous flowage and shearing (fig. 12B). These flowage lines are visible on aerial photos and were identified on the ground as lenses of steeply dipping vitrophyre and layered rhyolite. Large flows were erupted from the vent on Topaz Mountain and another vent in the northeastern Drum Mountains; each flow extends west-southwesterly about 4 km from the vent. A complex of at least four domes and short flows was erupted from separate vents along Antelope Ridge. Other vents are north and south of Colored Pass and north of Pismire Wash. Much of the rhyolite between Searles Canyon and Pismire Wash issued from a fissure vent that is clearly discernible on aerial photos as a lineament bounded by subparallel flow lines. Some of the vents were first located by Staatz and Carr (1964), who measured the attitude of flow layering throughout the rhyolite. These attitudes and additional observations by me were used to confirm the orientation of flow lines seen on aerial photos.

Figure 12.--Topaz Mountain Rhyolite. A) Aerial view looking north at Topaz Mountain, showing section of stratified tuff (Tmt) and alkali rhyolite (Ttm) that issued from vent on top of Topaz Mountain. Photo also shows: crystal tuff member of Joy Tuff (Tjc) and Drum Mountains Rhyolite (Tdr) downdropped to west along the east side of Joy graben by the Topaz Mountain fault (bars and balls indicate downthrown sides of subsidiary faults), which is concealed by Topaz Mountain Rhyolite on Topaz Mountain; and lineament of Topaz Valley fault (arrows). B) Aerial view looking northeast at isolated flow of alkali rhyolite in northeastern Drum Mountains (centered at sec. 7, T. 14 S., R. 10 W.), showing alinement of dark lenses of vitrophyre (arrows) that are concentric around the vent area.



A.

### Keg Mountain



B.

Vitrophyre and rhyolite evidently accumulated to considerable heights around a vent, and then spread laterally under their own weight and by force from injection of new lava within the vent, producing concentric flowage lines of sheared vitrophyre and flow-layered rhyolite. Williams (1932, p. 142-145) described a similar origin for the dacite domes of Lassen Peak, California. Vitrophyre zones in the Topaz Mountain Rhyolite were formed at the outer chilled margin of each succeeding injection of lava. Lenses of vitrophyre and parallel flow layering in rhyolite dip steeply; in short flows and domes, the dip is generally toward the vent, but in larger flows and in flows situated between vents the dip of layering may be either toward or away from the vent. Horizontal lineations, perpendicular to the overall direction of flowage and in the plane of layering, are common in some flows; lineations are defined by rod-shaped vesicles and sets of parallel striations in both vitrophyre and rhyolite. Rhyolite on Antelope Ridge evidently cooled prior to flowage because it contains vesicles with geopetal structures of layered silica that were originally deposited in horizontal position but which now dip steeply toward the vent. The rhyolite also contains many small-scale flowage folds that vary considerably in attitude; these folds probably formed near the vent and became reoriented during outward spreading of the rhyolite.

The Topaz Mountain Rhyolite typically contains about 13 percent phenocrysts that consist mainly of euhedral sanidine, partially resorbed quartz, and lesser amounts of red oxidized biotite and plagioclase (table 4). Small flows and domes in Dugway Valley and at Antelope Ridge contain as much as 37 percent phenocrysts. The groundmass is composed entirely of fine-grained quartz, cristobalite, potassium feldspar and scattered tiny grains of calcite and specular hematite. Traces of zircon with high uranium content (as much as 11,000 ppm U) occur as tiny (0.05-0.10 mm) subround gray to pink grains. Cavities filled with vapor phase quartz, opal, and topaz are common, and locally these contain fluorite, pink beryl, garnet, bixbyite, and pseudobrookite (Staatz and Carr, 1964, p. 102-108). Both mosaic and spherulitic groundmass textures are common. Chemical analyses show that most of the flows and domes are alkali rhyolite. The distinctive composition of the rhyolite --anomalous F, Be, Li, Nb, U, Th, and Y--has been noted often (Staatz and Griffiths, 1961; Shawe, 1966; Lindsey, 1977).

Stratified tuff--Stratified tuff occurs at many places beneath flows of alkali rhyolite in the Thomas Range. At any one section, the tuff is overlain by breccia, vitrophyre, and alkali rhyolite flows. The tuff units are rarely more than 30 m thick and vary greatly in thickness over short distances; the thickest sections occur in paleovalleys over older formations and flows of Topaz Mountain Rhyolite. A paleosurface having more than 30 m of relief (fig. 13A) was developed on older alkali rhyolite, the Joy Tuff, and Paleozoic rocks beneath Topaz Mountain.

The heterogeneous composition and variable primary structure of the tuff suggest that it was formed by a combination of processes. Massive to stratified tuff consisting mostly of pumice is probably of air-fall

origin (fig. 13B); such air-fall tuffs are abundant in the southern part of The Dell. Massive unsorted beds of pumice and lithic fragments (top of figs. 13A, 13C), seen in tuff around Topaz Mountain, resemble thin ash-flow tuffs described by Sparks, Self, and Walker (1973). The tuff has been interpreted also as a water-laid deposit (Shawe, 1972; Lindsey, 1977) because of extensive stratification (fig. 13A), abundant clasts derived from underlying formations (fig. 13C), and unconformities at the base of the tuff. Epiclastic tuffaceous sandstone with abundant quartz and sanidine derived from the Dell Tuff comprises most of the tuff north of Wildhorse Spring; such sandstone is probably water-laid. Angular fragments of older volcanic rocks as large as 1 m in diameter are locally abundant in the tuff (Lindsey, 1975); these may have been blasted from nearby vents or have been washed into the tuff from nearby paleohills. I favor a combination of pyroclastic eruption of ash and rock from vents accompanied by deposition by air fall, small ash-flows of local extent, and sheetwash from adjacent highlands, to produce the stratified tuffs of the Topaz Mountain Rhyolite.

The uppermost few meters of tuff are reddened and fused to welded tuff by overlying flows of alkali rhyolite. This fusing contrasts with the welding of ash-flow tuffs, which generally are most densely welded toward the middle and lower parts of cooling units. Similar fused tuffs beneath rhyolite flows have been described from southern Nevada (Christiansen and Lipman, 1966).

Pumice and shards are the dominant constituents of the tuff (fig. 13B); these accompany variable amounts of mostly volcanic rock fragments (fig. 13C), and less than 20 percent broken crystals consisting of quartz, sanidine, plagioclase, biotite, and traces of heavy minerals. Some of the tuff is glassy, but large areas have been altered by diagenesis to clinoptilolite, potassium feldspar, and cristobalite. Chemical analyses indicate that the tuff has a rhyolitic composition that, before diagenesis, was probably very close to the composition of the alkali rhyolite. Additional details of the mineral and chemical composition of the tuff have been reported elsewhere (Lindsey, 1975).

Figure 13.--Features of the stratified tuff in the Topaz Mountain Rhyolite. A) Stratified tuff filling paleovalley in Joy Tuff east of Topaz Valley (sec. 9, T. 13 S., R. 11 W.). Inclination of strata is believed to result from initial dip and compaction. B) Pumice and scattered dark obsidian fragments in air fall tuff on Antelope Ridge (sec. 13, T. 13 S., R. 11 W.). C) Angular fragments of volcanic rock and limestone (at pencil point) in tuff west of Topaz Valley (sec. 16, T. 13 S., R. 11 W.).

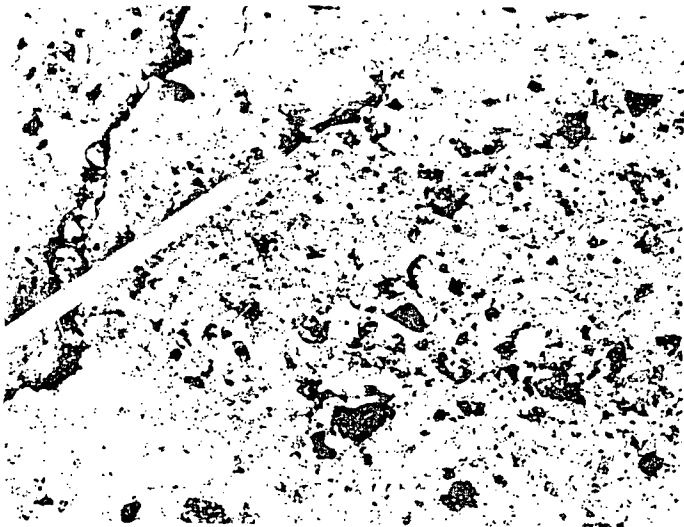




A.



B.



C.

## STRUCTURAL GEOLOGY

The Thomas Range and northern Drum Mountains are part of a caldera complex that has been extensively modified by basin-and-range block faulting. The Thomas caldera (Shawe, 1972) is the major structural feature of the area (fig. 2); its western outline is delineated by the ring fracture zone of the Joy fault and the Dell fault system, and faults now buried beneath Topaz Mountain Rhyolite in the Thomas Range. The remainder of the caldera margin has been projected in the western part of the Keg Mountains (Shawe, 1972), outside the area of this study. The Thomas caldera contains, nested within it, the younger Dugway valley cauldron. The Dugway Valley cauldron, whose topographic expression is now obscure, underlies much of Dugway Valley; its western margin is marked by faults and landslide deposits in the northeastern Drum Mountains, but its east side has not been located. The margin of a third cauldron may account for landslide deposits north of Spor Mountain, but other evidence for its existence is lacking. Basin-and-range structures cut across the caldera complex; two of the most prominent are the Joy graben and the horst of the north-central Drum Mountains. Highlands at Spor Mountain and the northwestern and central Drum Mountains compose the rim of the caldera complex; these also have been modified by basin-and-range faulting.

Outlines of the Thomas caldera and the Dugway Valley cauldron are based partly on the distribution of exposed and buried faults and partly on the thickness and distribution of ash-flow tuffs and landslide deposits. In other well-studied caldera complexes, such as those of the San Juan Mountains (Steven and Lipman, 1976) and southern Nevada (Byers and others, 1976), ash-flow tuffs associated with caldera collapse ponded to great thicknesses within the source caldera, but are thin or absent outside the margin of the caldera; landslides along the caldera margins left lenses of breccia and megabreccia interbedded with the intracauldron ash flows (Lipman, 1976). All of these features have been identified within the Thomas caldera and Dugway Valley cauldron, and are used here to establish the extent and history of cauldron subsidence.

The faulted structure of the caldera complex, also including post-caldera basin-and-range faults, has been revealed by mapping of numerous lineaments in the alluvium and the Topaz Mountain Rhyolite (fig. 2). These lineaments are interpreted as concealed faults; little or no offset is visible in alluvium and Topaz Mountain Rhyolite along most of the lineaments, but the lineaments are visible on aerial photographs as a result of slight fault movement, compaction, or settling of the covering unit. Many of the lineaments pass into well-exposed faults in rocks older than the Topaz Mountain Rhyolite, thus confirming their identification as concealed faults. Fracturing and small offsets are visible along lineaments in Topaz Mountain Rhyolite at Colored Pass and east of Topaz Mountain, as noted also by Staatz and Carr (1964).

## The Thomas caldera

The Thomas caldera began to subside about 39 m.y. ago in response to eruption of the Mt. Laird Tuff from vents in the northern Drum Mountains. More than 500 m of Mt. Laird Tuff and interbedded lacustrine sediment accumulated in a depression as much as 15-25 km across. Later eruptions of the Joy Tuff (38 m.y. ago) and the Dell Tuff (32 m.y. ago) largely filled the caldera, and local cauldron collapse in Dugway Valley and perhaps north of Spor Mountain modified the Thomas caldera. In the Thomas Range and Drum Mountains, the western half of the Thomas caldera is well-defined by 1) the ring fracture zone of the Joy fault and the Dell fault system, 2) the caldera wall-collapse breccia at Spor Mountain, and 3) the confinement of most of the post-subsidence Joy and Dell Tuffs within the caldera.

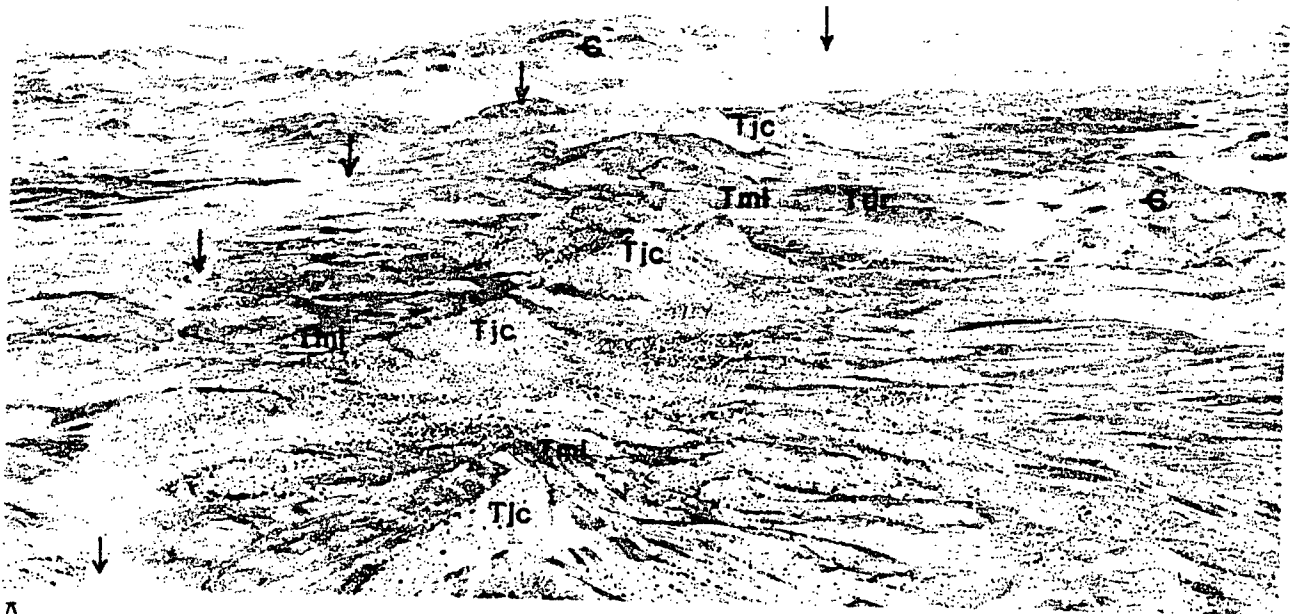
Initial subsidence of the Thomas caldera is believed to have accompanied eruption of the Mt. Laird Tuff about 39 m.y. ago. The source of the Mt. Laird Tuff was near Joy townsite, as indicated by tuff breccias associated with probable vents there and by intrusive plugs and dikes resembling Mt. Laird Tuff in the Drum Mountains south of Joy townsite. The intrusive equivalents may represent resurgence of Mt. Laird magma outside the caldera, but none occurs within the caldera or in the ring fractures. Subsidence of the caldera was most pronounced in Dugway Valley, where numerous ash flows of the Mt. Laird Tuff flowed into a lake, leaving a record of more than 500 m of tuff and lacustrine sediments.

The south and west walls of the Thomas caldera are defined by an extensive system of ring fractures, faults, and lineaments that extend nearly the entire length of the mapped area (figs. 14A, B). The ring fracture of the caldera is exposed as the Joy fault in the Drum Mountains, where it has both a structural and topographic expression. The Joy fault is exposed only in a few prospects in jasperoid and iron-stained Cambrian rocks near Joy townsite. The Joy fault connects with the Dell fault system along the east side of Spor Mountain (figs. 14B, 15) and extends northward beneath the Topaz Mountain Rhyolite as a system of lineaments. Lineaments in alluvium near the junction of the beryllium road and the Sand Pass Road and in Topaz Mountain Rhyolite, 2 km northwest of the road junction, may be the surface expression of buried faults in the ring fracture zone where it extends northward into The Dell. All northerly trending faults mapped in The Dell are downthrown on the east side, indicating that they form part of a complex, steplike boundary on the west side of the Thomas caldera at this locality (fig. 15). The buried northwest corner of the caldera may be quite angular, as indicated by prominent intersecting north- and east-trending buried faults in the northern part of the Thomas Range.

There is good evidence that the ring fracture and topographic wall of the Thomas caldera existed as early as 38 m.y. ago. The 38 m.y. crystal tuff member of the Joy Tuff is completely confined to the east side of the Joy fault, and does not occur on the west side of the Drum

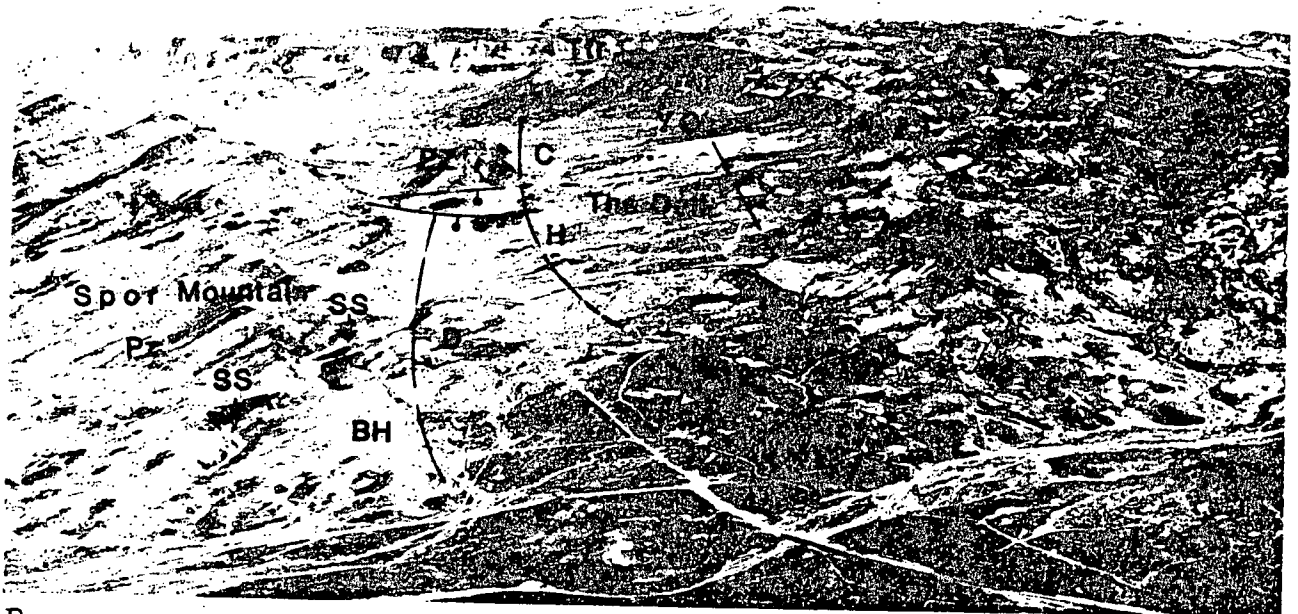
Figure 14.--Aerial views of the ring fracture zone of the Thomas caldera showing (A) the Joy fault, and (B) its northward extension in The Dell. A) View looking northwest from above Joy townsite, showing the arcuate trace of the Joy fault (arrows) and the caldera rim of northwestern Drum Mountains. C, Cambrian sedimentary rocks; Tdr, Drum Mountains Rhyodacite; Tml, Mt. Laird Tuff; Tjc, crystal tuff member of Joy Tuff. B) View looking looking north at The Dell, showing the Dell fault system, remnant of the caldera rim of tilted Paleozoic rocks on Spor Mountain, and the location of mines and prospects, which are the Yellow Chief mine (YC), Bell Hill mine (BH), Claybank (C), Hogsback (H), Oversight (O), and Buena No. 1 (B). Location of superposed stream (SS) may mark the position of the Dell drainage system during time of unconformity C and deposition of the beryllium tuff member of the Joy Tuff. PZ, undifferentiated Paleozoic rocks; Ttm, Topaz Mountain Rhyolite.

Fish Springs Range



A.

Dugway Range

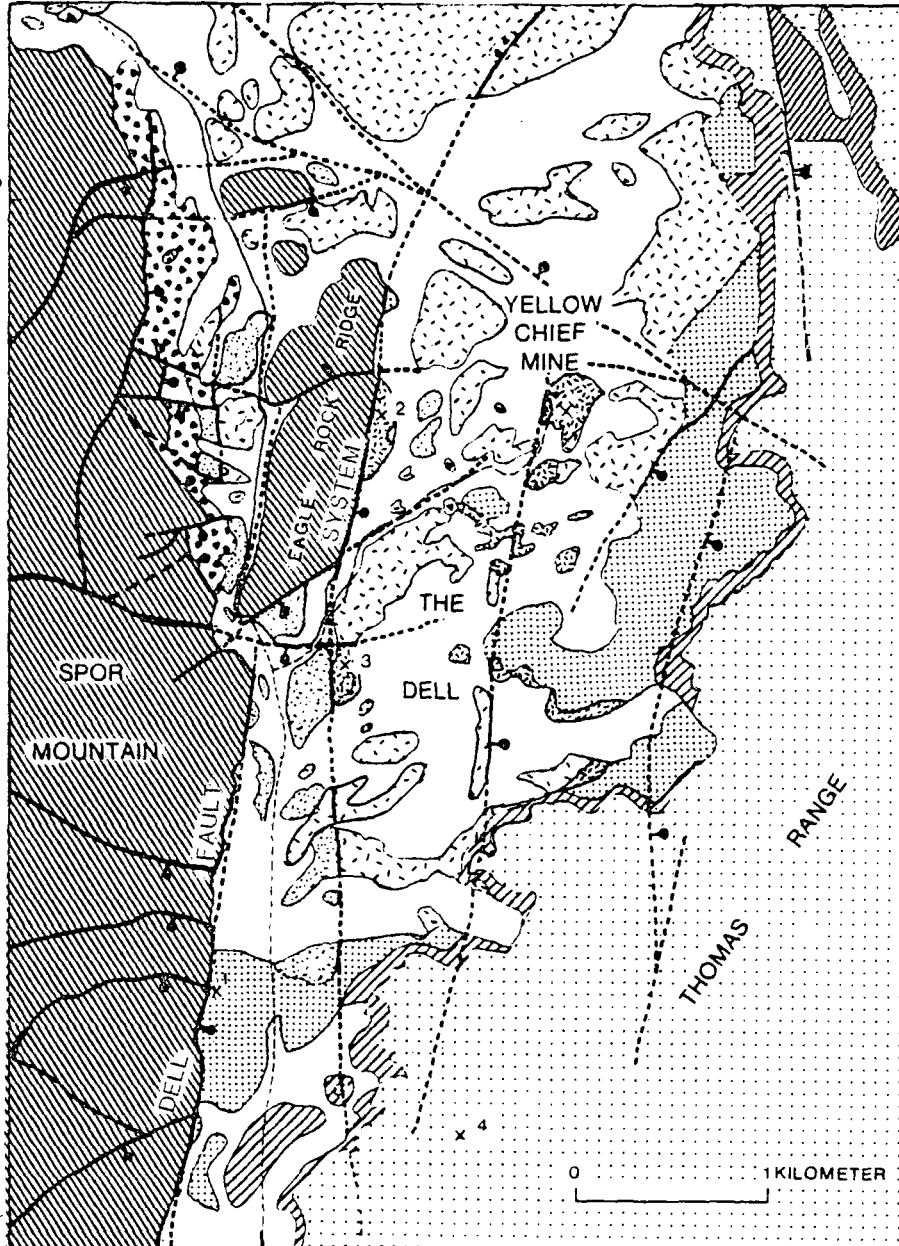


B.









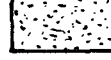

Figure 15.--Geologic map showing the structure of The Dell and the setting of uranium mines and prospects. Base from U.S. Geological Survey orthophoto enlarged to 1:40,000.

113°10

39°  
45'



EXPLANATION

-  QUATERNARY  
Alluvium and colluvium
- TERTIARY
-  Topaz Mountain Rhyolite (6-7 m.y.)
-  Alkali rhyolite--flows and extrusive domes of topaz-bearing alkali rhyolite
-  Stratified tuff--vitric and zeolitic tuff underneath and interbedded with alkali rhyolite  
angular unconformity  
Spor Mountain Formation (21 m.y.)
-  Porphyritic rhyolite member--plugs and flows of topaz-bearing alkali rhyolite
-  Beryllium tuff member--tuffaceous breccia with clasts of carbonate rock; includes bentonite and tuffaceous sandstone at Yellow Chief mine  
angular unconformity
-  Dell Tuff (31 m.y.)--rhyolitic ash-flow tuff with abundant crystals of quartz and sanidine  
unconformity
-  Landslide breccia, breccia at Spor Mountain--breccia with clasts derived from rocks of early Paleozoic age  
angular unconformity
-  Drum Mountains Rhyodacite (42 m.y.)--flows and breccias of porphyritic rhyodacite  
angular unconformity
- PALEOZOIC
-  Undifferentiated dolomite, limestone, quartzite, and shale
- Contact
- Fault, dashed where inferred, dotted where concealed by younger strata, ball and bar on downthrown side
- 1 Oversight prospect (uraniferous fluorspar in fault)
- 2 Claybank prospect (Be and U in beryllium tuff along fault)
- 3 Hogsback prospect (Be and U in beryllium tuff)
- 4 Buena No.1 (uraniferous opal in Topaz Mountain Rhyolite)
- Road



Mountains, where the Needles Range Formation lies directly on the Mt. Laird Tuff. The distribution of the Joy Tuff indicates ponding against the scarp of the Joy fault 38 m.y. ago. A small occurrence of Joy Tuff has been found by drilling in the subsurface of Fish Springs Flat west of Spor Mountain, however, indicating that the caldera wall did not block all westward flow of ash north of the Drum Mountains. Some movement of the Joy fault occurred after 38 m.y. ago, as indicated by faulted contacts of the Joy Tuff.

The ring fracture of the Thomas caldera has a long history of movement in The Dell; here, movement can be inferred or documented between 42 and 32 m.y. ago, 32 and 21 m.y. ago, and 21 and 7 m.y. ago (fig. 15). Reinterpretation of the breccia at Spor Mountain as a landslide deposit that may have formed along a fault scarp between 42 and 32 m.y. ago indicates that this part of The Dell fault system was active at that time. Restriction of the Dell Tuff to the east side of Spor Mountain indicates ponding against the scarps of the Dell fault system 32 m.y. ago. Faults of the Dell system cut the Dell Tuff and older rocks throughout The Dell; they cut the Spor Mountain Formation in the central part of The Dell, but are seen as lineaments covered by the Spor Mountain Formation in the southern part of The Dell (fig. 15). These relationships are interpreted to mean that the faults moved prior to 21 m.y. ago, probably during collapse of the Thomas caldera, and were rejuvenated in some sections during basin-and-range faulting after 21 m.y. ago.

#### Dugway Valley cauldron

The Dugway valley cauldron is defined by 1) an area of vent breccias in the crystal tuff member of the Joy Tuff of Topaz Mountain, 2) restriction of the black glass tuff member of the Joy to the area of vent breccias, and 3) the occurrence of faults and landslide breccias along the cauldron margin in the northeastern Drum Mountains (fig. 2). The Dugway Valley cauldron contains much greater thicknesses of volcanic rocks than the western segment of the Thomas caldera. The center of the Dugway Valley cauldron lies northeast of Antelope Ridge; the west side of the cauldron consists of three fault blocks that are downthrown stepwise into Dugway Valley. The Topaz Valley fault marks the west side of the faulted blocks and extends north beneath Topaz Mountain. The Antelope Ridge west fault is exposed in the northeastern Drum Mountains, where it drops the black glass tuff member of the Joy Tuff and the overlying landslide megabreccia of the northern Drum Mountains down on the east side. The fault extends north in the subsurface west of Antelope Ridge. The Antelope Ridge east fault extends south from Antelope Ridge into the subsurface. The northwestern extent of the margin of the Dugway Valley cauldron is problematical, but it may extend northward from Topaz Mountain and then eastward, encircling Dugway Valley. Faults in the western part of the Keg Mountains, mapped by Shawe (1972) as the east side of the Thomas caldera, may also mark the east side of the Dugway Valley cauldron.

The Dugway Valley cauldron collapsed suddenly 38 m.y. ago during eruption of the Joy Tuff from vents located along the western side of Dugway Valley. Large areas of tuff breccia in Joy Tuff along the west margin of the Dugway Valley cauldron probably formed during simultaneous eruption and collapse. After eruption of the black glass tuff member of the Joy Tuff, which was restricted to the Dugway Valley cauldron, the west wall of the cauldron collapsed and slid over the cauldron fill of Joy Tuff, forming the megabreccia of the northeastern Drum Mountains.

#### Basin-and-range structure

Faults of basin-and-range age are widespread in the Thomas Range and northern Drum Mountains and have modified the caldera structure extensively. Modification was accomplished by rejuvenation of earlier faults that were formed during cauldron subsidence and by initiation of new, north-trending faults. As a result of basin-and-range faulting, the Joy graben and an adjacent horst in the north-central Drum Mountains probably were formed. Numerous faults of basin-and-range age cut the rim outside the Thomas caldera.

The Joy graben was formed partly by subsidence of the Thomas caldera and partly by basin-and-range faulting. All of the structures associated with the ring fracture of the Thomas caldera, such as the Joy fault and the Dell fault system, were formed during caldera subsidence. The Dell fault system was rejuvenated after 21 m.y. ago, as shown by large offsets of the Spor Mountain Formation. The east side of the Joy graben and the adjacent horst of the north-central Drum Mountains probably were formed during basin-and-range faulting. The age of the horst presents a problem for the caldera model; the horst had to be absent for caldera-filling ash flows of the Joy Tuff to travel west across the present location of the horst to the caldera wall, but a highland had to exist soon after eruption of the Joy Tuff so that the landslide megabreccia of the northeastern Drum Mountains could slide over the Dugway Valley cauldron. The eastern side of the Joy graben is defined by the Schoenburger Spring fault, which strikes northwest and intersects the north-trending Topaz Mountain fault in the north-central Drum Mountains. The Topaz Mountain fault passes beneath the Topaz Mountain Rhyolite (fig. 12A), where it is aligned with a system of lineaments and vents in rhyolite that extends north into the Dugway Range, a distance of about 20 km. These structures cut across the caldera, and therefore are considered to be of basin-and-range origin.

The rim of the Thomas caldera contains numerous faults of basin-and-range age. Almost all major faults on Spor Mountain, whatever their trend, extend beyond the Paleozoic rocks and cut the Spor Mountain Formation and volcanic rocks of Oligocene and Eocene ages (figs. 2 and 15). Previous mapping did not show offset of volcanic rocks by many faults, so only a few were assigned a Tertiary age (Staatz and Carr, 1964, p. 128-129). Faulting of basin-and-range age is most evident around the beryllium mines southwest of Spor Mountain, where northeasterly and easterly trending high-angle normal faults displace the Spor

Mountain Formation by as much as 200 m or more, throwing the beryllium tuff and porphyritic rhyolite members into large blocks that have been tilted 15-30 degrees northwest. East of Spor Mountain, easterly and northeasterly trending faults extend into The Dell, where they cut volcanic rocks as young as the Spor Mountain Formation, also. The Drum Mountains are traversed by many westerly, northerwesterly, and northerly trending faults, some of which offset rocks of Tertiary age. Faults cut the Drum Mountains Rhyodacite at many places southwest of Joy townsite. South of the Sand Pass Road, faults cut rocks as young as the Needles Range Formation.

Basin-and-range faulting was accompanied by voluminous eruptions of alkali rhyolite. The first eruption, of the Spor Mountain Formation 21 m.y. ago, predated most basin-and-range faulting, although the two may have been closely related. After most basin-and-range faulting had ceased, the Topaz Mountain Rhyolite was erupted 6-7 m.y. ago. Basin and Range faults, and earlier faults rejuvenated by basin-and-range faulting, were a major influence on the locus of eruption of the Topaz Mountain Rhyolite. Numerous vents in the Topaz Mountain Rhyolite are situated at or near fault intersections beneath the rhyolite; these include vents in the north-central Thomas Range, south of Colored Pass, on Topaz Mountain (fig. 12A), on Antelope Ridge and in the northeastern Drum Mountains (fig. 12B). Vents north of Colored Pass and in the northeastern part of the Thomas Range occur near faults or along their projections beneath rhyolite. The vent north of the head of Searles Canyon was a fissure; the extent of the fault is still visible as an east-west lineament between subparallel flow lines in rhyolite. Only minor block-faulting continued after eruption of the Topaz Mountain Rhyolite.

#### Structural evolution

The structural evolution of the Thomas Range and Drum Mountains during part of Tertiary time can be inferred from the distribution of the products of volcanism and sedimentation and the timing of fault movements, as already discussed. The evidence has been integrated in a series of maps depicting the most probable structural evolution of the region (fig. 16) although evidence for the existence and timing of some events is lacking or equivocal. It must be emphasized that the degree of confidence in the maps decreases farther back in the Tertiary, with the maps of Eocene and Oligocene time being partly conjectural and those for Miocene time mainly factual.

The map of the time of unconformity B, about 38-39 m.y. ago, reflects the eruption of the Mt. Laird Tuff and accompanying subsidence of the Thomas caldera. Both the Mt. Laird Tuff and accompanying lacustrine sediments accumulated in Dugway Valley, whereas the tuff was erupted over a wide area beyond the caldera margin. Eruption of the Mt. Laird Tuff followed eruption of flows, breccias, and tuffs from small central volcanoes in the Black Rock Hills and the Little Drum Mountains, and possibly from fissures in the Thomas Range and Drum Mountains. The

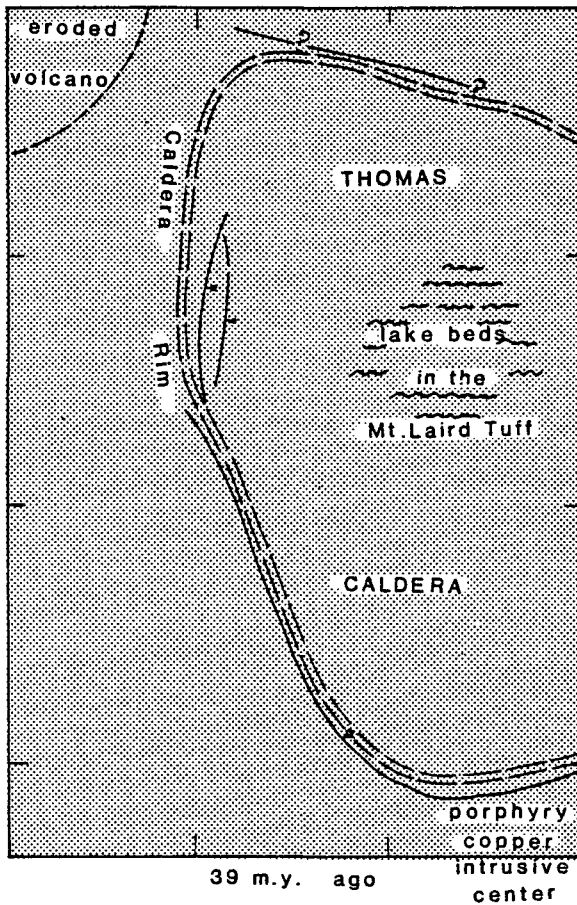
Joy Tuff had not been erupted yet.







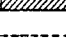
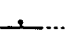

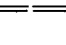

The Thomas caldera was filled with the mostly intracauldron Joy and Dell Tuffs 38-32 m.y. ago (figs. 18B and 18C). Eruption of the Joy Tuff 38-37 m.y. ago was accompanied by subsidence of the Dugway Valley cauldron, a subsidiary depression nested within the larger Thomas caldera. This subsidence left a segment of the Thomas caldera as a high rim relative to the Dugway Valley cauldron; the rim collapsed and slid over the west side of the cauldron after 37 m.y. ago (fig. 18B). Also, between 42 and 32 m.y. ago, the wall of the Thomas caldera at Spor Mountain collapsed; this event may have accompanied initial subsidence of the Thomas caldera or may reflect additional subsidence of the caldera during eruption of the Joy Tuff. Filling of the Thomas caldera was completed 32 m.y. ago by eruption of the Dell Tuff from an unknown source within the Thomas caldera (fig. 18C). The Dell Tuff covered some of the landslide breccia at Spor Mountain and ponded against scarps of the Dell fault system. Ash-flow tuff of the Needles Range Formation, which entered the southern part of Fish Springs Flat about 30 m.y. ago, probably was not locally derived and thus would have played no part in the structural development of the area.

The interval between deposition of the intracauldron ash-flow tuffs (about 32 m.y. ago) and the Spor Mountain Formation (21 m.y. ago) must have been a period of erosion of the caldera rim, including Spor Mountain, and perhaps of volcanic highlands in the Thomas Range (fig. 16C), but the only depositional record of erosion is the detritus incorporated in the beryllium tuff member of the Spor Mountain Formation. There is no evidence for cauldron resurgence (Smith and Bailey, 1968) during this interval; such resurgence should be evident from a moat filling of thick volcanoclastic sediments, intrusive rocks, and lavas along the margin of the caldera. These rocks would have formed soon after ash-flow eruption and cauldron subsidence. None of these features has been observed. The beryllium tuff is a local member that rarely exceeds 60 m in thickness; its conformable relationship with the overlying 21 m.y.-old porphyritic rhyolite member suggests an age close to the latter rather than close to that of the ash-flow tuffs. The oldest post-cauldron intrusive rocks and flows belong to the 21 m.y.-old porphyritic rhyolite, indicating a hiatus in local volcanism of nearly 11 m.y.

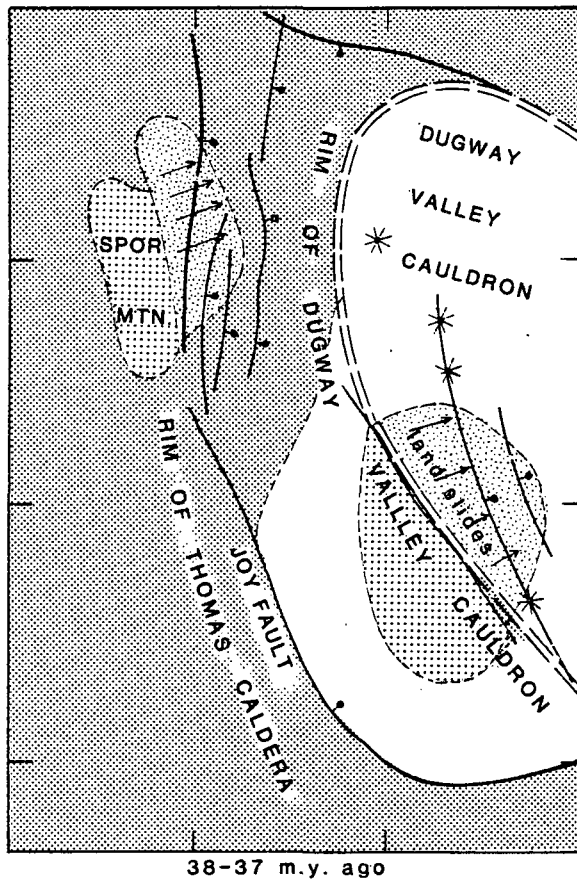
The tuff, tuffaceous sediments, and rhyolite of the Spor Mountain Formation were deposited on the erosional surface that became unconformity C at 21 m.y. ago (fig. 16D). Spor Mountain began to rise above a body of alkali rhyolite magma and to shed detritus into the surrounding area; plugs and vents of the porphyritic rhyolite member formed highlands to the north and east of Spor Mountain and erupted volcanic detritus that became incorporated in the beryllium tuff. A small south- and southwest-flowing stream system developed in The Dell and received detritus from Spor Mountain on the west and volcanic highlands on the east. This detritus collected in local tilted fault blocks, such as the one at Yellow Chief mine. The stream in The Dell

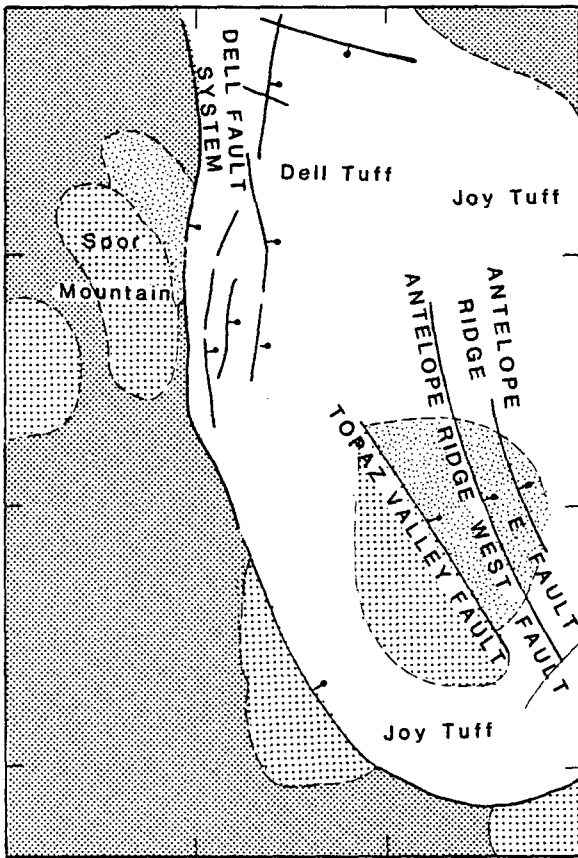
Figure 16.--Structural evolution of the Thomas Range and northern Drum Mountains. A) Map showing surface of unconformity B, about 38-39 m.y. ago, after eruption of the Mt. Laird Tuff and subsidence of the Thomas caldera. B) Map showing results of eruption of the Joy Tuff 38-37 m.y. ago, accompanying subsidence of the Dugway Valley cauldron, and collapse and sliding of cauldron walls. C) Map showing surface of unconformity C, about 30-21 m.y. ago. The Thomas caldera has been filled with intracauldron Joy and Dell Tuffs. The Needles Range Formation has been omitted. D) Map showing volcanism and sedimentation at the time of the Spor Mountain Formation 21 m.y. ago. E) Map showing surface of unconformity D, resulting from block-faulting and erosion 21-7 m.y. ago. F) Map showing results of volcanism 7-6 m.y. ago during the time of the early 11 m.y.



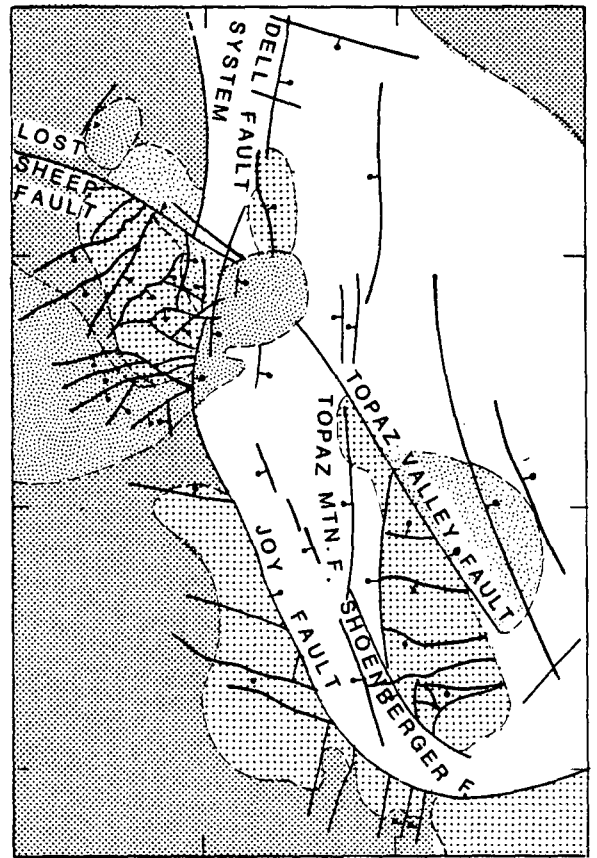
- EXPLANATION
-  Topaz Mountain Rhyolite-- dashed outlines show individual flows and domes
  -  Spor Mountain Formation-- arrows show direction of streamflow inferred for beryllium tuff member
  -  Landslide deposits-- arrows show direction of sliding
  -  Ash-flow Tuffs erupted during or after the Dugway Valley cauldron-- includes Joy Tuff and Dell Tuff
  -  Flows, breccias, and ash-flow tuff erupted prior or during the Thomas caldera-- includes Drum Mountains Rhyodacite and Mt. Laird Tuff
  -  Sedimentary rocks of Devonian to Precambrian age
  -  Undifferentiated rocks (F only)
  -  Depositional or erosional limit (contact)
  -  Fault, dotted where concealed, ball and bar on downthrown side
  -  Probable vent
  -  Structural margin of caldera or cauldron queried (?) where location uncertain

0 8 KILOMETERS



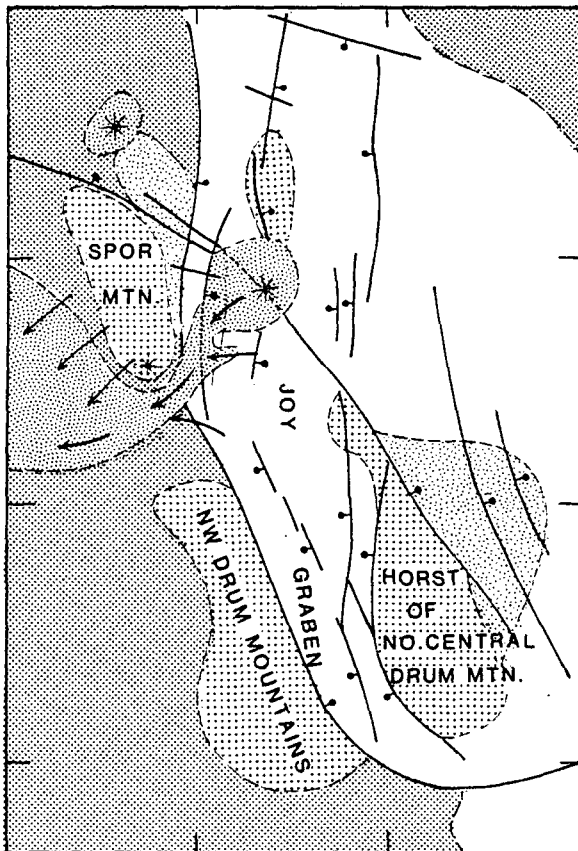


32 m.y. ago

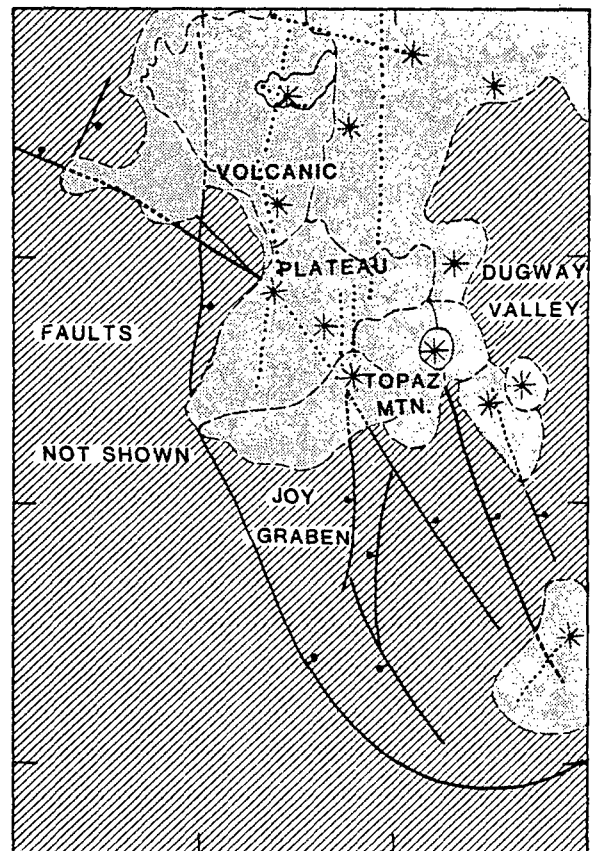


21-7 m.y. ago

0 4 8 KM.



21 m.y. ago



7-6 m.y. ago

flowed across the southern end of present-day Spor Mountain, where its probable location is marked by a modern entrenched drainage that has been superposed across the structural grain of the Spor Mountain block (marked by "SS" on fig. 14B). Fish Springs Flat lay directly downstream from The Dell and received detritus from it and from smaller streams that probably drained southwesterly from Spor Mountain. At the same time, small air falls and flows of ash and pumice from nearby vents covered the drainage basin and were partly reworked by small streams. The tuffs and sediments deposited in this volcano-sedimentary environment--a mixture of tuffaceous breccia containing abundant carbonate clasts, stratified tuff, and epiclastic tuffaceous sandstone and conglomerate--comprise the beryllium tuff member of the Spor Mountain Formation.

Unconformity D represents a long period of block faulting and erosion, from 21 m.y. to 7 m.y. ago, that followed the eruption of the porphyritic rhyolite member of the Spor Mountain Formation (fig. 16E). The period coincides with the time of widespread basin-and-range faulting, during which some faults that formed by cauldron subsidence in the Thomas Range and Drum Mountains were rejuvenated. Blocks of Paleozoic rocks were uplifted at Spor Mountain and in the Drum Mountains. The Spor Mountain Formation was broken into many fault blocks and eroded, so that only part of it remains.

Voluminous flows and domes of the Topaz Mountain Rhyolite began to erupt from vents along old faults about 7 m.y. ago; they covered much of the erosional surface of unconformity D in the Thomas Range (fig. 16F). Quiescent periods of as much as 0.5 m.y. duration interrupted intense rhyolitic volcanism. By the end of volcanism at 6 m.y. ago, rhyolite flows and domes had coalesced to form a large plateau; upland areas of the Thomas Range are still flat, attesting to the once great extent of the plateau surface. During the early stages of eruption, the rhyolite vents erupted abundant pumice and rock fragments which, mixed with detritus from nearby hills, filled valleys and low-lying areas with stratified tuff. The depression left by the Dugway Valley cauldron was nearly filled with tuff and rhyolite at this time.

#### Some unsolved problems

I have sought to integrate the structural development and volcanism of the Thomas Range and northern Drum Mountains into one model which relies on a framework of caldera subsidence and basin-range faulting. The model may require modification if new information can be obtained concerning some problems. These include 1) the location of the east side of the Thomas caldera; 2) the occurrence of large areas of basement within the Thomas caldera that might date from the time of subsidence; 3) the apparent small volume of ash-flow tuff erupted from the caldera at the time of initial subsidence; and 4) the peculiar absence of individual tuffs from parts of the caldera.



Much work remains to be done to locate and verify the east side of the Thomas caldera and the adjacent Keg caldera proposed by Shawe (1972). The east side of the Thomas caldera was projected through the western part of the Keg Mountains by Shawe (1972), but detailed mapping by Staub (1975) in the Picture Rock Hills did not confirm evidence for the ring fracture there. Thick sections of Joy Tuff in the Picture Rock Hills and of the Dell Tuff east of Keg Pass suggests that the caldera margin may be farther east than that projected by Shawe. Dikes and plugs of rhyolite to quartz latite in the northwestern Keg Mountains have been dated at 32 m.y. (Lindsey and others, 1975); they may be intrusions along a ring fracture zone, which was interpreted to be that of the Keg caldera by Shawe (1972). The distribution of intracauldron tuffs and of possible ring-fracture related intrusive rocks and faults should aid in locating the Thomas caldera and smaller calderas nested within it. Additionally, breccias that might indicate tuff vents and collapse of caldera walls should be sought; wall-collapse breccias might be found in the northern part of the Keg Mountains, where volcanic and sedimentary rocks pre-dating ash-flow eruption abound.

The presence of basement areas dating from the time of cauldron subsidence may provide insight into the process of subsidence. Such an area of basement is the horst of the north-central Drum Mountains, a large block (about 14 X 4 km) of Paleozoic rocks that probably has existed since about 37 m.y. ago. The horst provided the source from which landslide megabreccias slid over 37 m.y.-old black glass tuff member after subsidence of the Dugway Valley cauldron. The horst did not exist 38 m.y. ago, when the crystal tuff member of the Joy Tuff flowed west to the wall of the Thomas caldera. Although the horst probably owes much of its present relief to basin-range faulting, its early existence seems likely. Two explanations for its origin are 1) uplift over resurgent magma, and 2) differential subsidence within the caldera complex. Uplift by resurgence is considered unlikely because no intrusive rocks or lava flows are associated with the horst. Consideration of differential subsidence leads to the interesting possibility that the entire caldera complex may reflect incomplete or variable degrees of subsidence. Drilling has revealed a high area of Paleozoic rocks beneath Topaz Mountain Rhyolite near Colored Pass, at the head of Pismire Wash in the Thomas Range, that may indicate another horst. If other positive areas are found within the caldera complex, and if these can be shown to be related to fault blocks that pre-date basin-range structure, then incomplete, differential subsidence will be verified.

The problem of insufficient ash-flow volume for subsidence may reflect inadequate information about the true extent and thickness of ash-flow tuffs. The volume of the Mt. Laird Tuff, believed to be associated with subsidence of the Thomas caldera, is somewhat roughly estimated at 50-100 km<sup>3</sup>. This volume seems small for the size of the Thomas caldera, which is at least 15-25 km across. The accuracy of the volume estimate is severely affected by lack of information about the extent of the 500 m-thick section east of Topaz Mountain. Additional

drilling or geophysical study is needed to determine the volume of tuff beneath Dugway Valley. The combined volume of the Joy and Dell Tuffs, which filled the Thomas caldera and overflowed it to the east, is estimated at approximately 150-200 km<sup>3</sup> if one assumes a once continuous distribution of 180 m of tuff from the Joy fault to Desert Mountain. Such a volume of tuff is compatible with the collapse of the Dugway Valley cauldron and perhaps additional undiscovered cauldrons.

Individual formations of ash flow tuff are absent from parts of the caldera; such distribution would not be expected if a single large area subsided at once. Although the distribution of individual tuffs is incompletely known because of cover and gaps in subsurface information, enough is known to cause suspicion that additional structures related to cauldron subsidence will be found. Such an example is the absence of the Mt. Laird and Joy Tuffs in the caldera throughout the west half of the Thomas Range, and of the Dell Tuff from the compliment of the caldera. Such a distribution may be caused by a separate time of subsidence for the northwest part of the caldera, perhaps later than the 39-38 m.y. eruptions of the Mt. Laird and Joy Tuffs. Nevertheless, no structure delineating a separate subsidence feature is evident. A second explanation is that of differential subsidence; the northwest part of the caldera may not have collapsed as much as the south and east parts; only after these were filled with tuff could the Dell Tuff flow into the northwest part of the caldera. A third explanation is that long periods of erosion removed so much ash-flow tuff that the present distribution beneath rhyolite flows and alluvium is spotty. Long gaps in the record of volcanism, as shown by the ages of volcanic formations, provide time for extensive erosion. If so, the detritus from such erosional epochs must have been carried beyond the volcanic field, because no volcanic sediments in the area are of sufficient volume to account for the detritus. Available evidence does not permit a definitive explanation for the exclusion of individual tuffs from parts of the Thomas caldera.

## CHEMICAL COMPOSITION OF VOLCANIC ROCKS

### Rock types

Most of the volcanic rocks of the Thomas Range and northern Drum Mountains are believed to have been derived from local vents. Only the ash-flow tuff of the Needles Range Formation may be from a distant source. Thus, from geographic considerations, magmas beneath the Thomas Range and Drum Mountains could have produced the entire volcanic sequence and the small plutons associated with it, with the possible exception of the Needles Range Formation. Accordingly, the composition of all volcanic units except the Needles Range is compared (fig. 17).

There are three time-dependent rock types among the indigeneous rocks of the Thomas Range and northern Drum Mountains. In the classification of Rittmann (1952), the three types are 1) rhyodacite and quartz latite of 42 and 39 m.y. ago (Drum Mountains Rhyodacite and Mt.

Laird Tuff), 2) rhyolite of 38 to 32 m.y. ago (Joy and Dell Tuffs), and 3) alkali rhyolite of 21 and 7-6 m.y. ago (Spor Mountain Formation and Topaz Mountain Rhyolite) (fig. 17). Rhyodacite and quartz latite, erupted as both flows and tuffs, are characterized by about 60-67 percent  $\text{SiO}_2$ , 14-19 percent  $\text{Al}_2\text{O}_3$ , 4-8 percent total Fe as  $\text{Fe}_2\text{O}_3$ , 2-4 percent MgO, 4-6 percent CaO, 2-4 percent each of  $\text{Na}_2\text{O}$  and  $\text{K}_2\text{O}$ , and 0.6-1.1 percent  $\text{TiO}_2$ . The rhyodacite and quartz latites are about the same age and close in overall composition to the intermediate-composition volcanic rocks in the Little Drum Mountains described as shoshonitic by Leedom (1974) and Pierce (1974). Rhyolite, erupted as ash-flow tuffs, and alkali rhyolite, erupted as flows and tuffs, both contain 74-79 percent  $\text{SiO}_2$ , 11-14 percent  $\text{Al}_2\text{O}_3$ , 1-2 percent total Fe as  $\text{Fe}_2\text{O}_3$ , and less than 1 percent MgO; both are of calc-alkalic affinity, as will be shown below. The two rock types differ from each other in that the alkali rhyolite contains slightly less CaO than the rhyolite (commonly less than 1.0 percent, but ranging as high as 2 percent, versus 1-2 percent for the rhyolite), more  $\text{Na}_2\text{O}$  (generally 3-4 percent versus 1-3 percent for the rhyolite), slightly more  $\text{K}_2\text{O}$  (generally 4-5.5 percent versus 3-5 percent for the rhyolite), and less  $\text{TiO}_2$  (generally 0.05-0.15 percent versus 0.2-0.3 percent for the rhyolite). Alkali rhyolite also differs from rhyolite in that it contains as much as 0.77 percent fluorine (Staatz and Carr, 1964, p. 110; Shawe, 1966). The high fluorine content of alkali rhyolite is reflected in the widespread occurrence of topaz in that rock.

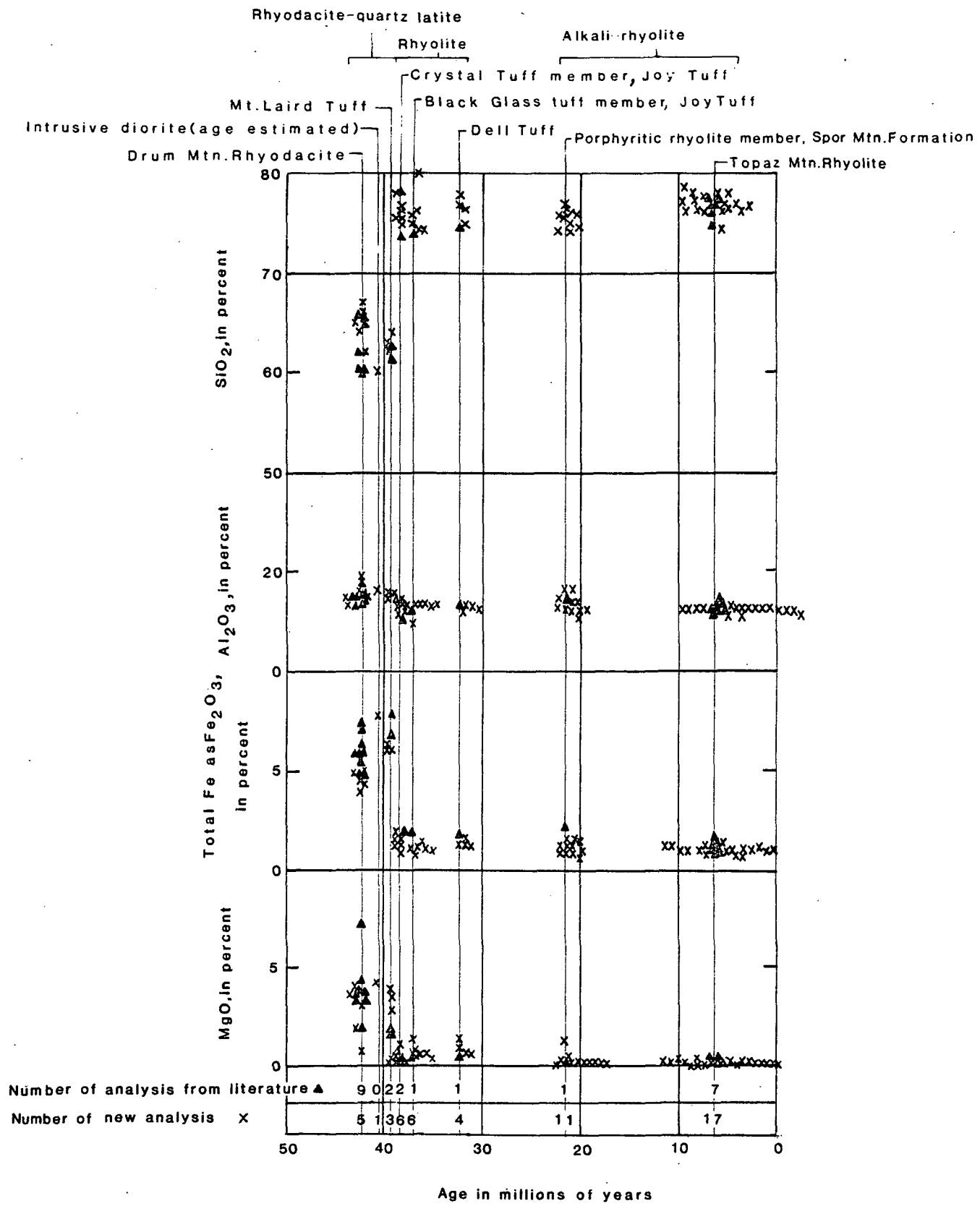
Rocks intermediate in composition between rhyodacite-quartz latite, rhyolite, and alkali rhyolite are not present (fig. 17). Shifts in composition from one rock type to the next were abrupt, not gradual. For example, the age of the Mt. Laird Tuff is intermediate between the Drum Mountains Rhyodacite and the Joy Tuff, but the composition of the Mt. Laird Tuff closely resembles that of the Drum Mountains Rhyodacite and is distinctly different from the slightly younger rhyolite of the Joy Tuff.

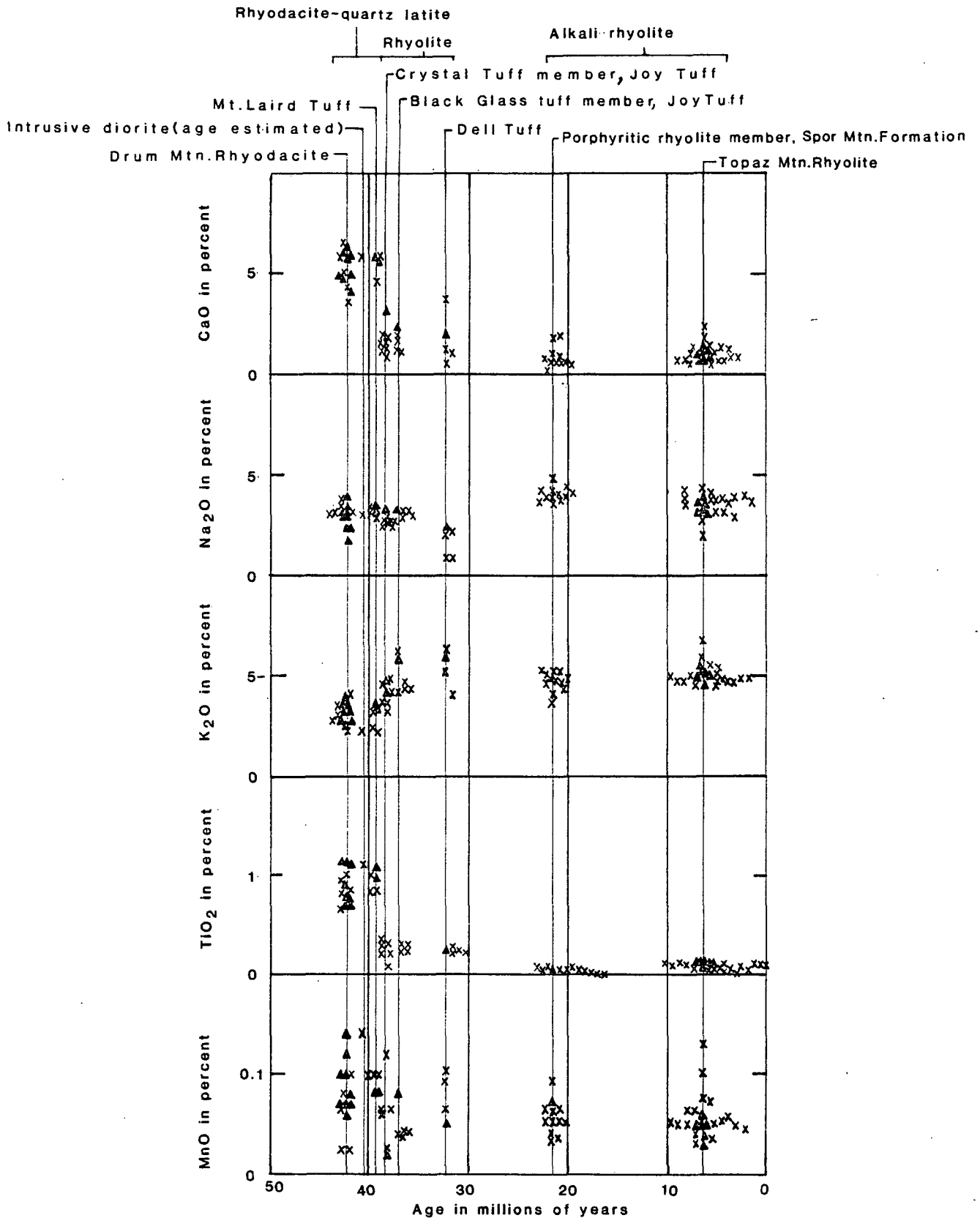
Comparison of total alkali versus silica contents of all three types indicates that they are within the field of subalkalic suites (fig. 18) (Irvine and Barager, 1971). The rocks also fall within the calc-alkalic field of Irvine and Barager on an AFM diagram (fig. 19). The three rock types tend to define separate fields in the alkali-silica and AFM diagrams, however, thus supporting the previous observation that volcanic products having compositions intermediate between these rock types are not present. The fields of rhyolite and alkali rhyolite occur close together and might be considered as one, but the rocks of each type plot as a coherent group having only partial overlap. Soda equals or exceeds potash in most of the rhyodacites and quartz latites, but potash dominates soda in the rhyolites and alkali rhyolites.

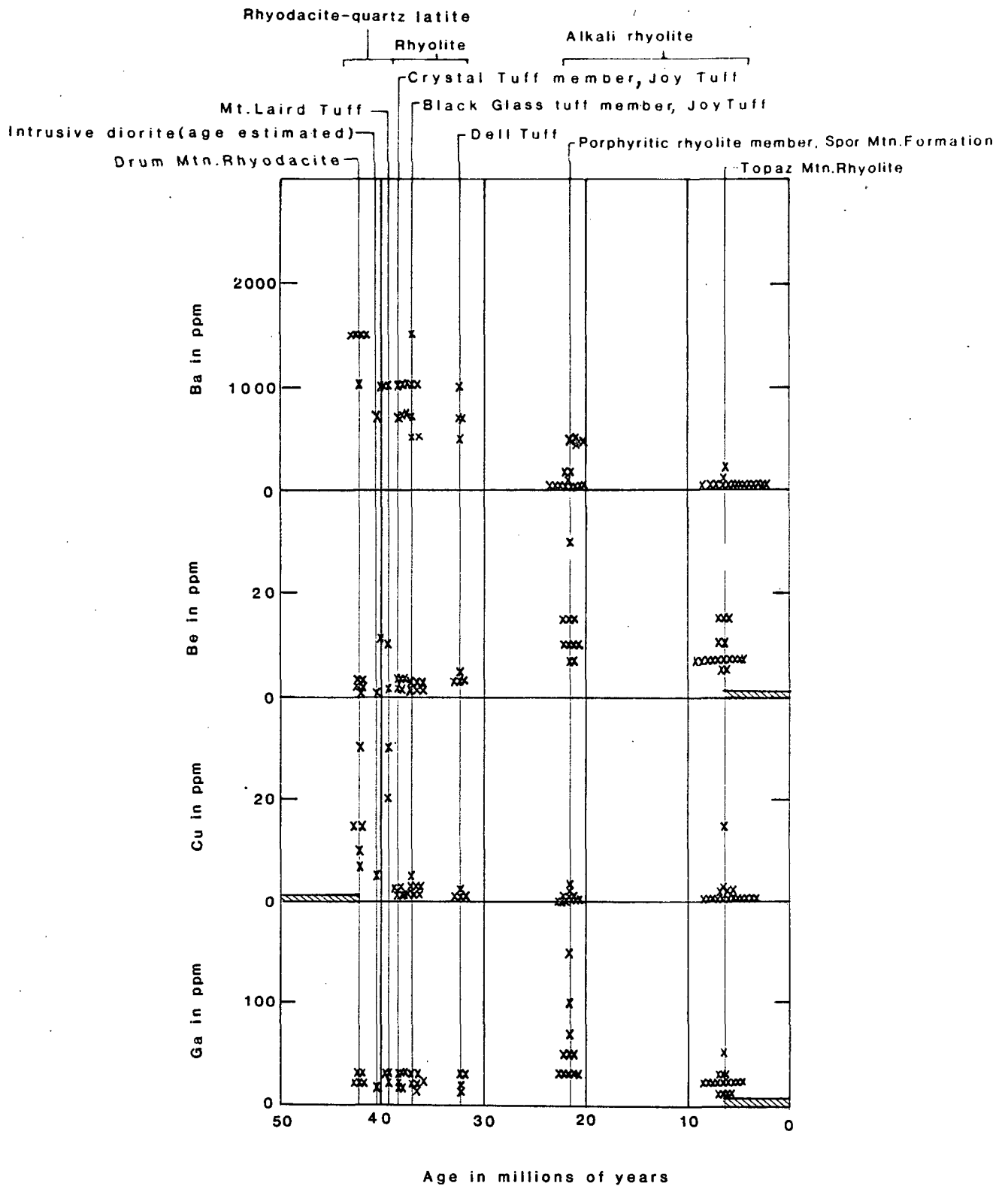
#### Trace element associations

The three rock types are sharply defined by their trace element association; rhyodacite-quartz latite contains chalcophile and

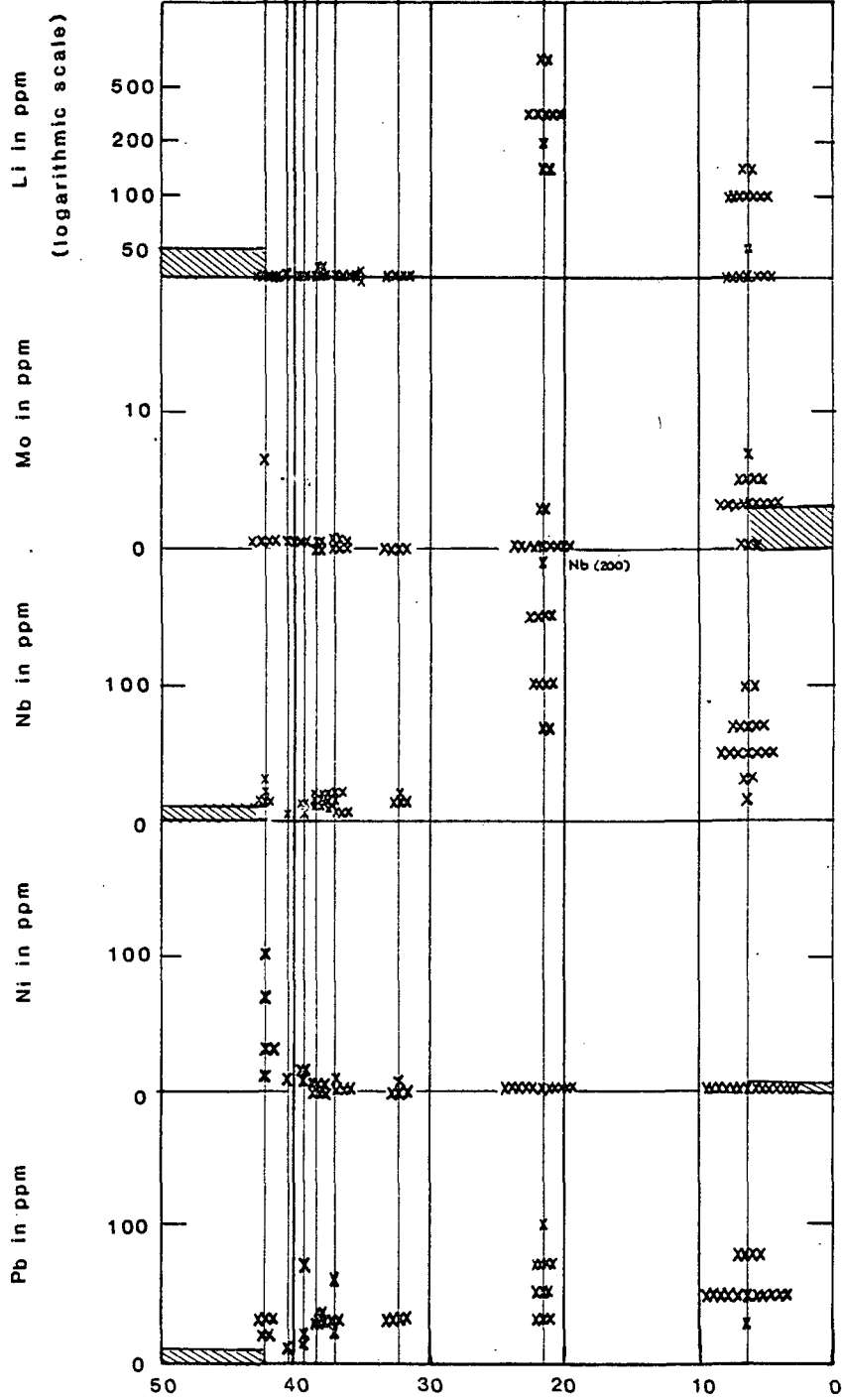
Figure 17.--Chemical compositions, including trace elements, compared to the ages of igneous rocks in the Thomas Range and northern Drum Mountains, Juab County, Utah. Shaded areas below some scales show limit of detection when some samples were below the limit. Analyses of major oxides from the literature are from Staatz and Carr (1964, p. 110), Newell (1971, p. 38), and Hogg (1972, p. 180). New chemical analyses are in table 8 (Appendix).







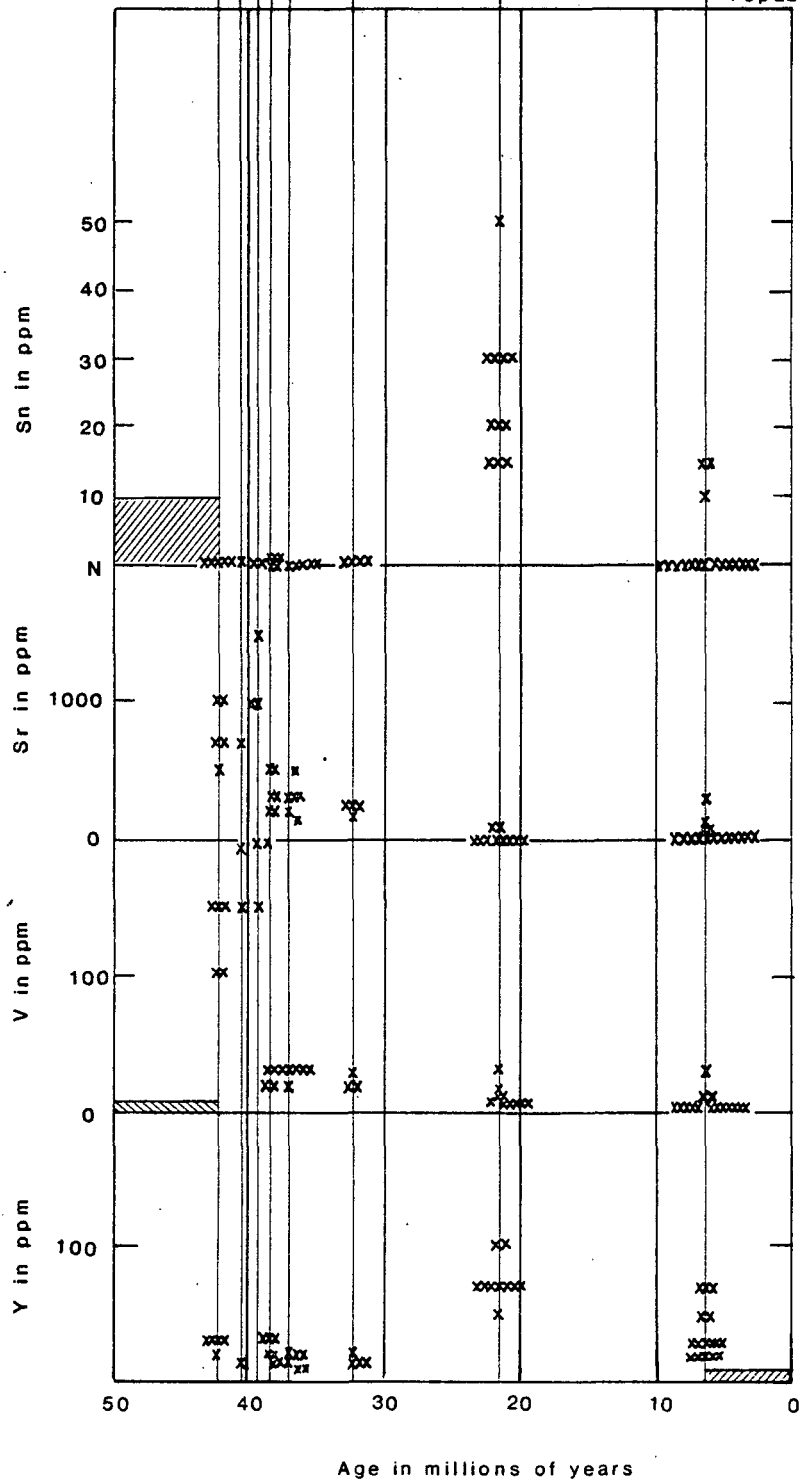
Rhyodacite-quartz latite  
 Rhyolite  
 Alkali-rhyolite  
 Crystal Tuff member, Joy Tuff  
 Mt. Laird Tuff  
 Black Glass tuff member, Joy Tuff  
 Intrusive diorite (age estimated)  
 Dell Tuff  
 Porphyritic rhyolite member, Spor Mtn. Formation  
 Drum Mtn. Rhyodacite  
 Topaz Mtn. Rhyolite



Age in millions of years



Rhyodacite-quartz latite  
 Rhyolite  
 Alkali rhyolite  
 Crystal Tuff member, Joy Tuff  
 Black Glass tuff member, Joy Tuff  
 Mt. Laird Tuff  
 Dell Tuff  
 Porphyritic rhyolite member, Spor Mtn. Formation  
 Intrusive diorite (age estimated)  
 Drum Mtn. Rhyodacite  
 Topaz Mtn. Rhyolite



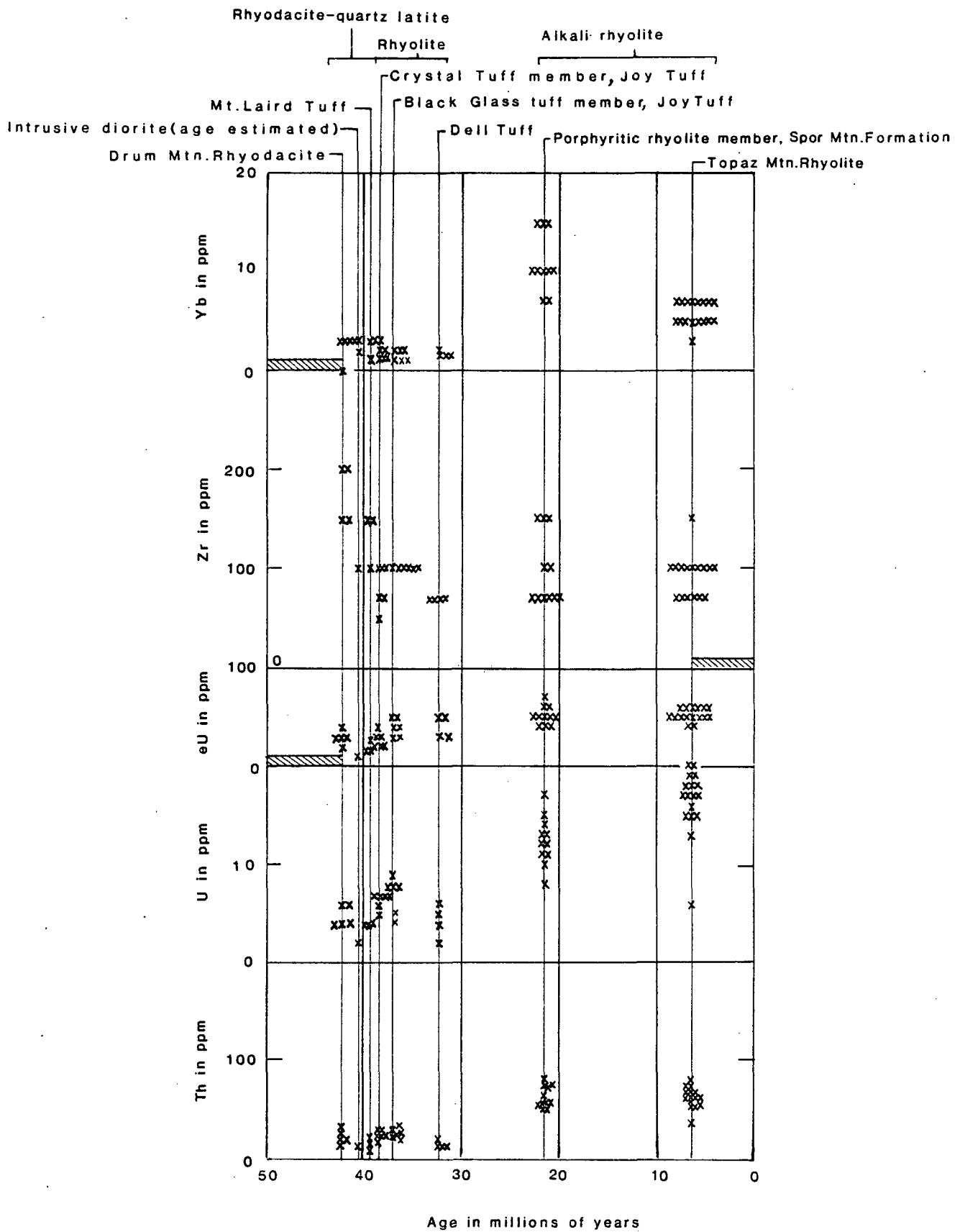
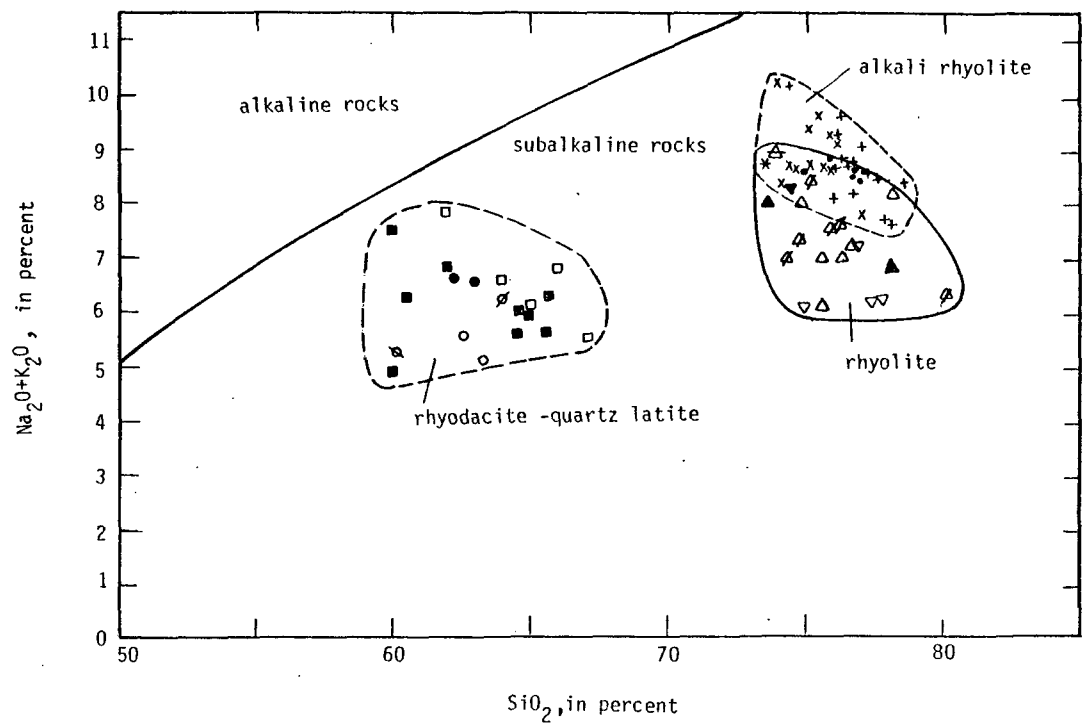
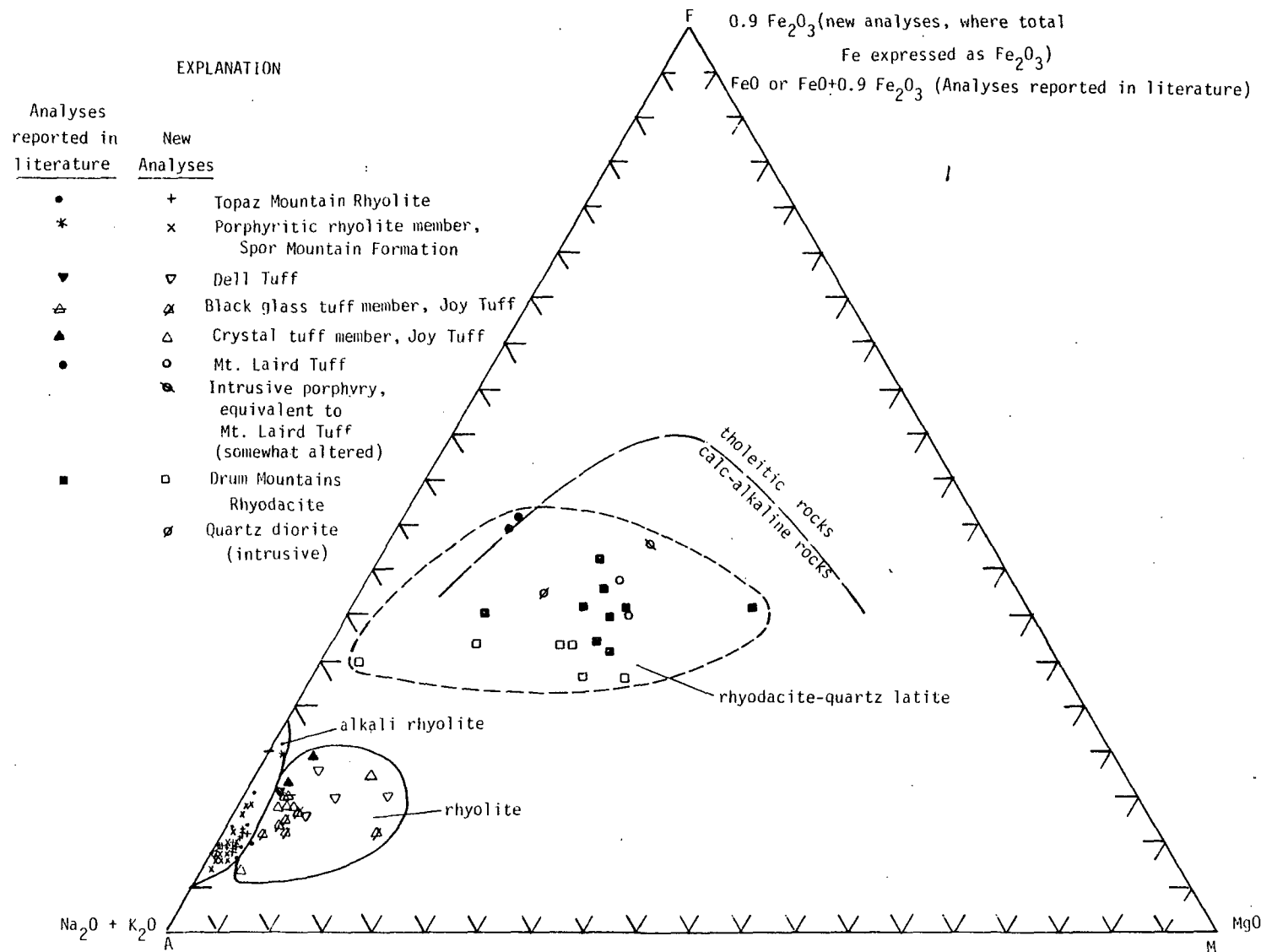


Figure 18.--Total alkalis ( $\text{Na}_2\text{O}$  plus  $\text{K}_2\text{O}$ ) versus silica content of igneous rocks of the Thomas Range and northern Drum Mountains. Analyses have been recalculated to total 100 percent and to exclude volatile components. Analyses reported in literature are from Staatz and Carr (1964, p. 113), Newell (1971, p. 43), and Hogg (1972, p. 180). Line separating alkalic from subalkalic rocks from Irvine and Baragar (1971).



EXPLANATION	
Analyses reported in literature	New analyses
•	+ Topaz Mountain Rhyolite
*	x Spor Mountain Formation, porphyritic rhyolite member
▼	▽ Dell Tuff
⊕	⊕ Joy Tuff, black glass tuff member
▲	△ Joy Tuff, crystal tuff member
●	○ Mt. Laird Tuff
⊗	⊗ Intrusive porphyry, equivalent to the Mt. Laird Tuff (somewhat altered)
⊗	⊗ Intrusive diorite
■	□ Drum Mountains Rhyodacite

Figure 19.--AFM diagram of igneous rocks of the Thomas Range and northern Drum Mountains. Analyses reported in literature are from Staatz and Carr (1964, p. 113), Newell (1971, p. 43), and Hogg (1972, p. 180). Line separating tholeiitic from calc-alkalic rocks from Irvine and Barager (1971).



concentration of uranium in alkali rhyolite, with individual crystals containing as much as one percent uranium. Uranium in zircon from rhyodacite-quartz latite and rhyolite does not exceed 1200 ppm. The high concentration of uranium in alkali rhyolite is considered to be magmatic.

The uranium content of all volcanic rocks in the Thomas Range and Drum Mountains is high, compared to that of volcanic rocks from orogenic belts. Only two rock samples having less than 4 ppm uranium were measured in the Thomas Range-Drum Mountains area, whereas uranium from volcanic rocks in orogenic belts is commonly as little as 1-4 ppm. Volcanic rocks collected from two transects in the central Andes generally did not contain more than about 4 ppm uranium (Zentilli and Dostal, 1977). Volcanic rocks of basaltic to rhyolitic composition in northern New Zealand contain less than 3.4 ppm uranium (Ewart and Stipp, 1968), and rocks of basaltic to intermediate composition in island arcs north of New Zealand generally contain less than 1 ppm uranium (Ewart and others, 1977). The uranium content of the Utah rocks is not unique in the western United States, however, where rhyolitic rocks containing 5-20 ppm uranium and more are common (Zielinski, 1978).

#### Relationship of volcanism to mineralization

The time-dependent rock types are associated with distinctive types of mineralization. Rhyodacite-quartz latite volcanism was associated with chalcophile and siderophile metal mineralization, rhyolite volcanism was barren, and alkali rhyolite volcanism was associated with lithophile metal mineralization. The types of mineralization are characterized broadly by the same trace elements that mark the types of igneous rocks.

Early rhyodacite-quartz latite volcanism was associated with sulfur-rich chalcophile mineralization, as illustrated by the occurrence of copper minerals and jarosite in small plutons that may overlie a blind mineralized pluton in the Joy area (Stalker, cited in Newell, 1971). Siderophile mineralization, as illustrated by the manganese, iron, gold-bearing jasperoid, and kaolin deposits of the Drum Mountains (Crittenden and others, 1961; McCarthy and others, 1969; Newell, 1971) probably belongs to the period of chalcophile mineralization when acid, sulfur-rich solutions leached these metals from country rock, concentrated them in fissures and fault zones, and left leached areas of pure clay. Most chalcophile and siderophile mineralization in the Drum Mountains appears to have been confined to rocks older than the Joy Tuff.

Most of the occurrences of the lithophile metals, including beryllium and uranium, are in the beryllium tuff member, which is the oldest representative of alkali rhyolite volcanism. Deposition of fluorspar pipes in Paleozoic rocks on Spor Mountain also probably accompanied alkali rhyolite volcanism. Sulfur is believed to have been sparse or absent during lithophile metal mineralization. Some

Table 6.--Analytical data for uranium content of zircon in volcanic rocks of the Thomas Range. Neutron dose determined by C. W. Naeser. Estimated ages of volcanic rocks are listed for comparison.

Sample number	Rock unit	Sample location in T. 12 S., R. 12 W.	Number of grains	Induced tracks in detector		Neutron dose (neutrons/cm <sup>2</sup> )	Uranium (ppm) <sup>1/</sup>		Estimated age (m.y.) of rock unit
				Number counted	Density (tracks/cm <sup>2</sup> )		Average	Range	
Alkali rhyolite									
U15	Topaz Mountain Rhyolite	SW1/4, sec. 14	20	597	7.46x10 <sup>6</sup>	9.06x10 <sup>13</sup>	4800	3200-11000	6.3-6.8 <sup>2/</sup>
U26	Porphyritic rhyolite member of Spor Mountain Formation	NE1/4, sec. 9	20	794	9.92x10 <sup>6</sup>	9.23x10 <sup>13</sup>	6300	1400-9400	21.3
U7A	do.	SW1/4, sec. 36	20	703	8.79x10 <sup>6</sup>	9.14x10 <sup>13</sup>	5700	4200-7600	21.3
U12B-1	Bentonite at Yellow Chief Mine (Beryllium tuff member of Spor Mountain Formation)	NW1/4, sec. 36	A <sup>3/</sup> 10	250	5.68x10 <sup>6</sup>	9.97x10 <sup>14</sup>	340	120-770	21.3 <sup>5/</sup>
			B <sup>4/</sup> 20	494	6.18x10 <sup>6</sup>	1.05x10 <sup>14</sup>	3500	2200-4500	
Rhyolite									
T54-A	Dell Tuff	SE1/4, sec. 26	20	717	8.96x10 <sup>6</sup>	1.00x10 <sup>15</sup>	530	220-1200	32.0
T42-A	do.	NW1/4, sec. 36	10	493	1.23x10 <sup>7</sup>	1.24x10 <sup>15</sup>	580	300-830	32.0
Rhyodacite-quartz latite									
U10A	Drum Mountains Rhyodacite	SW1/4, sec. 35	8	345	1.20x10 <sup>6</sup>	9.33x10 <sup>14</sup>	80	30-80	~42

<sup>1/</sup> U ppm =  $\frac{\text{Induced track density (5.88x10}^{10}\text{)}}{\text{Neutron dose}}$ . Concentrations of U are rounded to two significant digits.

<sup>2/</sup> Age estimated by association with dated flows.

<sup>3/</sup> Population A is about 10% of total zircon and contains low uranium zircon dated at 28.3±1.8 m.y. and 40.0±7.0 m.y.

<sup>4/</sup> Population B is about 90% of total zircon and contains high uranium zircon that could not be dated.

<sup>5/</sup> Based on geologic relations and correlation of high-uranium zircon (population B) with volcanism related to porphyritic rhyolite of Spor Mountain Formation.



beryllium, fluorite, and uranium were deposited after eruption of the Topaz Mountain Rhyolite 6-7 m.y. ago (Lindsey and others, 1975; Zielinski and others, 1977) but I now believe that late mineralization was relatively minor because of the lack of mineral deposits in the Topaz Mountain Rhyolite and their relative abundance in the older Spor Mountain Formation. The major period of lithophile metal mineralization probably occurred between 7 and 21 m.y. ago, when deposits of low-grade beryllium, uranium, and fluorite were formed in the beryllium tuff member of the Spor Mountain Formation. There is no evidence to associate uranium or other lithophile metal mineralization with the caldera cycle.

#### Origin of volcanic rocks

The volcanic rocks of the Thomas Range and the northern Drum Mountains were formed in three distinct stages, much as originally proposed by Shawe (1972). (1) Older flow rocks and tuffs of rhyodacite-quartz latite composition were erupted from small central volcanoes and fissures in late Eocene time. Initial subsidence of the Thomas caldera accompanied eruption of the Mt. Laird Tuff. Volcanism was accompanied by emplacement of small plutons and by chalcophile and siderophile metal mineralization. (2) The composition of volcanic products switched abruptly to rhyolitic ash-flow tuff in latest Eocene and Oligocene time. Eruption of tuff was accompanied by collapse of the Dugway Valley cauldron. Rhyolitic ash-flow volcanism in latest Eocene and Oligocene time probably was not followed by cauldron resurgence and probably was not accompanied by mineralization. (3) Alkali rhyolite volcanism accompanied basin-and-range faulting in Miocene time, producing tuffs, flows, and small plutons. Block faulting of basin-and-range type rejuvenated earlier faults and was accompanied by local erosion and sedimentation that mixed detritus with the tuffs. Fluorine and lithophile metal mineralization accompanied alkali rhyolite volcanism. Reconnaissance studies by Shawe (1972) and me indicate that, in general, the Tertiary history of the Keg Mountains resembles that of the Thomas Range and Drum Mountains.

All of the volcanic rocks could have originated by crustal fusion; alternatively, they may have originated by partial melting of the mantle and contamination with considerable crustal material. These ideas are compatible with Sr data evidence for continental felsic rocks in general (Hedge, 1966) and with Sr isotopic compositions of plutonic rocks nearby (Moore and others, 1979). The high content of silica, alkalis, thorium, and uranium in the entire volcanic pile support a crustal contribution, and is in contrast to the low content of these elements in volcanic rocks that are clearly derived from the mantle or from oceanic crust (e.g., Ewart and others, 1977).

Abrupt switches from rhyodacite-quartz latite to rhyolite to alkali rhyolite volcanism through time, accompanied by contemporary changes in magmatic trace element associations and types of mineralization, suggest that each magma was produced by fusion of a different region of the

mantle or crust, or that differentiation proceeded in three steps. If the magmas originated by fusion, it may have been partial or complete; if the latter, differentiation may have been necessary to concentrate lithophile elements. Petrographic evidence for an ancestral mafic magma for the Drum Mountains Rhyodacite and Mt. Laird Tuff permit a magmatic history beginning with fusion in the upper mantle followed by upward migration and major contamination with crustal material. The magmas were deep enough, or lacked the necessary vapor pressures, to prevent collapse over magma chambers during most rhyodacite-quartz latite volcanism, except during eruption of the Mt. Laird Tuff. The Mt. Laird magma may have migrated to a relatively high level in the crust before explosive eruption and crustal subsidence, as indicated also by plugs and dikes of Mt. Laird composition in the Drum Mountains. The magma chambers of the rhyolitic tuffs were shallow enough and the vapor pressure great enough for subsidence to occur during eruption. Such rhyolitic tuffs have been regarded as differentiates of calc-alkalic magma like the Drum Mountains Rhyodacite (Lipman and others, 1972).

The extreme enrichment of lithophile metals in the alkali rhyolite magmas may have resulted from differentiation, or from fusion of Precambrian rocks already enriched in these elements. Origin by differentiation would yield a large volume of mafic magma; there is no evidence for mafic magmas except the very young (<1 m.y.) basalt at Fumarole Butte. Origin by crustal fusion would require lithophile-metal-rich rocks nearby. Granitic and clastic metasedimentary terranes of Precambrian age are exposed beneath Paleozoic rocks nearby, as in the Deep Creek Mountains (Bick, 1966), at Granite Mountain (Fowkes, 1964), and in the Simpson and Sheeprock Mountains (Cohenour, 1959). Partial fusion or remobilization of Precambrian terrane having a high content of lithophile metals has been proposed as a source for alkali rhyolite magma and mineralizing solutions that formed beryllium deposits at Spor Mountain (Moore and Sorensen, 1978). Metamorphism of Precambrian terrane during Tertiary time has been documented for the Grouse Creek and Raft River Mountains, located about 200 km north of the Thomas Range (Compton and others, 1977). Reheating of Precambrian granitic terrane may have occurred also at Granite Mountain, where Precambrian biotite-gneiss and granite are cut by beryl-bearing pegmatite veins of Tertiary age only 20 km north of the Thomas Range (Park, 1968; Moore and Sorensen, 1978).

The volcanic history inferred for the Thomas Range and Drum Mountains supports the broad outlines of volcanism and basin-and-range development as proposed by Lipman, Prostka, and Christiansen (1972) and Christiansen and Lipman (1972) and elaborated more recently by Snyder, Dickinson, and Silberman (1976). They proposed that calc-alkalic volcanism of early to middle Tertiary age developed in response to subduction of the Farallon plate beneath the American plate, that calc-alkalic volcanism and subduction ended in Miocene time when the Farallon plate was consumed west of the basin and range province, and that the basin-and-range structure and fundamentally basaltic volcanism, including bimodal basalt-rhyolite, developed in response to crustal

attenuation caused by strike-slip movement between the Pacific and American plates. Two imbricate, easterly dipping subduction zones, one under the present basin and range, and the other under the Rocky Mountains, were proposed to account for calc-alkalic volcanism of the type represented by rhyodacite-quartz latite and rhyolite in the Thomas Range and Drum Mountains.

In their model, Lipman, Prostka and Christiansen (1972, p. 237) noted the Thomas Range as one of two areas of volcanic rocks having high  $K_2O$  contents indicative of an anomalously shallow depth to the western Benioff zone, and thus possibly reflecting a zone where the descending slab was decoupled from the crust. Correct estimation of the depth to the Benioff zone in western Utah is complicated, however, by the very slight systematic variation of  $K_2O$  with  $SiO_2$  in rhyodacite and quartz latite (Hogg, 1972; Leedom, 1974). In any case, the switch from calc-alkaline to fundamentally basaltic volcanism, represented in western Utah by alkali rhyolite, occurred at 21 m.y., somewhat early for the plate tectonic model as refined by Snyder, Dickinson, and Silberman (1976).

Alkali rhyolite volcanism was probably contemporaneous with extensional basin-and-range faulting in the Thomas Range and Drum Mountains, as indicated by widespread faults in all rocks 21 m.y. and older and only a few faults in rocks 6-7 m.y. old. Basin-and-range faulting is generally regarded as having begun about 16-17 m.y. ago (McKee and others, 1970; Noble, 1972). In the Thomas Range, basin-and-range faulting included rejuvenation of caldera ring features, as indicated by evidence for recurring movement along the faults of The Dell.

## URANIUM OCCURRENCES

Uranium occurs in four diverse settings in the Thomas Range: 1) in fluorspar pipes in Paleozoic rocks of Spor Mountain, 2) associated with beryllium deposits in stratified tuff and tuffaceous breccia of the beryllium tuff member of the Spor Mountain Formation, 3) in tuffaceous sandstone and conglomerate of the beryllium tuff member at the Yellow Chief mine, and 4) in veinlets of opaline silica in volcanic rocks of all ages.

Production and reserves are limited, but resources may be large. The pipes have produced fluorspar, but no production of uranium has been reported. The uranium deposits in the beryllium tuff member are large but of low grade (0.0x percent); no uranium has been recovered as a byproduct of beryllium mining. The only production of uranium from the area has been from the Yellow Chief mine, which produced more than 90,000 metric tons of ore having a grade of 0.20 percent  $U_3O_8$  (Bowyer, 1963). Veinlets of uraniferous opal, such as those at the Buena No. 1 and Autunite No. 8, have been prospected but none has produced ore. Analyses of samples from several prospects indicate a maximum grade of about 0.2 percent uranium (Staatz and Carr, 1964, p. 152-154).

All of the uranium occurrences were formed as a result of alkali rhyolite volcanism that accompanied basin-and-range faulting; some were formed by hydrothermal activity and others by ground water leaching of the products of volcanism. The fluorspar pipes, beryllium deposits, and probably the uraniferous opal veinlets were formed by hydrothermal activity that accompanied volcanism. No primary uranium minerals have been found; uranium in fluorspar pipes and in nodules and veinlets in the beryllium deposits is dispersed in fluorite and opal. Yellow secondary uranium minerals are common. Deposits at the Yellow Chief mine consist entirely of secondary uranium minerals that were precipitated from ground water; the uranium there probably was derived by ground water leaching of nearby hydrothermal deposits or uranium-rich volcanic rocks.

### Uranium in fluorspar pipes

Uraniferous fluorspar pipes are numerous throughout Spor Mountain along faults and fractures in Paleozoic rocks; no new work was done and the information presented in this report is summarized from Staatz and Carr (1964). Analyses of fluorspar show a range of 0.003-0.33 percent uranium (Staatz and Carr, 1964, p. 135). Some of the most uraniferous fluorspar (0.10-0.20 percent range of  $U_3O_8$ ) occurs near the Bell Hill mine, at the southeastern end of Spor Mountain. Most of the pipes are small, the largest reported being 47 by 32 m, and they commonly diminish in size at depth (Staatz and Carr, 1964, p. 130).

## Uranium in the beryllium tuff member of the Spor Mountain Formation

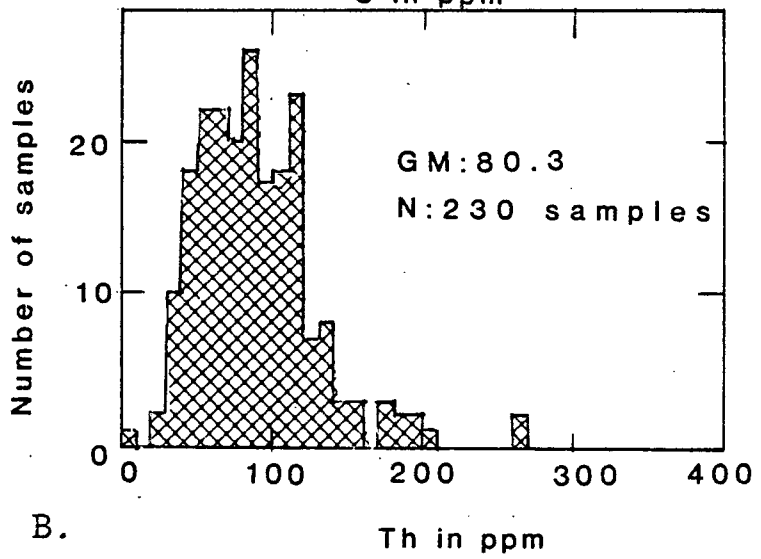
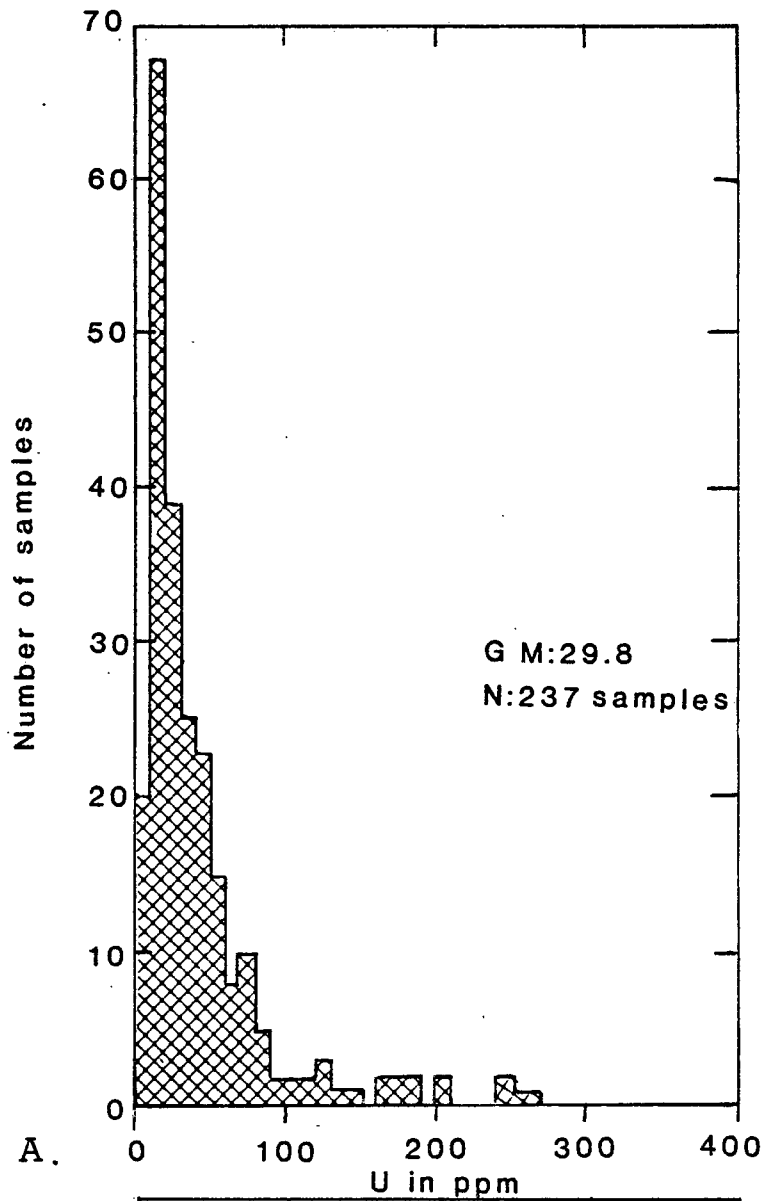
Stratified tuff and tuffaceous breccia of the beryllium tuff member contain low grade concentrations of uranium as well as economic deposits of beryllium. Epiclastic tuffaceous sandstone, a facies of the beryllium tuff at the Yellow Chief mine, contained minable quantities of beta-uranophane; this deposit will be discussed separately. Deposits of beryllium in tuff include the North End, Taurus, Sigma Emma, Monitor, Roadside, Fluro, Rainbow, and Blue Chalk claims southwest of Spor Mountain, and the Oversight, Hogsback, and Claybank claims in The Dell (fig. 2). Most of these claims contain uranium, also. Previous work has indicated that uranium in the beryllium tuff member is most abundant in and near beryllium ore (Park, 1968; Lindsey and others, 1973), but new data presented here contradict that presumption.

Uranium of hydrothermal origin (as much as 2000 ppm) occurs with beryllium in the structure of fluorite and opal in zoned nodules in the beryllium tuff member (Lindsey and others, 1973; Lindsey, 1978). Fission track maps of fluorite and opal nodules show uniform and zonal distributions of uranium, but no point sources that might indicate the presence of pitchblende or other uranium minerals. Such uranium must have been deposited with fluorite as a result of the breakdown of stable fluoride complex ions of beryllium and uranium (Lindsey and others, 1973), and thus is regarded to have been introduced by hydrothermal fluids. The absence of pyrite, other sulfide minerals, and tetravalent uranium minerals indicates that the mineralizing fluids had a very low  $a_{S^{2-}}$  and a high Eh and pH relative to the stability fields of sulfides and pitchblende.

Yellow secondary uranium minerals occur dispersed in the beryllium tuff member and these form ore deposits at the Yellow Chief mine. Such accumulations are evidently of ground water origin and may reflect leaching and remobilization of magmatic or hydrothermal uranium in the beryllium tuff member. Little is known about the possible residence of uranium in other minerals, such as smectite, which comprises most of the tuff in altered areas.

The overall abundance of uranium and thorium in part of the beryllium tuff member of the Spor Mountain Formation is indicated by analyses of drill hole cuttings from southwest of Spor Mountain (secs. 8 and 9, T. 13 S., R. 12 W.) (fig. 20). These cuttings, supplied to the U.S. Geological Survey by the Vitro Minerals Corporation, are from drill holes that penetrated most of the tuff section, and thus should adequately reflect the overall character of the tuff in the area of the drillholes. Histograms (fig. 20) are skewed toward high values of U and Th, indicating that the underlying frequency distributions may have been modified by processes that concentrated U and Th in the tuff. The original (premineralization) content of U and Th in the tuff is probably approximated by the modes of about 20 ppm U and about 80 ppm Th. The resulting Th/U ratio of about 4/1 is a reasonable value for these

Figure 20.--Histograms showing the abundance of A, uranium, and B, thorium in the beryllium tuff member, as shown by analysis of 237 samples from drill holes southwest of Spor Mountain. Analyses by delayed neutron method by H. T. Millard, Jr., A. J. Bartel, R. J. Knight, P. Hemming, J. O'Kelley, and R. White.



elements in igneous rocks, and it is close to that of about 5/1 for the overlying porphyritic rhyolite member of the Spor Mountain Formation. The porphyritic rhyolite contains a range of 50-79 ppm Th (average of 62 ppm) and 8-17 ppm U (average of 11 ppm).

The occurrence of uranium and thorium relative to beryllium in tuff is illustrated by analyses of cuttings from a drill hole at the Roadside beryllium deposit (hole 1 of Griffiths and Rader, 1963; and Lindsey and others, 1973) (fig. 21). There, beryllium-fluorite mineralization and attendant hydrothermal alteration were generally concordant to bedding and were most intense in the upper part of the tuff. Feldspathic tuff occupies the uppermost 18 m and lowermost 9 m of a drilled section; incompletely altered argillic tuff occupies the intervening space. The upper 6 m of tuff contains beryllium ore and conspicuous fluorite, the underlying 18 m of tuff contains abundant calcite and lithium (in trioctahedral smectite), and the remaining tuff contains abundant dolomite. The latter zonation reflects the increasing intensity of hydrothermal alteration from bottom to top. Uranium and thorium are most abundant below the beryllium ore, in the upper 10 m of the calcite-rich tuff. There, uranium ranges from 88 to 163 ppm. Tuff that contains more than 100 ppm Be and includes a beryllium ore zone contains only 38-74 ppm U. Thus, uranium and thorium tend to occur separately from beryllium ore.

The abundance of both uranium and thorium in drill hole cuttings of tuff support a magmatic-hydrothermal origin for these elements, but wide variation in the Th/U ratio indicates leaching and reconcentration of uranium with respect to thorium in some of the tuff. If an overall Th/U ratio of about 4/1 is used as a guide, it is evident that tuff having a higher Th/U ratio has been leached of uranium whereas tuff having a lower Th/U ratio has been enriched. A Th/U ratio of about one is associated with the highest concentrations of uranium in the drill hole cuttings (fig. 21), indicating that these uranium concentrations reflect enrichment of uranium; such enrichment may have been by hydrothermal fluids or by ground water.

Additional evidence that uranium concentrations occur in the beryllium tuff member separately from those of beryllium is provided by analyses of drill hole cuttings of selected mineralized zones (Glanzman and Meier, 1979) (fig. 22). These data are from drill cuttings provided to the U.S. Geological Survey by the Anaconda Company from the east side of Fish Springs Flat (secs. 6, 7, 8, 18, 19, T. 13 S., R. 12 W., sec. 1, T. 13 S., R. 13 W., and sec. 31, T. 12 S., R. 12 W.). Cuttings of tuff were selected from zones showing visible evidence of alteration and mineralization, such as clay and fluorite. The abundance of BeO, U, and Th in the selected cuttings show the expected effect of mineralization. Histograms of BeO and U (figs. 22A and 22B) are skewed positively toward high concentrations, as would be expected if some beryllium and uranium had been concentrated by mineralizing fluids. Many samples selected as being mineralized did not prove to be of



Figure 21.--Distribution of uranium with respect to beryllium ore in a drillhole at the Roadside beryllium deposit. Distribution of beryllium ore from Griffitts and Rader (1963). Uranium and thorium by delayed neutron method by H. T. Millard, A. J. Bartel, R. J. Knight, P. Hemming, J. O'Kelly, and R. White.

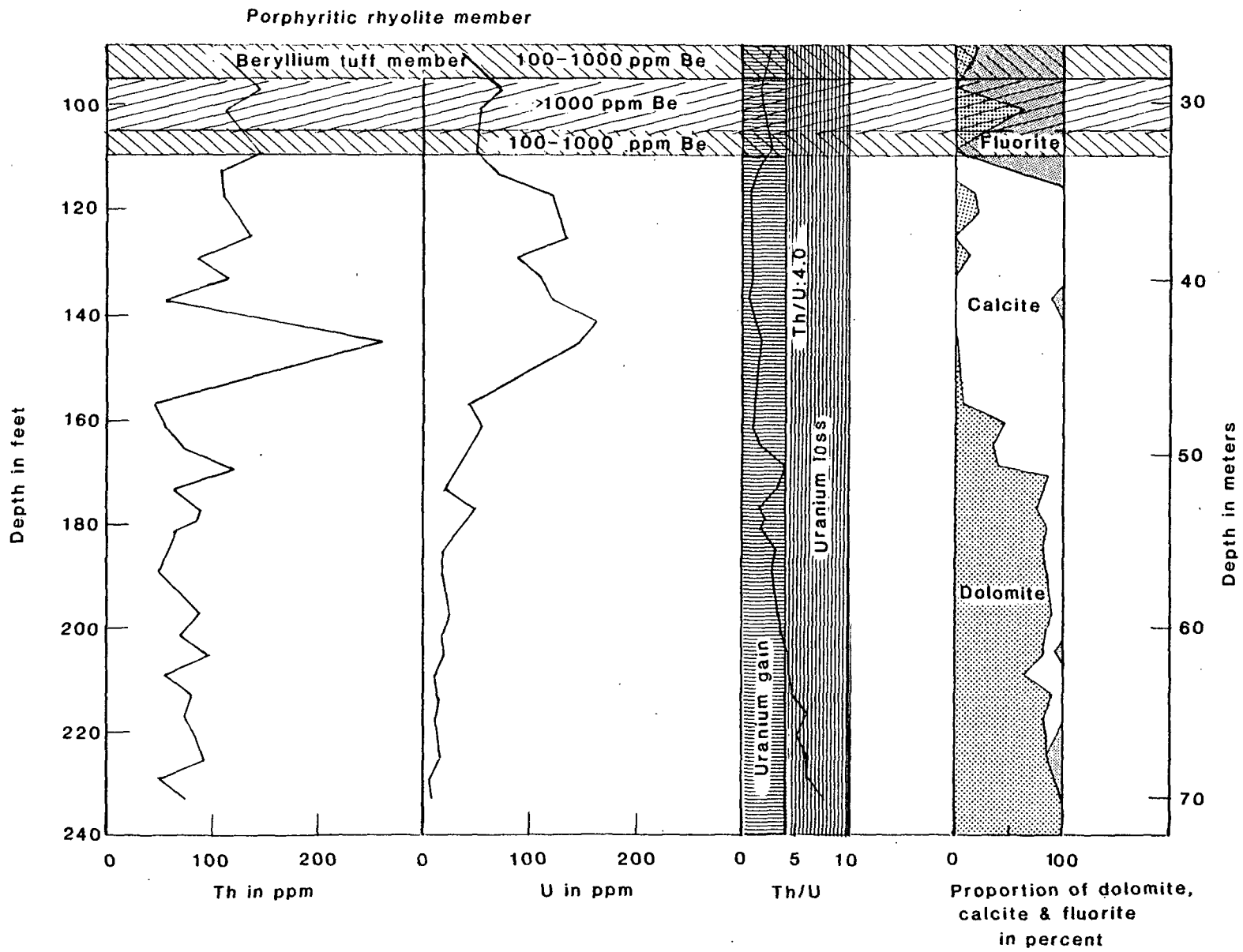
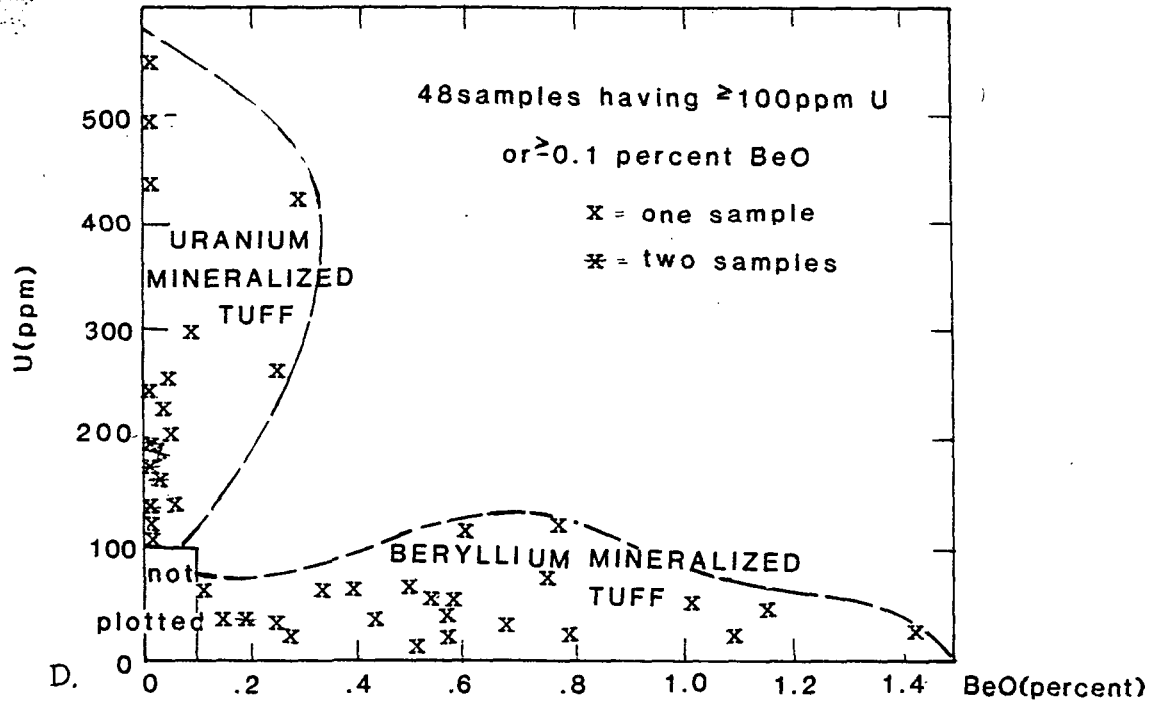
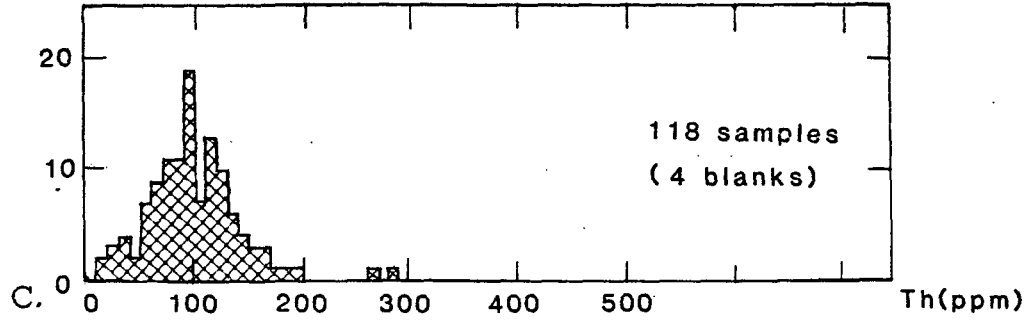
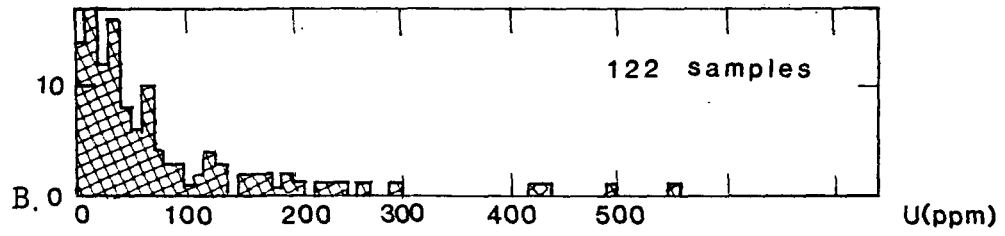
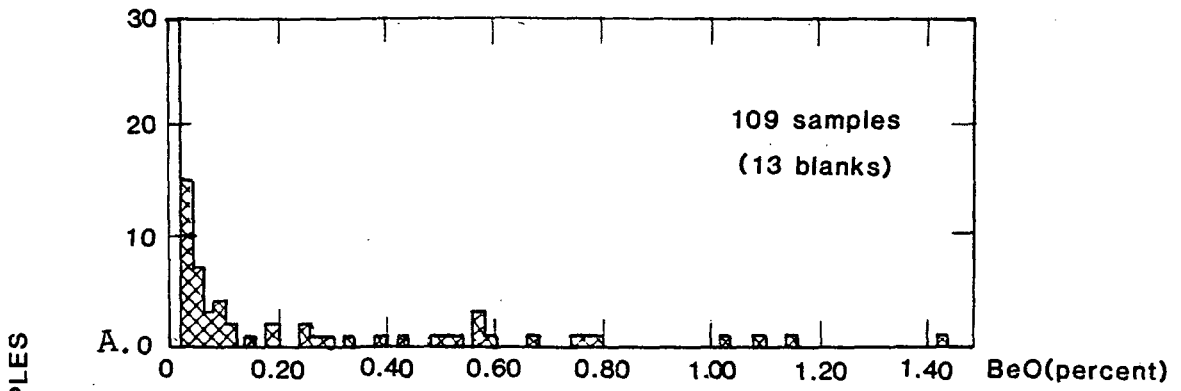


Figure 22.--Histograms showing the abundance of (A) beryllium oxide in percent, (B) uranium in parts per million, (C) thorium in parts per million, and (D) scattergram showing segregation of beryllium oxide and uranium in drill cuttings of mineralized zones in the beryllium tuff member of the Spor Mountain Formation. Data from Glanzman and Meier (1979).



beryllium ore grade, however, so that the samples cannot be regarded as representative of beryllium ore. Thorium is generally more abundant (about 100 ppm) in mineralized tuff than in the tuff overall (about 80 ppm), but the frequency distribution of thorium is not skewed positively (fig. 22C). The most significant aspect of the data is the separate occurrence of uranium from beryllium, as shown by a scattergram (fig. 22D) of 48 samples having  $\geq 0.1$  percent BeO or  $\geq 100$  ppm U. The scattergram defines two distinct groups of samples, one having high beryllium (0.1-1.42 percent BeO) and one having high uranium (100-556 ppm U). There is no correlation between beryllium and uranium. This relation corroborates that seen in the Roadside drill hole cuttings (fig. 21), where uranium tends to occur below beryllium ore.

Uranium occurs with beryllium and fluorite in small prospects that may represent exposures of feeders for hydrothermal fluids entering the beryllium tuff. These prospects include those associated with the contact zone of a pipe of porphyritic rhyolite at the south end of Spor Mountain (NW1/4 sec. 10, T. 13 S., R. 12 W.), and those associated with the Dell fault system, such as the Oversight and Claybank prospects. The Claybank prospect (figs. 14B, 15) is in faulted beryllium tuff along the east side of Eagle Rock Ridge, and the Oversight prospect is in hydrothermally altered fault gouge of the porphyritic rhyolite member at the south end of The Dell. A grab sample of fluorite-rich altered rhyolite from the contact zone of the pipe contained 1,000 ppm uranium and 50 ppm beryllium. A grab sample of fluorite-rich gouge from the fault on the Oversight prospect contained about 250 ppm uranium and 700 ppm beryllium. Nearby, drill holes have penetrated mineralized beryllium tuff beneath porphyritic rhyolite.

#### Yellow Chief Mine

The Yellow Chief mine is in a tilted fault block of volcanic rocks in The Dell (fig. 15). Tuffaceous sandstone and conglomerate in the lower part of the beryllium tuff member of the Spor Mountain Formation is the host for uranium ore at the Yellow Chief mine (fig. 10D). Westward tilting of the fault block has brought the Spor Mountain Formation down against the Dell Tuff along the footwall of the fault that marks the west side of the block. The fault at the west side of the Yellow Chief has been active over a long period of time, both before and after 21 m.y. ago; at the pit it downdrops a small erosional remnant of the 21 m.y. old porphyritic rhyolite and beryllium tuff. Farther south in The Dell, the fault is exposed in the Dell Tuff but is covered by the Spor Mountain Formation, with no displacement of that unit. Small faults having less than 1 m displacement cut the tuffaceous sandstone and conglomerate in the pit. The stratigraphic section at the Yellow Chief has been described in detail under the discussion of the beryllium tuff member of the Spor Mountain Formation.

The ore at the Yellow Chief is beta-uranophane ( $\text{Ca}(\text{UO}_2)_2(\text{SiO}_3)_2(\text{OH})_2 \cdot 5\text{H}_2\text{O}$ ), a pale-orange-yellow mineral (Bowyer, 1963). It occurs in lenses as much as 6 m thick and 90 m long that are

approximately concordant to the bedding in tuffaceous conglomerate and sandstone (Fig. 10D). The yellow mineral weeksite ( $K(UO_2)_2(Si_2O_5)_3 \cdot 4H_2O$ ) occurs in lenticular zones less than 1 m thick and 10 m long in the limestone conglomerate that overlies the tuffaceous sandstone (Staatz and Carr, 1964, p. 156). Both of these minerals occupy interstices and fractures, and coat sand grains and clasts in the conglomerate. Schroekingerite ( $NaCa_3(UO_2)(CO_3)_3(SO_4)F \cdot 10H_2O$ ) has been reported in veinlets in the tuffaceous sandstone (Staatz and Carr, 1964, p. 157) but has not been found in most of the ore. The host rock is partially altered to smectite, and some limestone clasts in the conglomerates have altered shells, but evidence for intense hydrothermal alteration is lacking. Small bits of earthy yellow jarosite are scattered about in the tuffaceous sandstone and conglomerate, and coarsely crystalline calcite cement and veinlets are widespread.

Two lenses of ore exposed on the face of the Yellow Chief pit (fig. 10D) were sampled to check for geochemical haloes and possible associations of trace elements that might suggest clues to the origin of the Yellow Chief ores. One ore lens sampled contains weeksite; the other, believed to be more typical of the Yellow Chief ore, contains beta-uranophane. The ore lenses were mapped in the field using a hand-held scintillator, and a series of samples was taken across the middle and ends of each ore lens (fig. 23). Equivalent uranium, analyzed by a counting technique, and uranium determined by delayed neutron analysis, are about the same in the ore lenses, indicating that uranium there is approximately in equilibrium. Equivalent uranium (eU) exceeds the concentration of uranium outside the ore lenses because at low concentrations (100 ppm and less) the content of potassium and thorium accounts for a significant part of the eU. Fluorine, beryllium, and lithium, which would be expected to indicate intensity of hydrothermal mineralization associated with beryllium deposits, show no systematic change in abundance across the middle or ends of the ore lenses. Fluorine and lithium are most abundant in the bentonite at the top of the pit wall, indicating that beryllium-related mineralization affected the clay-rich bentonite most. Uranium content of the bentonite is 100 ppm immediately above the weeksite ore, but only 15 ppm a meter above the ore. Copper, vanadium, chromium, lead, silver, and molybdenum were analyzed by spectrographic methods to look for evidence that the ores might chemically resemble those of the Colorado Plateau; no enrichment of these elements, except perhaps lead, and no systematic changes, were noted for either of the ore lenses.

The uranium deposits at the Yellow Chief mine are of uncertain origin. The paucity of fluorite and beryllium in the uranium ore suggests that the Yellow Chief deposits were not formed by the hydrothermal mineralization that produced the fluorspar and beryllium deposits. Overall, the ores do not resemble those of the Colorado Plateau, inasmuch as they do not contain uranous minerals, organic

Figure 23.--Location of geochemical samples in two ore lenses in the Yellow Chief mine. Ore lenses are located in figure 10D. A, A lens of weeksite ore at the top of limestone pebble and cobble conglomerate, and B, a lens of beta-uranophane ore in tuffaceous sandstone and conglomerate.

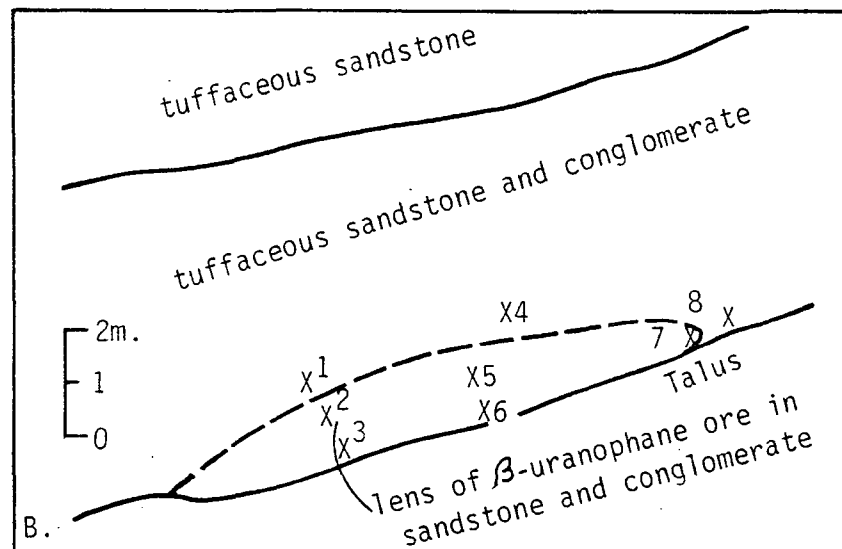
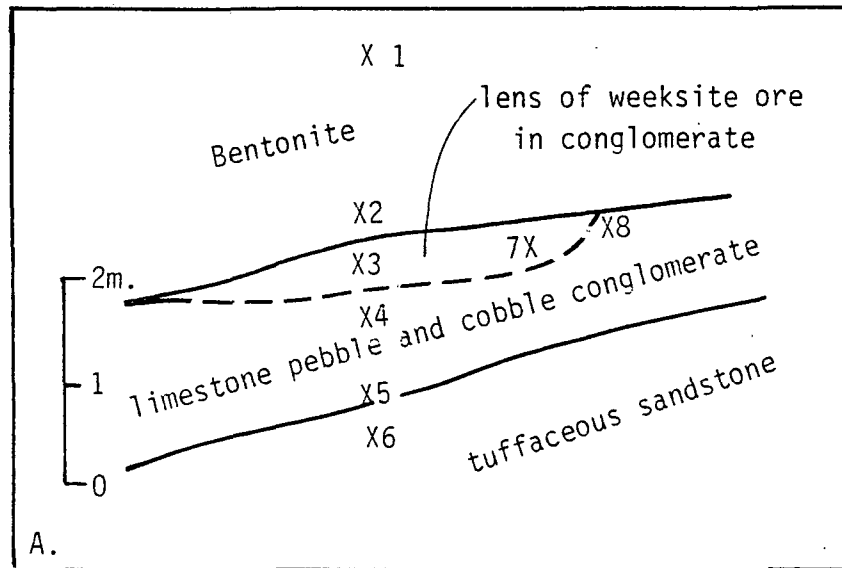




Table 7.--Chemical analyses of samples from two ore lenses in the Yellow Chief mine. Samples are located in figure 23.

[eU by beta-gamma scaler by Harriet Neiman; U and Th by delayed neutron method by H. T. Millard, Jr., A. J. Bartel, R. J. Knight, C. L. Shields, C. M. Ellis, R. L. Nelms, and C. A. Ramsey; F by specific ion electrode method by Harriet Neiman and Patricia Guest; Be, Li, Cu, V, Cr, and Pb by six-step semiquantitative spectrographic method by J. C. Hamilton. Ag and Mo not found at detection limits of 0.5 ppm and 3 ppm, respectively, by the spectrographic method. Leaders (--) indicate no data]

Sample number	Source of sample	Parts per million									
		eU	U	Th	F	Be	Li	Cu	V	Cr	Pb
A. Samples from vicinity of weeksite lens											
1	bentonite	30	15	57	3600	15	200	5	10	15	70
2	do.	90	100	68	6100	30	1000	7	30	30	70
3	ore in conglomerate	910	1002	-	800	20	150	10	30	70	300
4	barren conglomerate	50	34	14	1400	15	100	7	50	100	300
5	do.	50	21	14	1200	30	<50	7	70	100	100
6	sandstone	30	10	14	600	10	<50	3	30	10	50
7	ore in conglomerate	290	286	-	800	15	<50	7	30	70	70
8	barren conglomerate	70	49	21	1300	15	<50	7	30	100	30
B. Samples of sandstone from vicinity of uranophane lens											
1	outside ore lens	40	21	28	1200	50	<50	10	100	70	30
2	ore lens	120	76	35	1400	20	100	10	70	50	30
3	do.	80	39	26	1500	20	<50	10	70	100	30
4	outside ore lens	40	16	22	1000	30	<50	7	70	50	70
5	ore lens	3130	3343	-	1700	30	100	7	70	30	15
6	do.	610	602	-	1300	30	100	10	70	30	15
7	do.	2200	2316	-	1400	30	<50	15	150	70	70
8	outside ore lens	40	31	33	1500	5	<50	15	100	70	150

matter, or pyrite, although jarosite, noted in the host sandstone, might represent oxidized pyrite. Metals that are locally abundant in the beryllium ores (such as manganese, lithium, and zinc) and in the Colorado Plateau ores (such as vanadium, copper, and molybdenum) are not concentrated in the Yellow Chief ore. Uranium at the Yellow Chief may have been introduced by ground waters bearing silica and uranyl carbonate complex ions that dissociated when the calcite cement precipitated.

#### Uraniferous opal

Uranium occurs in the structure of opaline silica in fracture fillings in tuff at many places in the Thomas Range. The best known and most uraniferous opal occurs in the crystal tuff member of the Joy Tuff at the Autunite No. 8 prospect on the east side of Topaz Mountain. Fracture fillings of uraniferous opal occur also in the Topaz Mountain Rhyolite above the Autunite No. 8 prospect, at the Buena No. 1 prospect (Staatz and Carr, 1964, p. 152-154), and west of Topaz Valley; in the Dell Tuff in The Dell; with massive uraniferous opal in the beryllium tuff member at many locations; and in the dome of the porphyritic rhyolite member near Wildhorse Spring. Reconnaissance suggests that at least minute quantities of uraniferous opal can be found in any tuff in the Thomas Range. The fracture fillings are generally less than 1-2 cm wide and occur both singly and in zones less than 10 m wide and 30 m long. None has produced ore, and their small size and extent indicate that they are not of economic interest themselves.

The opal in fracture fillings is generally zoned, the zoning being defined by varying size of fibrous crystallites oriented perpendicular to the walls of the vein. The opal fluoresces bright yellow green under ultraviolet light, so that it can be readily distinguished from ordinary opal in the Thomas Range, which does not fluoresce. Calcite, quartz, fluorite, wecksite, and perhaps other secondary uranium minerals are common. Fission-track maps show that uranium is concentrated in the opal parallel to the zoning, so that there are large variations in uranium content between zones only a fraction of a mm thick (Zielinski and others, 1977).

The uraniferous opal is probably of hydrothermal origin; more specifically, such opal may have precipitated in hot springs. Both massive replacement opal and opal in fracture fillings occur in hydrothermal beryllium deposits in the beryllium tuff member. Uranium-lead apparent ages indicate deposition during or soon after beryllium-fluorite mineralization (K. R. Ludwig, 1979, oral commun.), and at least in part soon after eruption of the host Spor Mountain Formation. The close temporal relation between opal formation, beryllium-fluorite mineralization, and igneous activity indicates a genetic relation, also. Many of the fracture fillings show strong zoning of uranium concentration, which suggests wide fluctuation in the supply, rate, or conditions of precipitation of uranium. If silica, calcite, and fluorite were the major phases in equilibrium with the fluids, a likely

mechanism for controlling the rate of precipitation was change in temperature or pressure. Fluctuating temperature or pressure and the presence of fluorite support a hydrothermal source. For opal at the Autunite locality, temperatures of deposition in the range of  $\leq 36^{\circ}\text{C}$  were estimated from oxygen isotope composition (Henry, 1979), but this opal may have been deposited far from its presumed hydrothermal source.

#### Uranium in stratified tuff of the Topaz Mountain Rhyolite

A survey of stratified tuff in the Topaz Mountain Rhyolite showed that its original chemical composition was nearly identical to that of the associated alkali rhyolite, and that large areas of the once-vitric tuff had been altered to zeolite (Lindsey, 1975). Alteration was accomplished by open system ground-water leaching of the major alkalis,  $\text{Na}_2\text{O}$  and  $\text{K}_2\text{O}$ , and of minor elements including F, Rb, Mn, and Pb. No analyses of uranium were available for the study reported in 1975, but the content of equivalent uranium, which is dependent on  $^{40}\text{K}$ , Th, and U, was found to decline during zeolitization. The tuff was weakly affected by beryllium-fluorite mineralization, also.

A random selection of 20 samples used in the 1975 survey was analyzed for uranium and thorium by the delayed neutron method by H. T. Millard, Jr., C. McFee, and C. Bliss of the U.S. Geological Survey. These analyses show that the stratified tuff contains a range of 7-23 ppm U (average of 16 ppm) and 44-71 ppm Th (average of 55 ppm). Zeolitic tuff does not contain appreciably less U and Th than vitric tuff, but the small number of samples may be insufficient to detect differences. The analyses do show that the overall uranium and thorium content of the tuff is very close to that of alkali rhyolite. Seventeen samples of alkali rhyolite showed a range of 6-20 ppm (average of 16 ppm) and 36-76 ppm Th (average of 62 ppm). Although the wide range of uranium content in some of the tuff and rhyolite suggests that uranium has been mobile, study of similar tuffs in the Keg Mountains (R. A. Zielinski, 1979, oral commun.) indicates that most of the uranium has not been flushed from the tuff to be concentrated in ore deposits. No concentrations in excess of trace amounts of uranium, except in uraniferous opal, are known in the Topaz Mountain Rhyolite.

#### A model for uranium deposits and some suggestions for exploration

The uranium (and other lithophile metal) mineralization of the Thomas Range was associated with extensional block-faulting (basin-and-range faulting) and fluorine-rich alkali rhyolite volcanism beginning 21 m.y. ago. Uranium and other lithophile metals did not accompany the caldera cycle, which was complete by 32 m.y. ago. A hiatus of 11 m.y. separates uranium mineralization at Spor Mountain from the caldera cycle; thus uranium clearly is not associated with the caldera cycle or with earlier magmas that contained abundant sulfur and chalcophile metals.

Uranium in the Thomas Range has been concentrated by 1) magmatic fluids, 2) hydrothermal fluids, and 3) ground water. These methods of concentration correspond respectively to the 1) initial-magmatic, 2) pneumatogenic, and 3) hydroallogenic classes of volcanogenic uranium deposits proposed by Pilcher (1978). All of these fluids circulated in an environment of extensional faulting and alkali rhyolite volcanism, however, and their only relation to the caldera cycle was their introduction through fractures that were formed during cauldron subsidence and later reactivated during basin-and-range faulting. Uranium was concentrated by magmatic fluids in the beryllium tuff member (about 20 ppm) and in alkali rhyolite (10-20 ppm) of both the Spor Mountain Formation and the Topaz Mountain Rhyolite. Particularly large amounts of uranium, beryllium, and fluorine were concentrated in the magma of the Spor Mountain Formation, which underlay the vicinity of Spor Mountain and which was erupted as the beryllium tuff and porphyritic rhyolite members. Uranium was further concentrated in hydrothermal fluids rising through conduits that were opened by basin-and-range faulting. Such faulting tapped fluorine and lithophile-metal rich fluids in the top of the alkali rhyolite magma that underlay the vicinity of Spor Mountain. The fluids deposited uraniferous fluorspar in pipes along faults and fault intersections on Spor Mountain (Staatz and Carr, 1964, p. 130-148) and spread laterally into the beryllium tuff member, where they deposited disseminated fluorite, beryllium, lithium, and uranium (Lindsey, 1977). Uranium of hydrothermal origin was deposited in the structure of fluorite and opal; no tetravalent uranium minerals have been found. Uranium in the structure of fluorite at Spor Mountain may be tetravalent, but this possibility remains unproven.

The oxidizing chemical environment of hydrothermal uranium mineralization at Spor Mountain contrasts with the reducing chemical environments at McDermitt, Nevada-Oregon (Rytuba and Glanzman, 1978), and Marysvale, Utah (Cunningham and Steven, 1978). Pitchblende, pyrite, and fluorite are common in uranium ores at both McDermitt and Marysvale, but pitchblende and pyrite have not been found at Spor Mountain. At McDermitt, hydrothermal fluids containing sulphur, fluorine, mercury and uranium mineralized volcanic domes and moat sediments of the McDermitt caldera complex. At Marysvale, uranium-bearing hydrothermal fluids contained abundant fluorine, which complexed with uranium, and minor concentrations of sulfur, which was in the reduced state; uranium probably travelled as a tetravalent fluoride complex and was precipitated as the fluids cooled and the pH rose by reaction with wall rocks (Cunningham and Steven, 1978). At Spor Mountain, uranium probably travelled in hydrothermal fluids as hexavalent fluoride and silica complexes; precipitation of uranium occurred in response to precipitation of fluorite and silica and accompanying breakdown of complex ions. Fluorite and silica were probably precipitated by cooling of fluids; reaction of the fluids with carbonate rock and porous tuff caused the pH to rise and resulted in widespread smectite and K-feldspar alteration (Lindsey and others, 1973). Ground water has redistributed hydrothermal uranium at Spor Mountain and concentrated it locally in deposits of secondary minerals.

The potential for finding magmatic or hydrothermal deposits of pitchblende in the Thomas Range is uncertain. No pitchblende or other tetravalent uranium mineral has been found in the near-surface environment exposed at Spor Mountain, indicating that no reducing agent or environment was present to precipitate large amounts of uranium. No reducing agent, such as pyrite or carbonaceous matter, has been observed in the fluorspar pipes or in the beryllium tuff member by me, but such reductants might occur in deep environments. Some Paleozoic carbonate rocks on Spor Mountain are fetid and might serve as a local reducing environment along the walls of fluorspar pipes and rhyolite vents. The discovery of carbonaceous and pyritic lakebeds in the Mt. Laird Tuff of the subsurface northeast of Topaz Mountain indicates yet another reducing environment. The most favorable areas to look are near vents for alkali rhyolite lava, where the lava has passed through carbonate rocks or Tertiary lakebeds that contain carbonaceous matter. A mineralized plug of porphyritic rhyolite, located in the southern part of Spor Mountain, and vents of alkali rhyolite at Topaz Mountain, Antelope Ridge, and the northeastern Drum Mountain fit this criterion.

A deep hydrothermal environment at Spor Mountain may be present near a hypothetical pluton of alkali rhyolite that was the source of the beryllium tuff and porphyritic rhyolite of the Spor Mountain Formation, and of the beryllium-fluorite-uranium mineralization that followed. The vicinity of intrusion of the hypothesized pluton can be predicted from the distribution of the Spor Mountain Formation around Spor Mountain and the intensity of mineralization associated with that area. Also, Spor Mountain may have been lifted trap-door fashion by the pluton after eruption of the Spor Mountain Formation 21 m.y. ago. The hinge of the trap door would have been west of the mountain, and the region of greatest uplift would be along the Dell fault system where it displaces Spor Mountain Formation against Paleozoic rocks. Maximum upward projection of the pluton might be expected about 1 km west of Eagle Rock Ridge. The depth to the pluton is probably unpredictable without geophysical data, and the nature of the ores, if any, that might be associated with it seem equally difficult to predict. If sufficiently reducing environments are present at depth, the possibility for large concentrations of uranium and perhaps other metals is good. Anomalous traces of Mo, Sn, and W near the surface, concentrated in manganese oxide minerals near beryllium ore, may be generally indicative of other metals that would be expected below (Lindsey, 1977).

The Spor Mountain Formation and the Topaz Mountain Rhyolite are the most favorable source rocks for uranium deposited by ground waters. In general, the alkali rhyolites contain 10-20 ppm uranium, which is approximately 2-4 times as much as other volcanic rocks in the area. The beryllium tuff member probably contained 20 ppm uranium at the time of deposition and local concentrations of 2000 ppm or more were added in hydrothermal fluorite and silica. The stratified tuffs of the Topaz Mountain Rhyolite also contained 10-20 ppm uranium. The tuffs of both formations are porous and were initially glassy, and they are situated between relatively impermeable (though not totally impermeable) rhyolite

and other rocks, so that they provided a good conduit for fluids to leach and transport uranium. Thus it is not surprising that many occurrences of secondary uranium minerals, including the Yellow Chief deposit, are in the beryllium tuff member of the Spor Mountain Formation. Much secondary uranium, probably deposited by ground water, occurs in the beryllium tuff, as shown by the separate occurrence of uranium and beryllium in the tuff. The Yellow Chief deposit, which consists entirely of secondary uranium minerals, probably was formed by ground water also.

The potential for finding oxidized uranium deposits formed by ground water in the beryllium tuff member of the Spor Mountain Formation is moderate. The scarcity of reductants to precipitate uranium in tuff indicates that deposits of reduced uranium minerals such as uraninite and coffinite, which usually occur in deposits of the Colorado Plateau and Wyoming types, will not be found unless a hydrologic basin favorable to entrapment and precipitation of uranium can be located; none is exposed. The beryllium tuff member southwest of Spor Mountain has been drilled extensively in the search for both beryllium and uranium, so it is not likely that large high-grade deposits could have been overlooked. There may be much potential, however, for uranium-bearing tuff of low grade (0.0x percent). The best possibility for discovery of additional uranium deposits formed by ground water may be concentrations of secondary uranium minerals like those at the Yellow Chief. Favorable host rocks in The Dell may extend beneath the Thomas Range, where they may be expected in down-faulted blocks covered by Topaz Mountain Rhyolite.

Finally, another area of possible but very uncertain uranium potential, as yet mostly unexplored, is in the subsurface of Dugway Valley north and east of Antelope Ridge. The potential hosts there are stratified tuff of the Topaz Mountain Rhyolite and lakebeds of the Mt. Laird Tuff. Drilling and testing of Dugway Valley to 500-1,000 m will be necessary to evaluate its uranium potential. The cauldron environment there is a passive factor favoring occurrence of uranium; subsidence of both the Thomas caldera and the Dugway Valley cauldron created a depression filled with lakebeds and tuffaceous sediments that could act as a reducing trap for uranium leached by ground water from adjacent highlands of alkali rhyolite and tuff in the Thomas Range and Keg Mountains.

REFERENCES CITED

- Armstrong, R. L., 1970, Geochronology of Tertiary igneous rocks, eastern Basin and Range Province: *Geochimica et Cosmochimica Acta*, v. 34, no. 2, p. 203-232.
- Best, M. G., Shuey, R. T., Caskey, C. F., and Grant, S. K., 1973, Stratigraphic relations of members of the Needles Range Formation at type localities in southwestern Utah: *Geological Society of America Bulletin*, v. 84, no. 10, p. 3269-3278.
- Bick, K. F., 1966,, Geology of the Deep Creek Mountains, Utah: *Utah Geological and Mineralogical Survey Bulletin* 77, 120 p.
- Boyer, Ben, 1963, Yellow Chief Uranium Mine, Juab County, Utah, *in* Sharp, B. J., and Williams, N. C., eds., Beryllium and uranium mineralization in western Juab County, Utah: *Utah Geological Society, Guidebook to the geology of Utah* no. 17, p. 15-22.
- Byers, F. M., Jr., Carr, W. J., Orkild, P. P., Quinlivan, W. D., and Sargent, K. A., 1976, Volcanic suites and related cauldrons of Timber Mountain-Oasis Valley caldera complex, southern Nevada: *U.S. Geological Survey Professional Paper* 919, 70 p.
- Christiansen, R. L., and Lipman, P. W., 1966, Emplacement and thermal history of a rhyolite lava flow near Fortymile Canyon, southern Nevada: *Geological Society of America Bulletin*, v. 77, no. 7 p. 671-684.
- \_\_\_\_\_ 1972, Cenozoic volcanism and plate-tectonic evolution of the western United States. II. Late Cenozoic: *Royal Society of London Philosophical Transactions*, v. 271, p. 249-284.
- Cohenour, R. E., 1959, Sheeprock Mountains, Tooele and Juab Counties: *Utah Geological and Mineralogical Survey Bulletin* 63, 201 p.
- \_\_\_\_\_ 1963, The beryllium belt of western Utah, *in* Sharp, B. J., and Williams, N. C., eds., Beryllium and uranium mineralization in western Juab County, Utah: *Utah Geological Society, Guidebook to the geology of Utah* no. 17, p. 4-7.
- Cook, E. F., 1965, Stratigraphy of Tertiary volcanic rocks in eastern Nevada: *Nevada Bureau Mines Rept.* 11, 61 p.
- Compton, R. R., Todd, V. R., Zartman, R. E., Naeser, C. W., 1977, Oligocene and Miocene metamorphism, folding, and low-angle faulting in northwestern Utah: *Geological Society of America Bulletin*, v. 88, no. 9, p. 1237-1250.

- Crittenden, M. D., Jr., Straczek, J. A., and Roberts, R. J., 1961, Manganese deposits in the Drum Mountains, Juab and Millard Counties, Utah: U.S. Geological Survey Bulletin 1082-H, p. 493-544.
- Cunningham, C. G., and Steven, T. A., 1978, Postulated model of uranium occurrence in the Central Mining Area, Marysvale District, west-central Utah: U.S. Geological Survey Open-File Report 78-1093, 19 p.
- Erickson, M. P., 1963, Volcanic geology of western Juab County, Utah, in Sharp, B. J., and Williams, N. C., eds., Beryllium and uranium mineralization in western Juab County, Utah: Utah Geological Society, Guidebook to the geology of Utah no. 17, p. 23-35.
- Ewart, A., Brothers, R. N., and Mateen, A., 1977, An outline of the geology and geochemistry, and the possible petrogenetic evolution of the volcanic rocks of the Tonga-Kermadec-New Zealand island arc: Journal of Volcanology and Geothermal Research, v. 2, no. 2, p. 205-250.
- Ewart, A., and Stipp, J. J., 1968, Petrogenesis of the volcanic rocks of the central North Island, New Zealand, as indicated by a study of  $Sr^{87}/Sr^{86}$  ratios, and Sr, Rb, K, U, and Th abundances: Geochimica et Cosmochimica Acta, v. 32, no. 7, p. 699-736.
- Fowkes, E. J., 1964, Pegmatites of the Granite Peak Mountains, Tooele County, Utah: Brigham Young University Geology Studies, v. 11, p. 97-127.
- Glanzman, R. K., and Meier, A. L., 1979, Preliminary report on samples collected during lithium reconnaissance studies in Utah and Idaho: U.S. Geological Survey Open-File Report no. 79-279, 52 p.
- Griffitts, W. R., and Rader, L. F., Jr., 1963, Beryllium and fluorine in mineralized tuff, Spor Mountain, Juab County, Utah, in Geological Survey Research 1963: U.S. Geological Survey Professional Paper 476-B, p. B16-B17.
- Hedge, C. E., 1966, Variations in radiogenic strontium found in volcanic rocks: Journal of Geophysical Research, v. 71, no. 24, p. 6119-6126.
- Henry, C. D., 1979, Origin of uraniferous opal, in Henry, C. D., and Walton, A. W., eds., Final Report: Formation of uranium ores by diagenesis of volcanic sediments: U.S. Department of Energy report GJBX 22(79), ch. 10, 22 p.
- Hogg, N. C., 1972, Shoshonitic lavas in west-central Utah: Brigham Young University Geology Studies, v. 19, pt. 2, p. 133-184.



- Hollister, V. F., 1978, Geology of porphyry copper deposits of the western hemisphere: American Society of Mining, Metallurgical, and Petroleum Engineers, New York, 219 p.
- Irvine, N., and Barager, W. R. A., 1971, A guide to the chemical classification of the common volcanic rocks: Canadian Journal of Earth Sciences, v. 8, no. 5, p. 523-548.
- Krieger, M. H., 1977, Large landslides, composed of megabreccia, interbedded in Miocene basin deposits, southeastern Arizona: U.S. Geological Survey Professional Paper 1008, 25 p.
- Leedom, S. H., 1974, Little Drum Mountains, an Early Tertiary shoshonitic volcanic center in Millard County, Utah: Brigham Young University Geology Studies, v. 21, pt. 1, p. 73-108.
- Leedom, S. H., and Mitchell, T. P., 1978, Preliminary study of favorability for uranium resources in Juab County, Utah: U.S. Department of Energy report GJBX-23(78), 22 p.
- Lindsey, D. A., 1975, Mineralization halos and diagenesis in water-laid tuff of the Thomas Range, Utah: U.S. Geological Survey Professional Paper 818-B, 59 p.
- \_\_\_\_\_, 1977, Epithermal beryllium deposits in water-laid tuff, western Utah: Economic Geology, v. 72, no. 2, p. 219-232.
- \_\_\_\_\_, 1978, Geology of volcanic rocks and mineral deposits in the southern Thomas Range, Utah: Brigham Young University Geology Studies, v. 25, pt. 1, p. 25-31.
- \_\_\_\_\_, 1979, Geologic map and cross-sections of Tertiary rocks in the Thomas Range and northern Drum Mountains, Juab County, Utah: U.S. Geological Survey Miscellaneous Investigations Series Map I-1176.
- Lindsey, D. A., Ganow, H., and Mountjoy, W., 1973, Hydrothermal alteration associated with beryllium deposits at Spor Mountain, Utah: U.S. Geological Survey Professional Paper 818-A, 20 p.
- Lindsey, D. A., Naeser, C. W., and Shawe, D. R., 1975, Age of volcanism, intrusion, and mineralization in the Thomas Range, Keg Mountain, and Desert Mountain, western Utah: Geological Survey Journal of Research, v. 3, no. 5, p. 597-604.
- Lipman, P. W., 1976, Caldera-collapse breccia in the western San Juan Mountains, Colorado: Geological Society of America Bulletin, v. 87, no. 10, p. 1397-1410.

- Lipman, P. W., Prostka, H. J., and Christiansen, R. L., 1972, Cenozoic volcanism and plate-tectonic evolution of the western United States. I. Early and middle Cenozoic: Royal Society of London Philosophical Transactions, v. 271, p. 217-248.
- McCarthy, J. H., Jr., Learned, R. E., Botbol, J. M., Lovering, T. G., Watterson, J. R., and Turner, R. L., 1969, Gold-bearing jasperoid in the Drum Mountains, Juab and Millard Counties, Utah: U.S. Geological Survey Circular 623, 4 p.
- McKee, E. H., Noble, D. C., and Silberman, M. L., 1970, Middle Miocene hiatus in volcanic activity in the Great Basin area of the western United States: Earth and Planetary Science Letters, v. 8, no. 1, p. 93-96.
- Mehnart, H. H., Rowley, P. D., and Lipman, P. W., 1978, K-Ar ages and geothermal implications of young rhyolites in west-central Utah: Isochron/West, no. 21, p. 3-7.
- Moore, W. J., Hedge, C. E., and Sorensen, M. L., 1979, Variations in  $^{87}\text{Sr}/^{86}\text{Sr}$  ratios of igneous rocks along the Uinta trend, northwestern Utah (abs.): Abstracts with Programs, Rocky Mountain Section of Geological Survey of America, 32nd Annual Meeting, Ft. Collins, Colorado, p. 297.
- Moore, W. J., and Sorensen, M. L., 1978, Metamorphic rocks of the Granite Peak area, Tooele County, Utah (abs.): Abstracts with Programs, Rocky Mountain Section of Geological Society of America, 31st Annual Meeting, Provo, Utah, p. 234.
- Naeser, C. W., 1976, Fission track dating: U.S. Geological Survey Open-file Report 76-190, revised Jan. 1978 (unpaginated).
- Newell, R. A., 1971, Geology and geochemistry of the northern Drum Mountains, Juab County, Utah: Colorado School of Mines unpublished M. S. thesis, Golden, Colo., 115 p.
- Noble, 1972, Some observations on the Cenozoic volcano-tectonic evolution of the Great Basin, western United States: Earth and Planetary Science Letters, v. 17, no. 1, p. 142-150.
- Park, G. M., 1968, Some geochemical and geochronologic studies of the beryllium deposits in western Utah: University of Utah unpublished M.S. thesis, Salt Lake City, Utah, 105 p.
- Peterson, James, Turley, Charles, Nash, W. P., and Brown, F. G., 1978, Late Cenozoic basalt-rhyolite volcanism in west-central Utah (abs.): Abstracts with Programs, Rocky Mountain Section of Geological Society of America, 31st Annual Meeting, Provo, Utah, p. 236.

- Pierce, C. R., 1974, Geology of the southern part of the Little Drum Mountains, Utah: Brigham Young University Geology Studies, v. 21, pt. 1, p. 109-130.
- Pilcher, R. C., 1978, Classification of volcanogenic uranium deposits, in Mickle, D. G., ed., A preliminary classification of uranium deposits: U.S. Department of Energy report GJBX-63 (78), p. 41-51.
- Rittman, Alfred, 1952, Nomenclature of volcanic rocks: Bulletin Volcanologique, ser. 2, v. 12, p. 75-102.
- Rytuba, J. J., and Glanzman, R. K., 1978, Relation of mercury, uranium, and lithium deposits to the McDermitt caldera complex, Nevada-Oregon: U.S. Geological Survey Open-File Report 78-926, 28 p.
- Shawe, D. R., 1964, A late Tertiary low-angle fault in western Juab County, Utah, in Geological Survey Research 1964: U.S. Geological Survey Professional Paper 501-B, p. B13-B15.
- \_\_\_\_\_ 1966, Arizona-New Mexico and Nevada-Utah beryllium belts, in Geological Survey Research 1966: U.S. Geological Survey Professional paper 550-C, p. C206-C213.
- \_\_\_\_\_ 1968, Geology of the Spor Mountain beryllium district, Utah, in Ridge, J. D., ed., Ore deposits of the United States, 1933-1967 (Graton-Sales Volume): New York, The American Institute of Mining, Metallurgical and Petroleum Engineers, v. 2, pt. 8, p. 1149-1161.
- \_\_\_\_\_ 1972, Reconnaissance geology and mineral potential of the Thomas, Keg, and Desert calderas, central Juab County, Utah: U.S. Geological Survey Professional Paper 800-B, p. B67-B77.
- Shawe, D. R., and Stewart, J. H., 1976, Ore deposits as related to tectonics and magmatism, Nevada and Utah: American Institute Mining Engineers Transactions, 1977 Annual Meeting, Las Vegas, Nevada, v. 260, p. 225-232.
- Sparks, R. S. J., Self, S., and Walker, G. P. L., 1973, Products of ignimbrite eruptions: Geology, v. 1, no. 3, p. 115-118.
- Shreve, R. L., 1968, The Blackhawk landslide: Geological Society of America Special Paper 108, 47 p.
- Smith, R. L., and Bailey, R. A., 1968, Resurgent cauldrons, in Coats, R. R., Hay, R. L., and Anderson, C. A., eds., Studies in volcanology, Howell Williams volume: Geological Society America Memoir 116, p. 613-662.

- Snyder, W. S., Dickinson, W. R., and Silberman, M. L., 1976, Tectonic implications of space-time patterns of Cenozoic magmatism in the western United States: Earth and Planetary Science Letters, v. 32, no. 1, p. 91-106.
- Staatz, M. H., and Carr, W. J., 1964, Geology and mineral deposits of the Thomas and Dugway Ranges, Juab and Tooele Counties, Utah: U.S. Geological Survey Professional Paper 415, 188 p.
- Staatz, M. H., and Griffitts, W. R., 1961, Beryllium-bearing tuff in the Thomas Range, Juab County, Utah: Economic Geology, v. 56, no. 5, p. 946-950.
- Staatz, M. H., and Osterwald, F. W., 1959, Geology of the Thomas Range fluorspar district, Juab County, Utah: U.S. Geological Survey Bulletin 1069, 97 p.
- Staub, A. M., 1975, Geology of the Picture Rock Hills Quadrangle, Juab County, Utah: Salt Lake City, University of Utah unpublished M.S. thesis., 87 p.
- Steven, T. A., and Lipman, P. W., 1976, Calderas of the San Juan volcanic field, southwestern Colorado: U.S. Geological Survey Professional Paper 958, 35 p.
- Stewart, J. H., Moore, W. J., and Zietz, I., 1977, East-west patterns of Cenozoic igneous rocks, aeromagnetic anomalies, and mineral deposits, Nevada and Utah: Geological Society of America Bull., v. 88, no. 1, p. 67-77.
- Texas Instruments Incorporated, 1977, Aerial gamma-ray and magnetic survey of the Delta area--Utah: U.S. Department of Energy report GJBX-18(77).
- Williams, Howell, 1932, The history and character of volcanic domes: University of California Publications, Bulletin of the Department of Geological Sciences, v. 21, no. 5, p. 51-146.
- Zentelli, M., and Dostal, J., 1977, Uranium in volcanic rocks from the central Andes: Journal of Volcanology and Geothermal Research, v. 2, no. 3, p. 251-258.
- Zielinski, R. A., 1978, Uranium abundances and distribution in associated glassy and crystalline rhyolites of the western United States: Geological Society of America Bulletin, v. 89, no. 3, p. 409-414.

Zielinski, R. A., Ludwig, K. R., and Lindsey, D. A., 1977, Uranium-lead apparent ages of uraniferous secondary silica as a guide for describing uranium mobility, in Campbell, J. A., ed., Short papers of the U.S. Geological Survey Uranium-Thorium Symposium, 1977: U.S. Geological Survey Circular 753, p. 39-40.

## APPENDIX

Table 8.--Chemical analyses of igneous rocks from the Thomas Range and northern Drum Mountains, Juab County, Utah

[Silica,  $Al_2O_3$ , total Fe as  $Fe_2O_3$ , CaO,  $K_2O$ ,  $TiO_2$ , and some MnO by X-ray fluorescence by J. S. Wahlberg; MgO and  $Na_2O$  by atomic absorption by C. A. Gent, V. M. Merritt, and H. G. Neiman. Equivalent uranium (eU) determined by beta-gamma scaler by H. G. Neiman, V. M. Merritt, and C. A. Gent. Manganese and B through Zr determined by six-step semiquantitative spectrographic method by R. G. Havens and F. E. Lichte. For samples Sp-0, Sp-1, and Sp-2, Li determined by atomic absorption by V. M. Merritt. Uranium and thorium determined by delayed neutron method by H. T. Millard, Jr., C. Fee, C. Bliss, C. M. Ellis, and V. C. Smith. N, not detected; L, detected but below the limit of detection. Analyses do not total 100 percent because  $H_2O$  and volatile constituents were not determined; also,  $SiO_2$  by X-ray fluorescence is subject to considerable, but unmeasured, error.]

NAME AND LOCATION OF ROCKS ANALYZED

Sample No.	Location
Drum Mountains Rhyodacite, flow	
U3	SE 1/4, SW 1/4, sec. 2, T. 13 S., R. 12 W.
U10A	SE 1/4, SW 1/4, sec. 35, T. 12 S., R. 12 W.
U33	NW 1/4, NW 1/4, sec. 21, T. 13 S., R. 11 W.
U37	SW 1/4, NW 1/4, sec. 30, T. 13 S., R. 12 W.
U65	NW 1/4, NW 1/4, sec. 16, T. 14 S., R. 11 W.
Intrusive diorite	
U233	SW 1/4, SE 1/4, sec. 36, T. 14 S., R. 11 W.
Mt. Laird Tuff	
U57	SE 1/4, NE 1/4, sec. 21, T. 14 S., R. 11 W.
U62	NE 1/4, SW 1/4, sec. 16, T. 14 S., R. 11 W.
Intrusive porphyry, slightly altered, equivalent to Mt. Laird Tuff	
U222	SW 1/4, SW 1/4, sec. 35, T. 14 S., R. 11 W.
Joy Tuff, crystal tuff member	
U32	NW 1/4, NW 1/4, sec. 22, T. 13 S., R. 11 W.
U34	SE 1/4, NE 1/4, sec. 20, T. 13 S., R. 11 W.
U43	SE 1/4, SW 1/4, sec. 17, T. 13 S., R. 11 W.
U49	SW 1/4, SW 1/4, sec. 5, T. 13 S., R. 11 W.
U56	SE 1/4, NE 1/4, sec. 21, T. 14 S., R. 11 W.
T51-A	NE 1/4, NW 1/4, sec. 10, T. 13 S., R. 11 W.
Joy Tuff, black glass tuff member, basal black welded zone	
Sp-0	SW 1/4, SE 1/4, sec. 25, T. 13 S., R. 11 W.
U141B	NW 1/4, NE 1/4, sec. 36, T. 13 S., R. 11 W.
Joy Tuff, black glass tuff member, middle gray welded zone	
U141A	NW 1/4, NE 1/4, sec. 36, T. 13 S., R. 11 W.
U155	NW 1/4, SW 1/4, sec. 6, T. 14 S., R. 11 W.
Joy Tuff, black glass tuff member, upper unwelded zone	
Sp-1	SW 1/4, SE 1/4, sec. 25, T. 13 S., R. 11 W.
Sp-2	SW 1/4, SE 1/4, sec. 25, T. 13 S., R. 11 W.

NAME AND LOCATION OF ROCKS ANALYZED--cont.

Sample No.	Location
Dell Tuff	
U78	NE 1/4, NW 1/4 sec. 26, T. 11 S., R. 11 W.
U84	SE 1/4, NE 1/4, sec. 2, T. 13 S., R. 12 W.
T42-A	NW 1/4, NW 1/4, sec. 36, T. 12 S., R. 12 W.
T54-A	NE 1/4, SE 1/4, sec. 26, T. 12 S., R. 12 W.
Spor Mountain Formation, porphyritic rhyolite member, flow	
U2A	NW 1/4, NW 1/4, sec. 11, T. 13 S., R. 12 S.
U7A	SE 1/4, SW 1/4, sec. 36, T. 12 S., R. 12 W.
U11A	SE 1/4, SW 1/4, sec. 35, T. 12 S., R. 12 W.
U20A	NW 1/4, SE 1/4, sec. 9, T. 13 S., R. 12 W.
U97	NW 1/4, NE 1/4, sec. 25, T. 12 S., R. 12 W.
U122	SW 1/4, SE 1/4, sec. 25, T. 12 S., R. 12 W.
T53-TR-A	SW 1/4, NE 1/4, sec. 8, T. 13 S., R. 12 W.
T53-TR-B	SW 1/4, NE 1/4, sec. 8, T. 13 S., R. 12 W.
Spor Mountain Formation, porphyritic rhyolite member, plug	
U21C	NE 1/4, NW 1/4, sec. 10, T. 13 S., R. 12 W.
Spor Mountain Formation, porphyritic rhyolite member, extrusive dome	
U26	NW 1/4, SE 1/4, sec. 9, T. 12 S., R. 12 W.
U100	NE 1/4, SE 1/4, sec. 8, T. 12 S., R. 12 W.
Thomas Range Rhyolite, older flow	
U15	SW 1/4, SW 1/4, sec. 14, T. 12 S., R. 12 W.
U16	NW 1/4, SE 1/4, sec. 22, T. 12 S., R. 12 W.
U72	NE 1/4, NE 1/4, sec. 19, T. 12 S., R. 12 W.
T50-TR-A	NE 1/4, NE 1/4, sec. 28, T. 12 S., R. 11 W.
T50-TR-B	NE 1/4, NE 1/4, sec. 28, T. 12 S., R. 11 W.



NAME AND LOCATION OF ROCKS ANALYZED  
(continued)

Sample No.	Location
Thomas Range Rhyolite, younger flow	
T52-TR-A	NW 1/4, SW 1/4, sec. 15, T. 13 S., R. 11 W.
T52-TR-B	NW 1/4, SW 1/4, sec. 15, T. 13 S., R. 11 W.
T13-TR-A	SW 1/4, NE 1/4, sec. 1, T. 13 S., R. 12 W.
T13-TR-B	SW 1/4, NE 1/4, sec. 1, T. 13 S., R. 12 W.
T21-TR-A	NE 1/4, SE 1/4, sec. 28, T. 13 S., R. 11 W.
T21-TR-B	NE 1/4, SE 1/4, sec. 28, T. 13 S., R. 11 W.
Thomas Range Rhyolite, Topaz Mtn. flow	
T40-TR-A	NW 1/4, NE 1/4, sec. 16, T. 13 S., R. 11 W.
T40-TR-B	NW 1/4, NE 1/4, sec. 16, T. 13 S., R. 11 W.
Sp-13	NW 1/4, NW 1/4, sec. 16, T. 13 S., R. 11 W.
Thomas Range Rhyolite, extrusive dome	
U74	NE 1/4, NW 1/4, sec. 26, T. 12 S., R. 11 W.
T03-TR-A	SW 1/4, SW 1/4, sec. 14, T. 13 S., R. 11 W.
T03-TR-B	SW 1/4, SW 1/4, sec. 14, T. 13 S., R. 11 W.

Table 8.—Cont.

	Lower limit of detection	U3	U10A	U33	U37	U65
Composition in percent						
SiO <sub>2</sub>		59	62	63	62	61
Al <sub>2</sub> O <sub>3</sub>		13	14	14	13	15
Fe <sub>2</sub> O <sub>3</sub>		3.7	4.2	3.8	4.6	4.2
MgO		0.51	1.65	3.69	2.82	3.49
CaO		5.7	4.5	3.4	6.2	4.1
Na <sub>2</sub> O		3.6	3.11	2.98	2.93	3.43
K <sub>2</sub> O		3.8	3.3	2.2	2.9	2.3
TiO <sub>2</sub>		0.92	0.77	0.60	0.81	0.90
MnO	.05; 0001 <sup>3/</sup>	< .05	< .05	0.090	0.077	0.0065
Composition in parts per million						
B	20	N	N	L	N	L
Ba	1.5	1500	1000	1500	1500	1500
Be	1	3	2	3	2	1.5
Ca	150	200	L	N	L	300
Co	3	10	10	30	15	20
Cr	1	20	150	200	150	150
Cu	1	10	15	15	7	30
Ga	5	20	20	30	20	30
La	30	150	70	70	70	150
Li	50	N	N	N	N	N
Mo	3	N	N	7	N	N
Nb	10	30	20	15	15	15
Nd	70	100	70	N	70	150
Ni	5	10	30	70	30	100
Pb	10	30	20	30	30	20
Sc	5	7	15	15	15	30
Sn	10	N	N	N	N	N
Sr	5	1000	500	700	700	1000
V	7	100	100	150	150	200
Y	10	30	30	20	30	30
Yb	1	3	3	3	3	3
Zr	10	200	150	200	150	300
eU	10	20	30	30	29	40
U	-	6	4	4	4	6
Th	-	26	19	19	17	30

Table 8.—Cont.

	U233	U57	U62	U222 <sup>1/</sup>
Composition in percent				
SiO <sub>2</sub>	53	60	59	55
Al <sub>2</sub> O <sub>3</sub>	14	15	15	13
Fe <sub>2</sub> O <sub>3</sub>	6.8	5.7	5.5	5.2
MgO	3.6	3.24	3.49	2.20
CaO	5.1	5.3	5.1	3.9
Na <sub>2</sub> O	2.68	2.81	2.90	2.85
K <sub>2</sub> O	1.9	2.1	2.3	2.7
TiO <sub>2</sub>	1.0	0.80	0.80	0.90
MnO	0.12	0.090	0.090	0.09
Composition in parts per million				
B	N	L	L	N
Ba	700	1000	1000	1000
Be	N	1.5	1.5	L
Ce	N	N	N	N
Co	15	20	20	15
Cr	30	70	70	10
Cu	5	30	50	20
Ga	15	30	30	20
La	L	70	70	50
Li	N	N	N	N
Mo	L	N	N	L
Nb	N	10	10	N
Nd	N	70	70	N
Ni	7	15	15	10
Pb	10	20	70	15
Sc	30	30	30	15
Sn	N	N	N	N
Sr	700	1000	1500	1000
V	150	200	200	150
Y	15	30	30	15
Yb	2	3	3	1.5
Zr	100	150	150	100
eU	10	20	30	20
U	2	4	4	4
Th	11	12	13	16

Table 8.—Cont.

	U32	U34	U43	U49	U56	T51-A
Composition in percent						
SiO <sub>2</sub>	74	70	76	73	75	73
Al <sub>2</sub> O <sub>3</sub>	11	12	13	13	14	12
Fe <sub>2</sub> O <sub>3</sub>	0.70	1.4	1.3	1.6	1.3	1.4
MgO	0.33	0.39	0.46	0.96	0.46	0.31
CaO	0.77	1.6	1.4	1.7	1.3	1.4
Na <sub>2</sub> O	3.1	3.18	3.30	2.90	3.30	2.93
K <sub>2</sub> O	4.5	4.3	3.6	3.1	3.6	3.9
TiO <sub>2</sub>	0.067	0.29	0.30	0.30	0.20	0.21
MnO	0.11	0.057	0.065	0.065	0.065	0.022
Composition in parts per million						
B	L	20	20	L	30	20
Ba	700	1000	1000	700	1000	700
Be	1.5	2	3	3	3	1.5
Ca	L	N	N	N	N	L
Co	N	L	L	L	L	L
Cr	1	1.5	7	3	7	1
Cu	1.5	1.5	3	3	1.5	1.5
Ga	15	30	20	30	30	15
La	70	70	L	50	L	L
Li	N	N	N	N	N	N
Mo	N	N	N	N	N	L
Nb	15	15	15	15	15	15
Nd	N	N	N	N	N	L
Ni	N	N	N	L	L	L
Pb	30	30	30	30	30	30
Sc	L	L	5	7	5	L
Sn	N	N	N	N	N	N
Sr	200	300	500	500	300	300
V	20	30	30	30	30	20
Y	20	30	15	20	15	15
Yb	2	3	1.5	2	1.5	1.5
Zr	70	70	100	100	100	50
eU	20	20	40	20	30	30
U	7	6	7	5	7	7
Th	21	19	25	22	25	22

Table 3.—Cont.

	Sp-0	U141B	U141A	U155	SP-1 <sup>2/</sup>	Sp-2 <sup>2/</sup>
Composition in percent						
SiO <sub>2</sub>	70	74	71	76	76	66
Al <sub>2</sub> O <sub>3</sub>	12	13	13	13	9.9	12
Fe <sub>2</sub> O <sub>3</sub>	1.1	1.2	1.3	1.2	0.9	1.0
MgO	0.37	0.47	0.51	0.49	0.42	1.23
CaO	1.46	1.2	1.7	1.1	1.44	2.10
Na <sub>2</sub> O	3.03	3.18	2.73	3.06	1.00	1.99
K <sub>2</sub> O	4.80	4.0	4.2	4.4	4.82	4.13
TiO <sub>2</sub>	0.20	0.20	0.30	0.30	0.20	0.20
MnO	.039	.039	.039	.039	.026	.013
Composition in parts per million						
B	20	30	30	30	L	L
Ba	700	1000	1000	1500	500	500
Be	1	2	2	2	1	1
Ca	150	200	L	L	150	150
Co	N	L	L	L	N	5
Cr	5	10	15	15	7	10
Cu	3	3	5	3	2	2
Ga	20	30	30	20	15	20
La	70	100	70	70	50	70
Li	<10	N	N	N	<10	20
Mo	L	L	N	N	N	N
Nb	L	15	20	20	L	L
Nd	N	70	70	70	N	N
Ni	5	L	L	L	L	5
Pb	20	50	30	30	15	30
Sc	5	5	7	7	N	5
Sn	N	N	N	N	N	N
Sr	200	300	300	300	150	500
V	20	30	30	30	15	20
Y	20	20	15	20	10	10
Yb	1	2	2	2	1	1
Zr	100	100	100	100	100	100
eU	50	50	40	30	40	30
U	8	9	8	8	5	4
Th	27	23	23	24	21	27

Table 8.—Cont.

	U78	U84	T42-A	T54-A
Composition in percent				
SiO <sub>2</sub>	77	76	70	71
Al <sub>2</sub> O <sub>3</sub>	13	12	12	12
Fe <sub>2</sub> O <sub>3</sub>	1.3	1.3	1.3	1.5
MgO	0.61	0.73	1.16	0.8
CaO	0.50	1.1	1.1	3.5
Na <sub>2</sub> O	0.80	2.10	2.13	0.79
K <sub>2</sub> O	6.4	4.0	3.6	4.9
TiO <sub>2</sub>	0.20	0.20	0.25	0.23
MnO	0.065	0.09	-	0.096
Composition in parts per million				
B	L	L	30	L
Ba	1000	500	700	700
Be	3	5	3	3
Ca	N	N	N	L
Co	L	N	3	L
Cr	10	3	2	2
Cu	1.5	1.5	2	1.5
Ga	30	30	20	15
La	50	50	30	50
Li	N	N	N	L
Mo	N	N	N	N
Nb	15	15	20	15
Nd	N	N	N	L
Ni	N	N	N	L
Pb	30	30	30	30
Sc	5	L	7	L
Sa	N	N	N	N
Sr	200	200	200	150
V	30	20	20	20
Y	15	15	20	15
Yb	1.5	1.5	2	1.5
Zr	70	70	70	70
eU	50	50	30	30
U	4	5	2	6
Th	23	21	24	21

Table 8.--Cont.

	U2A	U7A	U11A	U20A	U97	U122
Composition in percent						
SiO <sub>2</sub>	68	64	72	73	72	73
Al <sub>2</sub> O <sub>3</sub>	11	12	13	12	15	15
Fe <sub>2</sub> O <sub>3</sub>	1.1	0.83	0.89	1.1	0.8	0.9
MgO	0.16	0.11	0.11	0.10	0.20	0.14
CaO	0.98	0.52	0.64	0.65	0.80	0.20
Na <sub>2</sub> O	3.8	4.2	3.9	3.8	3.5	4.1
K <sub>2</sub> O	4.7	4.5	4.9	4.8	4.5	4.3
TiO <sub>2</sub>	0.072	<0.05	0.050	0.079	<.05	<.05
MnO	<0.05	0.053	0.053	0.063	0.039	0.065
Composition in part per million						
B	50	30	30	30	20	L
Ba	100	30	30	150	70	30
Ba	10	15	10	15	7	10
Ce	L	L	L	L	L	L
Co	N	N	N	N	N	N
Cr	N	N	N	N	3	N
Cu	2	1	N	N	3	1
Ga	30	50	30	50	100	150
La	70	70	70	70	50	50
Li	150	300	300	300	150	700
Mb	N	N	N	N	N	N
Nb	100	70	100	150	150	200
Nd	70	70	N	100	N	N
Ni	N	N	N	N	N	N
Pb	100	70	30	50	70	70
Sc	N	N	N	N	N	L
Sn	15	30	50	15	20	30
Sr	30	15	15	20	15	15
V	15	10	N	7	N	30
Y	100	70	70	200	50	70
Yb	15	10	10	20	7	10
Zr	70	70	70	150	100	70
eU	50	40	60	50	70	50
U	12	11	10	14	8	13
Th	79	54	55	75	56	50

Table 8.--Cont.

	T53-TR-A	T53-TR-B	U21C	U26	U100
Composition in percent					
SiO <sub>2</sub>	76	74	73	72	74
Al <sub>2</sub> O <sub>3</sub>	14	13	12	11	12
Fe <sub>2</sub> O <sub>3</sub>	1.5	1.5	1.2	1.4	0.6
MgO	0.13	0.08	0.10	0.08	0.11
CaO	0.54	0.47	0.72	1.7	1.7
Na <sub>2</sub> O	3.60	3.73	3.8	4.1	3.98
K <sub>2</sub> O	4.9	4.7	5.0	4.0	3.5
TiO <sub>2</sub>	0.053	0.055	0.072	0.25	<0.05
MnO	0.034	0.036	0.050	<0.050	0.090
Composition in part per million					
B	70	30	30	20	L
Ba	15	20	150	50	50
Be	15	7	10	50	30
Ca	L	L	L	N	N
Co	N	N	N	N	N
Cr	L	L	N	N	3
Cu	L	L	1	N	N
Ga	30	30	50	30	70
La	70	70	70	L	L
Li	300	300	700	300	200
Mo	3	3	N	N	N
Nb	150	150	100	100	70
Nd	100	150	70	N	N
Ni	L	L	N	N	N
Pb	30	30	30	50	70
Sc	L	L	N	N	L
Sn	30	30	20	20	15
Sr	15	15	70	15	70
V	L	L	10	N	7
Y	70	100	70	70	70
Yb	15	15	10	10	7
Zr	150	150	70	70	100
eU	60	50	50	40	40
U	17	11	12	13	15
Th	71	72	64	51	53



Table 8.--Cont.

	U15	U16	U72	T50-TR-A	T50-TR-B
Composition in percent					
SiO <sub>2</sub>	74	72	78	75	76
Al <sub>2</sub> O <sub>3</sub>	12	12	11	12	12
Fe <sub>2</sub> O <sub>3</sub>	1.1	1.2	0.80	0.90	0.84
MgO	0.23	0.18	0.09	0.20	0.07
CaO	0.52	0.67	0.80	1.4	0.66
Na <sub>2</sub> O	3.5	3.5	2.68	1.95	3.51
K <sub>2</sub> O	4.6	4.8	4.8	6.6	4.6
TiO <sub>2</sub>	0.071	0.056	0.090	0.069	0.073
MnO	0.053	0.055	0.065	0.100	0.036
Composition in parts per million					
B	20	20	L	L	L
Ba	30	30	50	15	7
Be	15	15	10	7	7
Ca	N	N	L	L	L
Co	N	N	N	N	N
Cr	N	N	30	L	L
Cu	1.5	1	1	L	L
Ga	30	30	50	15	20
La	N	L	70	50	50
Li	150	150	L	L	L
Mo	N	N	3	L	3
Nb	100	100	70	50	50
Nd	N	N	N	L	N
Ni	N	N	N	L	L
Pb	50	50	70	30	50
Sc	N	N	L	L	L
Sa	10	15	15	N	N
Sr	30	30	70	300	20
V	10	10	L	L	L
Y	70	70	30	20	20
Yb	7	7	5	5	5
Zr	100	100	150	70	70
eU	60	50	60	60	50
U	15	17	18	19	17
Th	56	53	68	59	61

Table 8.--Cont.

	T52-TR-A	T52-TR-B	T13-TR-A	T13-TR-B	T21-TR-A	T21-TR-B
Composition in percent						
SiO <sub>2</sub>	75	75	75	77	73	62
Al <sub>2</sub> O <sub>3</sub>	12	12	12	12	12	10
Fe <sub>2</sub> O <sub>3</sub>	0.97	1.0	0.98	1.00	1.0	0.93
MgO	0.16	0.11	0.06	0.06	0.15	0.19
CaO	1.4	2.5	1.0	0.86	1.3	1.6
Na <sub>2</sub> O	3.25	3.14	3.71	3.58	3.51	3.49
K <sub>2</sub> O	4.7	4.7	4.7	4.8	4.7	4.9
TiO <sub>2</sub>	0.092	0.110	0.079	0.095	0.087	0.087
MnO	0.048	0.047	0.071	0.053	0.061	0.053
Composition in part per million						
B	L	L	L	L	L	L
Ba	20	70	10	15	10	20
Be	7	7	15	10	7	7
Ca	L	L	L	L	L	L
Co	N	N	N	N	N	N
Cr	L	L	L	L	L	L
Cu	L	L	L	L	L	L
Ga	15	15	20	20	20	20
La	70	70	50	70	70	70
Li	100	100	100	100	100	100
Mo	3	3	5	5	7	3
Nb	50	30	70	70	70	70
Nd	L	70	L	L	L	L
Ni	L	L	L	L	L	L
Pb	50	50	50	50	50	50
Sc	L	L	L	L	L	L
Sn	N	N	N	N	N	N
Sr	50	100	15	15	30	70
V	L	L	N	L	L	7
Y	20	20	30	30	30	20
Yb	5	3	7	7	7	5
Zr	100	70	100	70	100	100
eU	50	50	60	60	50	50
U	18	17	20	17	19	18
Th	61	65	64	74	73	76

Table 8.--Cont.

	T40-TR-A	T40-TR-B	SP-13	U74	TO3-TR-A	TO-3-TR-B
Composition in percent						
SiO <sub>2</sub>	64	62	74	75	71	74
Al <sub>2</sub> O <sub>3</sub>	10	11	11	11	12	12
Fe <sub>2</sub> O <sub>3</sub>	0.92	1.0	0.68	1.0	0.91	0.96
MgO	0.12	0.18	0.02	0.19	0.04	0.05
CaO	0.66	0.66	0.55	1.3	0.46	1.1
Na <sub>2</sub> O	3.39	3.34	3.45	2.76	4.07	3.58
K <sub>2</sub> O	4.6	4.9	4.2	4.4	4.5	4.7
TiO <sub>2</sub>	0.090	0.100	0.087	0.10	0.050	0.070
MnO	0.043	0.050	0.032	0.039	0.12	0.050
Composition in parts per million						
B	L	L	L	L	20	L
Ba	5	7	15	200	5	10
Be	7	7	5	5	7	7
Ca	L	L	150	L	N	N
Co	N	N	N	N	N	N
Cr	L	L	L	L	L	L
Cu	L	L	1	15	L	L
Ga	20	15	20	30	20	20
La	70	70	70	70	L	L
Li	L	L	50	L	100	L
Mb	5	3	5	3	3	3
Nb	50	50	15	30	50	50
Nd	L	L	N	N	L	L
Ni	L	L	N	N	L	L
Pb	50	50	50	70	70	70
Sc	L	L	L	N	N	L
Sn	N	N	N	N	N	N
Sr	50	50	10	70	7	15
V	L	L	L	20	N	L
Y	30	30	50	50	70	50
Yb	7	5	5	5	7	7
Zr	100	100	100	100	70	70
eU	50	50	60	40	50	40
U	15	15	13	6	20	16
Th	67	68	63	36	51	59

- 1/ Rock has been partly altered by hydrothermal fluids.
- 2/ Alkali metals may have been leached by ground water.
- 3/ Limits of detection for MnO are .05 percent by X-ray fluorescence;  
.0001 by six-step spectrographic method.